Summer 8-22-2020

Processing Modeling of Hot Air Convective Drying of Sugar Kelp (Saccharina Latissima)

Praveen Kumar Sappati
University of Maine, sappati.kumar@maine.edu

PROCESS MODELING OF HOT AIR CONVECTIVE DRYING OF SUGAR KELP (SACCHARINA LATISSIMA)

By

Praveen Kumar Sappati

M.Tech (Dual), Indian Institute of Technology Kharagpur, 2013

B.Tech, Indian Institute of Technology Kharagpur, 2013

A DISSERTATION

Submitted in Partial Fulfillment of the

Requirements for the Degree of

Doctor of Philosophy

(in Food and Nutrition Sciences)

The Graduate School

The University of Maine

August 2020

Advisory Committee:

Balunkeswar Nayak, Associate Professor of Food Processing, Advisor

Peter vanWalsum, Associate Professor of Chemical & Biomedical Engineering, Advisor

Denise Skonberg, Associate Professor of Food Science

Mary Camire, Professor of Food Science and Human Nutrition

Douglas Bousfield, Professor of Chemical & Biomedical Engineering

PROCESS MODELING OF HOT AIR CONVECTIVE DRYING OF SUGAR KELP (SACCHARINA LATISSIMA)

By Praveen Kumar Sappati

Dissertation Advisor: Dr. Balunkeswar Nayak

An Abstract of the Dissertation Presented
in Partial Fulfillment of the Requirements for the
Degree of Doctor of Philosophy
(in Food and Nutrition Sciences)
August 2020

Recent interest among consumers to avoid added chemical additives/preservatives has led to the recognition of seaweed as a healthy source of fibers, minerals, and antioxidants. Currently, global seaweed aquaculture is valued over US$ 6 billion and is increasing at a steady rate of 8% annually. Moreover, as per NOAA Fisheries the US imports more than 80% of the seafood consumed. This provides huge economic and workforce development opportunities in the seaweed aquaculture industry of Maine. Consequently, farming sugar kelp (*Saccharina latissima*), a brown seaweed, is gaining momentum along the northeast US coast. Due to its seasonal availability and limited shelf life, seaweeds are sun-dried or using hot-air to remove moisture, preventing oxidation and microbial growth. The goal of this research is to solve the bottlenecks of drying seaweed in Maine by developing an innovative technology focused on a clean, energy-efficient and closed drying system for producing top-notch and local finished products for American consumers. For this project, the effect of drying and storage conditions (temperature, humidity) on the physical, chemical and thermal properties of the final product are studied. Also, a mathematical drying model is developed to understand the drying kinetics and rate of moisture removal in hot-air driers. Investigations carried out throughout this experiment shows controlled environment drying can improve the predictability of drying dynamics significantly for the preservation of health-beneficial components in sugar kelp. The developed model showed drying can be optimized to create a carbon negative and sustainable seaweed processing industry in Maine.

DEDICATION

I dedicate this dissertation to the creator of the universe, my parents and friends for providing me the education, love, and support throughout my life.

ACKNOWLEDGEMENTS

My research project would not have been possible without the support of lucky stars and many people who always stood by my side and helped me in every possible way. First, I would like to thank both Dr. Balunkeswar Nayak and Dr. Peter vanWalsum for giving me this opportunity to pursue a doctoral degree at the University of Maine and for their invaluable mentorship throughout this project. I am grateful to my advisory committee members Dr. Denise Skonberg, Dr. Mary Camire and Dr. Doug Bousfield for their insightful guidance, moral support, and commitment towards my research. I would also like to thank the National Science Foundation award #1355457 on Sustainable Ecological Aquaculture Network (SEANET) for funding me to start this work and Seth Barker (Maine Fresh Sea Farms, Maine) for harvesting and donating fresh sugar kelp throughout this research work. I also appreciate my undergraduate lab assistants including Emily Duran-Frontera, Owen Mulrey, Kirsten Swimm, Sara Gundermann, Nikita Agarwal and Hanjuan Cao for helping and generating preliminary experimental data for this project. I would also like to thank the Advanced Manufacturing Center and Advanced Structures and Composite Center, University of Maine for giving access to the convective dryer and the Differential Scanning Calorimeter, respectively.

Special appreciation to Katherine Dentici for her selfless support throughout my stay at the University of Maine. She helped me in every aspect of my research including equipment location, training and conducting lab classes. I am also very grateful to my squash guru, Niclas Erhardt for open-hearted conversation, teaching an awesome sport and giving me the reason to not give up and aspire to become the best version of myself. I would also like to thank my past and current labmates (Tamanna Ramesh, Dr. Adeseye Lasekan, Yaohan Yin, Avinash Singh Patel, Suryaprakash Balasubramaniam, Richa Arya, Adoum) for modeling perseverance and optimism. To all my awesome friends Bouhee Kang, Dhriti Nayyar, Surbhi Khanna, Ankur Tiwari, Chitra Pandian, Prateek Kunwar, Dustin Nadjkovic, Amanda Barberi, Devin Bryne, Koorosh Kashkooli, Siddhart Chhatwal, Eeshaan Asaikar, Abigail Wiegand, Harikrishnan Medayil, Bhargavi Rane, Dhafer Alshaibani, Waem Alshaibani, Sami Humaid, Samuel

Akomeafrempong, Sayan Maitra, thank you guys for always being there. Lastly, very thankful to my parents for their hard work, dedication and endless support throughout the journey of my life.

TABLE OF CONTENTS

LIST OF TABLES

LIST OF FIGURES

CHAPTER 1

INTRODUCTION

1.1. Background

Seaweeds are marine macro-algae and are a rich source of dietary fibers, vitamins, minerals, antioxidants and medicinal bioactive compounds (Darcy-Vrillon 1993; Ito and Hori 1989; Morrissey et al. 2001; Tabarsa et al. 2012). Seaweeds are harvested wild from the ocean in most places in the world. Seaweeds are classified into three major groups; the green algae (Chlorophyta), the brown algae (Phaeophyta), and the red algae (Rhodophyta) (Hurd et al. 2014). Sugar kelp (*Saccharina latissima*) belongs to the brown class of seaweeds and is mostly cultivated in Asian countries such as China and Japan, some parts of Europe and in the coastal fronts of North America. It is named sugar kelp because of its sweet-tasting powder containing considerable amounts of mannitol (Hurd et al. 2014). The frond of sugar kelp grows quickly from November to April and it lives for 2 to 4 years (Hurd et al. 2014). Cultivation of sugar kelp does not need any application of chemical pesticides; hence the food products are free from pesticide residues compared to land-based products.

Drying is a phase change process governed by simultaneous heat and mass transfer (Mujumdar & Passos, 2000). It removes free water and makes food less susceptible to microbial attack, lipid oxidation and enzymatic browning (Argyropoulos et al. 2011; Zhang et al. 2006). To extend the shelf life of sugar kelp it is either conventionally sun-dried or hot air dried. Sun drying is one of the oldest techniques for food preservation, however, it is very slow, requires clear weather conditions and open drying may lead to pest, rodent and bird infestation (Ringeisen et al. 2014). Closed drying systems are energy-intensive but have proved to be better than sun drying in terms of nutrient retention and hygiene (Gallali et al. 2000; Murthy 2009). Higher drying temperatures (50 – 80°C) induce faster drying rates, but also lead to alterations in textural quality due to case hardening, undesirable color change and material shrinkage (Russo et al. 2012). Removal of free water attached to the solid matrix of food creates void space and stress at the cellular level, leading to material shrinkage. The material state (glassy or rubbery) can highly

influence its shrinkage while drying and hence, affects the textural properties and shelf-life. Hot air drying induces faster drying rate, but also leads to a reduction in heat-sensitive nutrients including vitamin C, antioxidants, phytochemicals, total flavonoid content and total phenolic content (Katsube et al. 2009; Shi et al. 1999). Also, the chemical and nutritional composition of seaweeds depends mostly on species, growth location, growth period, water temperature, salinity and light intensity (Miyashita et al. 2013; Schiener et al. 2015; Wells et al. 2016; Kumar et al. 2015, Suresh Kumar et al. 2015; Susanto et al. 2016). Hence, determining the thermal properties (thermal conductivity (k), thermal diffusivity (D), specific heat capacity (C)) of sugar kelp is important for predicting the drying rate under different drying conditions and its effect on the nutritional profile, functional and bioactive properties of the dried kelp.

Thermal properties of foods vary with temperature and moisture content during thermal processing due to the changes in texture and/or composition (Karunakar et al. 1998). Furthermore, void formation during drying as a result of moisture removal can be characterized macroscopically by structural properties such as true density, bulk density, porosity, and shrinkage. General models for the prediction of thermal properties of food products (i.e., thermal conductivity, specific heat, thermal diffusivity and material density) as functions of basic food components (i.e., fat, protein, moisture, carbohydrate, fiber, and ash) of land-based products were developed by Choi and Okos (1986). However, in the case of seaweeds, empirical modeling has known limitations since the primary constituent groups in seaweeds consist of complex polysaccharides (alginates, cellulose, laminarin, mannitol, and fucoidan) that are completely different from those in land-based products. There have been many published experimental values of the thermophysical properties of foods and mathematical models to represent these data (Gonzo 2002; Wang et al. 2006; Carson 2006). However, there is no similar work done on the seaweeds.

Mathematical modeling and simulation play a key role in designing and optimizing the processing of foods. Process models are increasingly being used to solve process problems and to help in decision-making for the process parameters. Real-world systems are generally simulated using complex

algorithms however, they never exactly imitate the real-world system. Therefore, a model needs to be verified and validated to the degree required for the model's intended purpose and application. The verification and validation of the simulation model can only be done after initial model development using certain process specifications identified at distinct levels and compared with the real-world experiments. This is an iterative process that takes place throughout the development of a simulation model. Measured thermal properties of sugar kelp will be essential for the modeling and evaluation of food processing operations involving heat and mass transfer, especially when energy costs, food quality and safety are the main considerations.

1.2. Objectives

The main objective of this study is to develop an innovative technology focused on a clean, energy-efficient and closed drying system for producing top-notch and local finished products for American consumers.

The specific objectives of this research are as follows:

1) Studying the moisture sorption isotherm and the effect of glass transition temperature on the shrinkage during hot-air convective drying for establishing storage parameters.
2) Studying the effect of drying parameters (temperature, humidity and time) on the physico-chemical properties of sugar kelp for establishing processing conditions.
3) Studying the thermophysical properties of sugar kelp and developing the heat and mass transfer model during the hot-air drying for optimizing process parameters.

CHAPTER 2

LITERATURE REVIEW

2.1. History of Seaweeds

Seaweeds or sea vegetables are marine macroalgae essential to the complex ecosystem required to support marine life. They act as a continuous source of oxygen in water by converting the inorganic carbon dioxide into organic compounds using solar radiation during photosynthesis (Thiel et al. 2007; Vásquez et al. 2013). Besides, they also provide dissolved organic matter mainly in the form of polysaccharides, an important food source for the marine microfauna and habitat for the marine animals higher in the food chain (Graham et al. 2007; Vásquez. 1992). They have also been an important part of the human diet for thousands of years in China, Japan, Korea, Chile, and Ireland (Dillehay et al., 2008; Fleurence and Levine, 2016; Nash, 2010). In Japan, the lack of goiter is attributed to the high seaweed consumption in the form of dried nori sheets used in the preparation of sushi. In China, seaweeds are utilized for medicinal purposes including *Sargassum* for goiter, *Gelidium* for intestinal afflictions, and *Laminaria* for the dilation of the cervix in difficult childbirths (Dawson, 1966). In southeast Asian countries such as Malaysia and Indonesia, seaweeds are consumed fresh as salad. In North America and Europe, a red alga named *Chondrus crispus*, has been used for its medicinal properties in treating urinary tract infections, diarrhea, breast infections, and tuberculosis (Dawson, 1966). Due to antifungal and antibacterial properties, seaweed extracts were also historically used to cure fevers in 18th century England, headaches in Alaska, USA and scabies in New Zealand (Chapman and Chapman, 1980). In the European Union, seaweeds were primarily used for the commercial production of hydrocolloids for both food and nonfood applications e.g., alginates and agar. In Ireland and Scotland, seaweeds were used as fertilizers for farms. Currently, seaweeds are projected as the next superfood for the human diet, health, and well-being and are applied in several sectors including biopolymers, cosmetics, animal feed, and functional food additives with various health benefits.

2.2. The Economy of the Seaweed Industry

Harvesting wild seaweeds from natural stocks is a common practice in Europe whereas in Asian countries seaweeds are cultivated for various applications. Currently, over the globe, the export value of the five cultivated genera including *Laminaria*, *Undaria*, *Gracilaria*, *Porphyra* and *Eucheuma/Kappaphycus* is valued at between US$ 10-16 billion and is increasing steadily at 8% annually (Tiwari and Troy 2015) (FAO 2014). From 1995-2012, the amount of seaweed consumption has been increased by 176%; largely contributed by the growth of farming of seaweeds in Indonesia, China, and the Philippines. In terms of sustainability, seaweed cultivation has resulted in the decline of wild harvesting practice from 52% in 1995 to only 4% of the net production of seaweed in 2012. The values reported above indicate only the export value of the seaweed and do not give a true estimate of the industry size as most of the seaweeds are produced and consumed locally. Also, there is a lack of data on the individual dollar value of the variety of seaweed and type of product.

2.3. Seaweeds: What are They?

Seaweeds, the term includes over 9000 species of macroalgae, are majorly classified into three categories based on their primary appearance due to the presence of specific pigments: red (Rhodophyta), green (Chlorophyta) and brown (Phaeophyta). Among those three major groups, red seaweeds are the most diverse representing 73% followed by brown and green seaweeds with 21% and 6% of the total seaweed species, respectively. Brown seaweeds have the largest thalli or body size. Green algae are multicellular, oxygenic and photosynthetic eukaryotic algae. Ninety percent of all green algae are predominantly found in freshwater whereas the remaining 10% inhabits the marine environment (Smith, 1955). Green seaweeds are found on the shallow coastal shores and eutrophic zones due to high nutrient tolerance. Ulva is commonly found on rocky shores and due to its resemblance to the land-based lettuce, it is also known as sea lettuce. The red seaweeds are the oldest eukaryotic algae and widely found in filamentous shape around the world in temperate, tropical and arctic waters. They are characterized as having eukaryotic cells, a complete lack of flagellar structure, food reserves of floridean starch, the presence of phycobilins,

chloroplasts without stacked thylakoids, and no external endoplasmic reticulum. They can grow in deep seawater with low light intensity due to the presence of an additional pigment known as phycobiliproteins such as R-phycoerythrin and R-phycocyanin. Most common of the red seaweeds are *Porphyra*, popularly known as "nori" in Japan, "laver" in the UK, USA and Canada, and *Gracilaria*. Brown seaweeds are characteristically brown due to the presence of fucoxanthin and are found in between subpolar and equatorial regions. They are morphologically different as compared to the other groups of seaweeds and biologically evolved to uptake more carbon dioxide under blue light. Brown and red seaweeds are an important source of hydrocolloids including alginates, agar, and carrageenan. They are found commonly in sheltered waters on rocky substrata in the intralittoral zone and their sporophyte is differentiated into a basal holdfast, a firm cylindrical stipe slightly flattened at the top and the highly variable structure of a single, undivided blade (Braune and Guiry 2011). Sugar kelp (*Saccharina latissima*) belongs to the brown class of seaweeds and is named sugar kelp because of its sweet-tasting powder containing considerable amounts of mannitol (Hurd et al. 2014). It is mostly harvested in Asian countries such as China and Japan, some parts of Europe and in the coastal fronts of North America. Sugar kelp is the most common brown seaweed produced in the state of Maine, USA. Its spores are grown on a seedstring in a nursery system on land with proper environmental controls (i.e. intensity of light, water temperature, water filtration and circulation, nutrient supply, etc.). After 5-7 weeks, the kelp attains 1-2 mm in size and the seedstring is outplanted on the longlines supported by the buoy systems at a particular site in the ocean with good nutrient flow, especially nitrogen. Afterward, the kelp is allowed to grow without any application of fertilizers between the period of mid-September and late March to attain the desired size. Finally, the fully-grown kelp is harvested from the longlines from April until June. In the wild, the frond of sugar kelp can live for 2 to 4 years (Hurd et al. 2014).

2.4. Chemical Composition of Brown Seaweeds and Health Benefits

Recent interest among consumers to avoid added chemical additives/preservatives in food products has led to the recognition of seaweed as a source of natural and healthy food. Moreover, reports

on the nutritional value of seaweeds have contributed to a growing demand for seaweed food products (Suleria et al. 2015). Seaweeds are a rich source of vitamins, minerals, antioxidants, omega-3 fatty acids and especially medicinal bioactive compounds in the form of dietary fibers (alginates, carrageenan, fucoidan, laminarin, porphyran, ulvan) and secondary polyphenolic metabolites (fucoxanthin, phlorotannins) (Campo et al. 2009; Darcy-Vrillon 1993; Ito and Hori 1989; Kang et al. 2012; Kotake-Nara et al. 2005; Mori et al. 2004; Morrissey et al. 2001; Tabarsa et al. 2012; Wang et al. 2009; Yang and Zhang 2009; Zubia et al. 2008). However, the chemical composition and nutritional content of seaweeds depend on multiple factors including: species, geography, location, season, water temperature, salinity and light intensity (Kumar et al. 2015; Miyashita et al. 2013; Schiener et al. 2015; Suresh kumar et al. 2015; Susanto et al. 2016; Wells et al. 2016). The active metabolites found in seaweed have been documented to exhibit various biological activities based on their chemical structure and species, including: anticancer, antitumor, antiviral, anti-inflammatory and anti-angiogenic effects (Beppu et al. 2009; Cumashi et al. 2006; Damonte et al. 2004; Ikeguchi et al. 2011; Sugawara et al. 2006). Brown seaweeds contain fats predominantly in the form of saturated fatty acids (SFA) (myristic acid (14:0), palmitic acid (16:0), stearic acid (18:0)) and poly unsaturated fatty acids (PUFAs) (linoleic acid (18:2), γ-linolenic acid (18:3n-6), α-linolenic acid (18:3), stearidonic acid (18:4), arachidonic acid (20:4), eicosapentaenoic acid (20:5n-3)), each group of fatty acids representing about 40% of the total fat/lipid content. PUFAs are abundant in seaweeds, especially ω -3's and ω-6's, which are essential fatty acids not biosynthesized by humans and must be consumed through the diet (Khotimchenko et al. 2002). The positive impact of these PUFA's on human health are well studied, including: reduction in cardiovascular diseases (Burtin 2003), anti-cancer properties (Khotimchenko and Gusarova 2004) and pre-postnatal development of the brain (Guesnet and Alessandri 2011).

Brown seaweeds generally contain very low amounts of proteins as compared to the other types of seaweeds (Fleurence and Levine 2016). The highest protein content (24 g $(100\ g)^{-1}$ dry solids) is recorded in *Undaria pinnatifida* and in most species, it can vary from 3 - 15 g $(100\ g)^{-1}$ dry solids

(Fleurence and Levine 2004; Smith and Young 1955). The carbohydrates in sugar kelp exist in two forms: structural (alginates and cellulose) and storage (laminarin, mannitol and fucoidan) and vary depending on the harvest season and environmental conditions (Schiener et al. 2015). Alginates exist primarily in the cell wall of brown algae, consisting of linear monomeric chains of β-D-mannuronic acid (M) and α-L-guluronic acid (G) residues (Kraan 2012). These chains are comprised of GG, MM or GMGM blocks depending on the species, source and time of harvest (Lee and Mooney 2012). G-blocks of alginate are responsible for hydrogel forming activity in the presence of cations such as Ca^{2+} by intermolecular cross-linking (George and Abraham 2006). Laminarin is also a linear polysaccharide consisting of glucose monosaccharide units linked by β-1,3-glycosidic bonds or β-1,6-glycosidic bonds (Rioux et al. 2010). It can represent around 2 – 34 g $(100\ g)^{-1}$ dry solids in the brown macroalgae (Kraan 2012). Mannitol is a six-carbon polyol that can vary between 12 – 30 g $(100\ g)^{-1}$ dry solids depending on the species and time of harvest (Holdt and Kraan 2011; Zubia et al. 2008). Fucoidans are the sulfated polysaccharides found in brown seaweeds up to 10 g $(100\ g)^{-1}$ dry solids (Holdt and Kraan 2011). Many studies have found that the consumption of high dietary fiber present in seaweed could help the prevention of obesity related disorders and metabolic syndrome (Lee et al. 2010; Yeh et al. 2011). Seaweeds are also an excellent source of calcium and phosphorus, the two essential minerals for calcification of the protein matrix, possibly lowering the risk of osteoporosis and bone mineral loss (Aslam et al., 2013; MacArtain et al., 2007; Yamaguchi et al., 2001). The mineral content found in sugar kelp is higher than in any terrestrial plants and is the highest among the seaweeds (Omotoso 2006; Rupeŕez 2002). Because of this, it is a very good nutritional source of primary macro and trace elements in the decreasing order: Potassium (K), Sodium (Na), Calcium (Ca), Magnesium (Mg), Iodine (I), Strontium (Sr), Iron (Fe), Arsenic (As), Aluminum (Al), Zinc (Zn) and Titanium (Ti) (Scheiner et al. 2015).

A vast range of pigments that absorb light in the visible spectrum for photosynthesis is found in the macroalgae, based on whether they are classified as brown, green or red seaweeds. In brown seaweeds chlorophyll a, chlorophyll c, fucoxanthin, violaxanthin and a precursor of vitamin A (β – carotene) are the

important light-harvesting pigments. Among these, fucoxanthin is the predominant pigment, it is generally yellowish-brown in color and masks the green color of chlorophyll, giving an overall appearance in the range of olive green to dark brown (Jefferey et al. 1997). Brown seaweeds have enormous amounts of phenolic compounds which are also known for exhibiting antioxidant activities (Dang et al. 2017; Gupta et al. 2011; Lann et al. 2008; Rajauria et al. 2010). These phenolic compounds include mainly chlorogenic acid, phloroglucinol, caffeic acid, kaempferol, 2, 5-dihydroxy benzoic acid, coumaric acid, cirsimaritin, ferulic acid, gallic acid, and syringic acid (Chakraborty et al. 2017; Rajauria et al. 2016). The continuous increase in life expectancy and low fertility rates have resulted in demographic shifts, causing an increase in neurological diseases such as autism, epilepsy, psychiatric disorders, neuropathic pain, or Alzheimer's and Parkinson's diseases among older adults. Several studies have documented that the natural bioactive compounds and minerals present in marine algae can act as a potential candidate for preventing neurodegenerative disease with no side effects as compared to the synthetic neuroprotective drugs (Cho et al., 2012; Ogara et al., 2015; Suganthy et al., 2010).

2.4. Farming, Harvesting and Processing of Seaweeds

Growing seaweeds in aquaculture has increased three-fold since 1997 from 7 million tons to 24 million tons (FAO 2014). Food products for human consumption constitute around 83% of the annual cultivation, while the rest is used in developing hydrocolloids, fertilizers and animal feeds (Craigie, 2011). This tremendous growth in production of seaweeds can potentially complement the land-based agricultural products. The productivity of some of the seaweed species is comparable with agricultural crops, for instance, the yield of giant kelp (*Macrocystis* spp.) is equivalent to sugar cane annually. Some of the research indicates that only 10% of the total ocean surface is required to produce fish and seaweeds equivalent to all the agricultural yield without the need for freshwater (Radulovich 2011). Brown seaweeds are present in shallow coastal waters attached to rocky substrates to receive adequate sunlight for photosynthesis. They absorb nutrients throughout their thallus and do not have true roots. Most commonly, brown seaweed propagules are attached to a string in the nursery to provide a substrate for

their growth and after maturation, they are transferred on thick nylon long lines supported by buoys allowing them to grow underwater with access to required sunlight, carbon dioxide, and nutrients. Seaweed cultivation in dead eutrophic zones of oceans can remove excess nutrients and thus help in rebalancing the local ecosystem. Growing similar species in different water can be challenging due to changes in water salinity, different ecosystems leading to the presence of vertebrate and invertebrate herbivores or biofouling organisms. In Damariscotta Bay, Maine, USA, the seaweeds are grown downstream from oyster farms. The waste from oyster cages provides nutrients along with naturally present ocean nutrients.

Fig 2.1 Sugar kelp grown on nylon long lines (Damariscotta Bay, Maine, USA)

Harvesting seaweeds, especially sugar kelp, is a very labor intense and tedious process for the seaweed farmers in Maine, USA from April to June on sunny days. It involves lifting a section of the long line above water (**Fig. 2.2**), inspecting and washing it with ocean water to remove any biofouling (**Fig 2.3**), cutting the stipes along the line, and collecting and transporting kelp in hygienic totes to the coast for further processing (**Fig 2.4**) (**Fig 2.5**). This whole process is repeated along the several long lines attached to buoys parallel to each, other resembling row-like structure. On the coast, each blade of harvested kelp is loaded manually on the hanging lines inside the drying room assisted with solar drying and air

ventilation. Kelp blades are dried inside the drying chamber for approximately 48 hrs. to attain a final moisture content below 20% wet basis.

Fig. 2.2 Sugar kelp farmers lifting a section of sugar kelp line

Fig. 2.3 Sugar kelp farmers inspecting and washing a section of sugar kelp line with ocean water

Fig. 2.4 Cut and an uncut section of sugar kelp line

Fig 2.5 Sugar kelp totes unloading zone on the coast

Seaweeds are stored in the dark in low-temperature ocean water to extending their storage life with low mesophilic microbes and satisfactory textural conditions (Paull and Chen 2008) (Liot et al. 1993). Ninety percent of the total mass of fresh sugar kelp consists of water which makes it a lot harder to maintain its shelf life at room temperature. Therefore, fresh sugar kelp is processed using several methods including removal of water during drying (freeze-drying, sun drying and hot air drying) (Sappati et al. 2019), addition of starter culture and fermenting to below a pH of 4.6 (Hermann et al. 2015), hot water blanching followed by freezing, and dry salting and refrigerated storage (Perry et al. 2019) (Nayyar and Skonberg 2019) for extending shelf life as well as imparting certain physical and sensory characteristics.

Drying was one of the earliest techniques for food preservation and is governed by simultaneous heat and mass transfer effects on liquid-vapor phase change (Mujumdar and Passos 2000). At present, dried seaweeds are commercially produced under direct sunlight or by using a convective hot air dryer

based on propane or natural gas heating. Many areas, especially in the equatorial and subtropical zone of many developing countries in the Asia and Pacific region, use open drying systems to capture sunlight. However, sun drying has very limited application in the US state of Maine, due to lack of exposure to sunlight, warm dry air and clear weather conditions during the harvesting season of the year. In contrast, conventional convective dryers are energy-intensive but have proved to be better than sun drying in terms of nutrient retention and hygiene (Gallali et al. 2000; Murthy 2009). Hybrid drying technology such as solar-assisted with heat pumps (Fadhel et al. 2010), infrared-assisted (Fasina 2003) and microwave-assisted drying (Wang et al. 2004) is being promoted along with several non-thermal pretreatments including CO_2 drying, pulsed electric field (PEF), osmotic dehydration (OD) and ultrasound (Jin et al. 2017) to increase food safety and reduce the drying time and power consumption.

2.6. Drying Effects on the Chemical Composition, Physical and Thermal Properties

Fresh seaweeds contain very high moisture content (~75% - 90% w.b) and are highly perishable due to enzymatic deterioration, lipid oxidation, and microbial attack. The functional properties, bioactive compounds, volatile compounds (aroma, flavor) and antioxidant activity in the finished seaweed product are highly affected by the drying method applied, depending on the disintegration of the food matrix during the process (Costa et al. 2015; Dang et al. 2016; Gupta et al. 2011; Lann et al. 2008; Ling et al. 2015; Neoh et al. 2016; Tello-Ireland et al. 2011; Vairappan et al. 2014; Wong and Cheung 2001). The most widely used method of drying seaweeds is open sun drying. It is currently the main drying method used in many areas, especially in the equatorial and subtropical zone of many developing countries in Asia and the Pacific region. Sun-drying (SD) has very limited application in the US state of Maine, due to lack of exposure to sunlight, warm dry air and clear weather conditions during the harvesting season of the year. For improving drying conditions, alternate methods like vacuum freeze-drying (FD) (Chan et al. 1997; Le Lann et al. 2008), hot air oven drying (HAD) (Chan et al. 1997; Le Lann et al. 2008), hydrothermal drying (Rajauria et al. 2010), microwave drying (Dang et al. 2016) and dehumidified drying (Djaeni and Sari 2015) have been employed for drying several species of seaweeds. In brown alga *Hormosira banksii*, the levels of total phenolic compounds (TPC), total flavonoid content (TFC) and

proanthocyanidins were found to be higher as a result of vacuum drying, freeze-drying and dehumidified drying as compared to the sun and oven drying (Dang et al. 2016). Similarly, lower phytochemical contents were also reported in the case of sun-dried and sauna dried red seaweed *Kappaphycus alvarezii* (Ling et al. 2015). The chemical profile of seaweeds is also highly dependent on the season of harvest as the proximate components undergo massive fluctuation depending on the temperature, pH, and the salinity of water and other environmental changes (Astorga-España et al. 2015; Kumar et al. 2015; Schiener et al. 2015). HAD is the most common alternate method and is less expensive than FD, however it leads to reduction in heat-sensitive nutrients including vitamin C, antioxidants, phytochemicals, total flavonoid content and total phenolic content (Katsube et al. 2009; Sablani et al. 2011; Shi et al. 1999; Yang et al. 2010). HAD also causes alterations in textural quality due to case hardening, undesirable color change and undesirable levels of material shrinkage (Kurozawa et al. 2012; Russo et al. 2012). Even though FD can yield better quality products in terms of maintaining the integrity of nutrient, texture and flavor profile in the finished product, its high-energy requirement, and capital costs make it unprofitable for large scale operations (Wojdylo et al. 2016). Heat pump based (HPD) drying systems are novel and promising for drying heat-labile food products as the drying systems consume little energy, ensure product quality and allow de-coupled control of drying conditions (air temperature, relative humidity, air velocity) (Deng et al. 2011; Othman et al. 2011). In a study performed on squids, HPD systems proved to result in better myosin integrity and the highest volatile content as compared to HAD (Deng et al. 2015). Costa et al. 2015 reported that HPD systems have 40% lower drying time than conventional tray dryers (CTD) while dehydrating *Spirulina* at a temperature of 50ºC. In the same study, while drying at 50ºC, they also found the total phenolic compounds and total antioxidant activity in *Spirulina* to be 60% and 10% higher, respectively, in HPD as compared to CTD. These changes in the chemical profile due to seasonal variation and processing methods can have major impacts on the functional and bioactive properties of the dried seaweeds.

The drying process of seaweeds generally occurs under a falling rate period (Djaeni and Sari 2015; Gupta et al. 2011; Moreira et al. 2016; Sappati et al. 2017). During this period, the moisture present in the porous structure of food material undergoes simultaneous vapor diffusion through the void pores due to vapor pressure gradient and outward liquid movement in the capillaries (Geankoplis 1993). Within the same species of seaweed, the morphological and structural differences of the tissue, its age, size, growing environment and seasonality influence the total moisture content (MC) of the fresh seaweed (Clendenning 2009). The water activity (a_w) of a food is the ratio between the vapor pressure of the food to the saturated vapor pressure of pure water under the same temperature (Heldman 2013). It is the energy state of water in the food or simply a measure of the amount of free water available in the food. The a_w has been used as an important factor in predicting the growth of bacteria, yeasts, and molds and hence provides a good estimate for the shelf life, microbial stability, undesired bioreactions and physical properties of dried kelp. The shelf life of the dried product under given conditions can be increased by controlling its acidity level (pH) or the level of a_w or a suitable combination of the two (Singh and Shalini 2016). It has been reported that the limiting water activity for all life forms (bacteria, mold, yeast) of 0.6 is achieved in the final dried seaweed if its final moisture content is less than 20% on a dry basis (Stevenson et al. 2015).

Vitamin C consists of ascorbic acid and dehydroascorbic acid and is an important antioxidant found predominantly in fruits and vegetables. Some of the common seaweeds contain high amounts of Vitamin C such as *Eucheuma cottonii, Caulerpa lentillifera* and *Sargassum polycystum* (0.35 mg g^{-1} wet sample) (Matanjun et al. 2009). Pure ascorbic acid is stable in the presence of oxygen, light and room temperature for long durations. However, its stability is compromised in food systems and is vastly dependent on the storage conditions, pH, processing temperature, photo-oxidation and the presence of enzymes and metal ions (Moser and Bendich 1991). Several authors have investigated the role of air temperature in degradation kinetics of vitamin C in various foods (Erenturk et al. 2005; Goula and Adamopoulos 2006; Kaya et al. 2010).

Microscopic structural changes (pore formation) during drying as a result of moisture removal can be characterized macroscopically by structural properties such as true density, bulk density, porosity, and shrinkage. True density or particle density in the case of granular food is determined by the densities of its constituents and it decreases with an increase in the moisture content. The bulk density of granular food is measured experimentally depending on how the food is packed in the container. A vast amount of data has been presented on the structural properties of food (true density, bulk density, and porosity) with respect to its moisture content and temperature (Boukouvalas 2006a; Boukouvalas 2006b). It has been observed that the true density is always greater than the bulk density and lies in between the density of pure water and dry solids. The applied drying method and processing conditions can also highly influence the porosity of the dried product (Rahman 2003; Sablani and Rahman 2002). Choi and Okos have proposed empirical models based on the proximate composition of the food for predicting the thermal properties such as thermal conductivity (k), specific heat capacity (C), diffusivity (D) and bulk density (ρ) over a wide range of processing temperatures (Choi and Okos 1986). For instance, this model has been used to estimate the thermal properties of several different foods such as bakery products and carrot and meat alginate particles by considering all the major food components present including water, protein, fats, carbohydrate, fiber and ash (Sablani et al. 2002; Hassan and Ramaswamy 2011). However, the application of empirical modeling in the case of seaweeds has known limitations since the primary constituent groups in seaweeds consist of complex polysaccharides (alginates, cellulose, laminarin, mannitol and fucoidan) completely different from those in land-based products. Moreover, transport properties of food such as thermal conductivity, specific heat capacity and diffusivity are dependent on structural properties, especially porosity, and therefore the volume fraction of air should be considered while calculating the thermophysical properties from individual constituents (Rahman 2009). Alternatively, thermophysical properties (k, D) can be measured directly in a single experiment by the modified heat probe method using a dual needle probe (Carslaw and Jaeger 1959; Sweat 1974). In this method, a central heat source generates heat pulses, and the temperature response is monitored by the thermocouple placed parallel to the heating source at a fixed distance. The solution algorithm of this

method only accommodates conduction as the primary mode of heat transfer. Consequently, during the heating stage, a large temperature gradient can induce convective currents in low viscous foods and might change the food structure at the microscopic level, resulting in an inaccurate measurement. The pycnometer is currently used as the standard method for measuring the ρ of foods (Coimbra et al. 2006; Phinney et al. 2017; Rojas et al. 2013). The volume of the fixed mass of the food placed in the pycnometric flask is measured by displacing the non-wetting working liquid, indirectly allowing the density of the sample to be determined. The C of the various food samples including potato (Wand and Brennan 1995), chicken breast patties (Tang et al. 1991), lentil seeds (Sopade et al. 2006), and honey (Hua et al. 2011) has been measured in the past by the standard method of differential scanning calorimetry (DSC). DSC measures the specific heat by applying a constant rate of heating and measuring the temperature difference between the unit mass of the food material and the empty reference. Specific heat capacity can also be measured indirectly by measuring thermal conductivity, density, and thermal diffusivity by using equation (5.5) presented in this paper.

CHAPTER 3

EFFECT OF GLASS TRANSITION ON THE SHRINKAGE OF SUGAR KELP (*SACCHARINA LATISSIMA*) DURING HOT AIR CONVECTIVE DRYING

Nomenclature

a, Constant of Eq. (9)

A_o, Superficial area at instant t = 0 (m^2)

A_t, Superficial area at instant t (m^2)

$a_{w,}$ Water activity

b, Ratio of unfreezable water to the total solid content

B, Constant related to net heat of sorption

C, Constant related to monolayer heat of sorption

c, Constant of Eq. (9)

D_{ef}, Effective diffusion coefficient (m^2/s)

E, Molecular mass ratio of water to solids

k, Gordon Taylor parameter

K, Constant related to multilayer heat of sorption

L, Sample half thickness (m)

M_b, BET monolayer water content (kg H_2O/kg dry solids)

M_g, GAB monolayer water content (kg H_2O/kg dry solids)

$M_{w,}$ Moisture content of the sample (kg H_2O/kg dry solids)

MR, Moisture ratio

n, Coefficient of Suzuki model

t, Time period (s)

T_{gm}, Glass transition temperature of mixture (^oC)

T_{gs}, Glass transition temperature of solids (^oC)

T_{gw}, Glass transition temperature of pure water (^oC)

X_{eqb}, Equlibrium moisture content (kg H_2O/kg solids dry basis)

X_o, Initial moisture content (kg H_2O/kg solids dry basis)

X_s, Mass fraction of solid (kg solid/kg sample wet basis)

X_t, Moisture content (kg H_2O/kg solids dry basis) at any given time t

X_w, Mass fraction of water (kg H_2O/kg sample wet basis)

δ, Freezing point depression

β, Molar freezing point constant of water (kg K/kg mol.)

λ_w, Molecular mass of water (g/mol.)

ρ_0, Initial density (g/cm^3)

3.1. Introduction

Sugar kelp is highly perishable due to its high moisture content (~ 92% w.b). To extend its shelf life it is either conventionally sun-dried or hot air dried. Sun drying is one of the oldest techniques for food preservation, however, it is very slow, requires clear weather conditions and open drying may lead to pest, rodent and bird infestation (Ringeisen et al. 2014). Closed drying systems are energy-intensive but have proved to be better than sun drying in terms of nutrient retention and hygiene (Gallali et al. 2000; Murthy 2009). Drying is a phase change process governed by simultaneous heat and mass transfer (Mujumdar & Passos 2000). It removes free water and makes food less susceptible to microbial attack, lipid oxidation and enzymatic browning (Argyropoulos et al. 2011; Kurozawa et al. 2012; Zhang et al. 2006). The drying rate is highly dependent on several process parameters including drying temperature, moisture diffusion coefficient, the difference in the partial pressure of water vapor in food and the surroundings, material thickness, surface area and phase transition (from glassy to rubbery state) (Lewicki and Jakubczyk 2004; Van Arsdel 1973). Higher drying temperatures (50 - 80°C) induce faster drying rates, but also lead to reduction in heat-sensitive nutrients including vitamin C, antioxidants, phytochemicals, total flavonoid content and total phenolic content (Katsube et al. 2009; Sablani et al. 2011; Shi et al. 1999; Yang et al. 2010) and alterations in textural quality due to case hardening, undesirable color change and material shrinkage (Kurozawa et al. 2012; Russo et al. 2012). Removal of free water attached to the solid matrix of food creates void space and stress at the cellular level, leading to the material shrinkage. The material state (glassy or rubbery) can highly influence its shrinkage while drying and hence, affects the textural properties and shelf-life. Shelf-life of a food product depends on a number of intrinsic and extrinsic properties of the processed or stored product such as: water activity (available moisture), pH, available oxygen and nutrients, redox potential and glass transition temperature

(Buera et al. 2011; IFST 1993) and storage conditions such as temperature and relative humidity (Badii et al. 2014; Gonda et al. 2012).

Glass transition temperature (T_g) in a food corresponds to the thermodynamic unsteady state at which the amorphous form of water, bound to the solid food matrix, transitions between the rubber and glassy states (Rahman 2012; Roos 2010; Sablani et al. 2010) In high moisture foods like seaweed, the amorphous water behaves as in the rubber state at the beginning of drying, until the moisture and temperature drop sufficiently to reach the glass transition state. In the rubbery state, the molecular movement is much higher than that in the glassy state and volume reduction during shrinkage in this stage is directly proportional to the moisture loss (Karathanos et al. 1996). Further, shrinkage in the rubbery state of a food product is compensated with the amount of moisture loss during dehydration i.e. volume of moisture loss is equivalent to the change in material volume (Bhandari and Howes 1999; Mayor and Sereno 2004). Below the glass transition temperature, the molecular diffusivity decreases significantly due to high viscosity (in the range of 10^{12}-10^{13} Pa s) that restricts the movement of water and other organic components responsible for a rigid product (Bhandari and Howes 1999; Mayor and Sereno 2004). Highly concentrated water in the glassy state is dynamically immobile and does not support or become involved in any chemical reactions. Thus, the glass transition temperature can be taken as a reference temperature to assess the quality, safety and stability attributes of products during storage and to determine shelf-life.

Shrinkage while drying reduces the path length for moisture diffusion and results in lower moisture diffusion coefficients as compared to models that assume no shrinkage. Several authors have compared models with and without shrinkage and found a significant difference between moisture diffusion coefficients. In cases of papaya (Kurozawa et al. 2012), fish muscle (Park 1998) and carrot (Zielinska and Markowski 2010) the moisture diffusion coefficients were (18.75% - 31.81%), (42% - 43.5%) and (15.68% - 77.5%) lower, respectively, as compared to models that assumed no shrinkage, depending on the air-drying temperature and velocity. However, in this study shrinkage is not considered

while solving Fick's diffusion equation because sugar kelp's thickness is very small (~ 2.5mm) as compared to its superficial area dimensions.

This work aims to evaluate the effect of glass transition phenomenon on shrinkage of sugar kelp by achieving these specific objectives: 1) Determine the moisture sorption isotherm, 2) Study the glass transition temperature, 3) Model drying kinetics, and 4) Investigate the application of dehumidification at lower temperatures for decreasing drying time.

3.2. Materials and Methods

3.2.1. Materials

Fresh sugar kelp (*Saccharina latissima*) grown in Damariscotta bay, Maine, was donated by Maine Fresh Sea Farms, Walpole, ME, USA. The holdfasts at the end were cut off and the blade and stipe parts were washed with running fresh water to remove the attached biofouling and salts. The seaweed samples were kept at -20^{o}C for 24 hours before freeze-drying (Virtis Ultra 35EL, SP scientific, Warminster, PA, USA) at different cycles of temperature (-20^{o}C, -10^{o}C, 0^{o}C, 10^{o}C, and 25^{o}C) for 4 hours each with vacuum maintained at 20 Pa. The initial moisture content of fresh sugar kelp was observed to be 0.924 kg H_2O/kg sample (wet basis) before freeze-drying. After a 20-hour cycle of freeze-drying, the dried sugar kelp was pulverized to a fine powder using mortar and pestle and stored in an opaque brown container at 4^{o}C until further analysis. The moisture content of the freeze-dried sample was 0.0592 kg H_2O/kg solids (dry basis).

3.2.2 Proximate Analysis

The moisture content of freeze-dried sugar kelp samples was measured using a gravimetric method. One gram of sample in triplicates was dried in an oven (VWR, VWR International, Radnor, PA, USA) at 105 ^{o}C until there was no further change in weight +/- 0.001 g (AOAC 1999). For measuring ash content, 0.5g of sample in triplicates was kept at 550 ^{o}C in a muffle furnace (Thermolyne Model F-

A1730, Dubuque, IA, USA) for 6h (AOAC 1999). Total nitrogen content was determined using a dry combustion analyzer (TruMac CNS, LECO Corporation, MI, USA) (AOAC 1990). The total crude protein was calculated using an average nitrogen-to-protein conversion factor of 5.3 for sugar kelp (Schiener et al. 2015). The fat content of the sample was measured using the acid-hydrolysis method for seafood (AOAC 2005). The total carbohydrate content was calculated using the difference method (Merill and Watt 1973). The total soluble solids (TSS) of the supernatant was measured using refractive index (Palette Digital Refractometers 0-45^{o}, ATAGO U.S.A Inc., WA, USA) on a sample prepared by taking 0.5 g of sample homogenized (Polytron homogenizer, Brinkmann Instruments, Westbury, NY) in 4.5 mL of water for 2 min and centrifuged at 7000 x g for 10 min.

3.2.3 Moisture Sorption Isotherm

For estimating the moisture sorption isotherm, the freeze-dried sugar kelp powder was kept in airtight glass jars in the presence of saturated salt solutions with known water activities at room temperature ~ 22°C. Triplicates of 1 gram freeze-dried samples were kept for three weeks to attain equilibrium in airtight bormioli rocco glass jars (500 ml) (Bormioli Rocco North America, NY, USA) in the presence of a salt solution (150 mL), with thymol (10 g) added to avoid microbial growth. The salts used for this experiment were: LiCl, CH_3COOK, $MgCl_2.6H_2O$, K_2CO_3, $MgNO_3.6H_2O$, NaCl, NH_4Cl, KCl and KNO_3, with equilibrium water activities of: 0.113, 0.225, 0.328, 0.432, 0.529, 0.754, 0.792, 0.851 and 0.946, respectively (Greenspan 1977). Change in weight of samples was recorded each day until there was no weight variation of +/- 0.0005 g. Final equilibrium moisture content (EMC) in dry basis was measured by the change in final and initial weight.

3.2.3.1 Water Sorption Isotherm Modeling

Water sorption isotherms of sugar kelp powder were modeled using the BET (Brunauer–Emmett–Teller) and GAB (Guggenheim–Anderson–de Boer) models. The BET model provides the best fit for water activity in the range of (0.05-0.45) (Rahman 1995). The GAB model can be fitted for a vast range of water activity up to 0.9.

Eq. (3.1) represents the BET model

$$M_w = \frac{M_b B a_w}{[(1-a_w)(1+(B-1)a_w)]} \tag{3.1}$$

Eq. (3.2) represents the GAB model

$$M_w = \frac{M_g C K a_w}{[(1-Ka_w)(1-Ka_w+CKa_w)]} \tag{3.2}$$

GAB is an extended version of the BET model. The parameter K compensates for the modified properties in the multilayer region and bulk liquid properties. Non-linear optimization technique was used for estimating the BET and GAB model constants.

3.2.4 Glass Transition Temperature

Differential scanning calorimetry (DSC Q2000, TA instrument, New Castle, DE, USA) was performed on the freeze-dried sugar kelp to obtain thermal transition curves of heat flow with respect to temperature. Triplicates of samples having moisture content in the range of 0.05 to 3 kg H_2O/kg dry solids were used for this experiment. The samples (4-10mg) were placed and sealed in standard aluminum hermetic pans. An empty aluminum pan was used as the reference. The instrument was calibrated using indium fusion. The samples were cooled to -80^{o}C from room temperature (22^{o}C) using a mechanical cooling unit using ramp function and allowed to attain equilibrium for 10 minutes. Initially, the samples with low moisture (< 0.3 kg H_2O/kg solids) were scanned through a temperature range of -80 to 100^{o}C at 2, 5 and 10 ^{o}C/min scan rate. The scan rate of 2 ^{o}C/min was chosen for future analyses. Glass transition is generally indicated by the vertical shift in the thermogram. TA universal analysis software was used for analyzing the thermogram for the arrival, mid-point, and end of the glass transition temperature. The thermogram for samples with high moisture content (0.3 to 3 kg H_2O/kg solids) also showed the melting curve. The enthalpy of melting (ΔH) was obtained by computing the area under the melting curve. The endpoint of the freezing curve (T_m) was given by the intersecting point of the baseline with the given

melting endotherm. The freezing point (T_f) of the high moisture samples was determined by making a tangent to the left side of the endotherm (**Fig. 3.5**). During the DSC scan, high moisture content samples were subjected to annealing at (T_m - 1) for 30 minutes (Bai et al. 2001; Syamaladevi 2009). After annealing, the freeze-dried sample was cooled to -80 ^oC from (T_m - 1) using ramp function and again heated from -80^oC to 100^oC at 5 ^oC/min. The glass transition phenomenon is influenced by the amount of moisture in the amorphous food system and is most commonly modeled using the Gordon and Taylor equation (1952) as given below:

Eq. (3.3) represents the Gordon Taylor equation

$$T_{gm} = \frac{X_s T_{gs} + kX_w T_{gw}}{X_s + kX_w} \tag{3.3}$$

T_{gm}, T_{gs} and T_{gw} are the glass transition temperature of the mixture, dry solids and pure water, respectively. The glass transition T_{gw} of pure water was considered to be -135^oC (Johary et al. 1987).

Freezing point depression is a colligative property dependent on the concentration of solute. Freezing lines for ideal and dilute solutions are generally modeled using the Clausius-Clapeyron equation and is expressed in the given form:

Eq. (3.4) represents the Clausius-Clapeyron equation

$$\delta = \frac{-\beta}{\lambda_w} \ln\left[\frac{1 - X_s}{1 - X_s + EX_s}\right] \tag{3.4}$$

Due to its limited application, an extended form of the Clausius-Clapeyron equation was developed by Chen (1986). A new parameter b, which is the ratio of unfreezable water to the solid content, was introduced and is commonly used for modeling freezing point depression in food systems. Chen's model is expressed as given below (5).

Eq. (3.5) represents the Chen's equation

$$\delta = \frac{-\beta}{\lambda_w} \ln\left[\frac{1 - X_s - bX_s}{1 - X_s - bX_s + EX_s}\right] \tag{3.5}$$

The parameters b and E are estimated using a non-linear optimization technique in Microsoft Excel.

3.2.5 Drying Kinetics

For drying kinetics of fresh sugar kelp, samples of approximately 50g (blades and stipes) were dried on perforated pans at an air temperature of either 40°C or 70°C with relative humidity levels of 25%, 50% and 80% and air velocity of 10.0 m/s using convective dryer (Cincinnati sub-zero, CSG, OH, USA). The drying system consisted of automated air circulation, temperature and humidity control. During drying, the sample was weighed using a precision balance with a resolution of 0.01 g at regular intervals until no further change in weight was observed. Several authors have reported that the drying process of leafy plants occurs under the falling rate period (Demir et al. 2004; Doymaz 2006; Lebert et al. 1992; Temple and Van Boxtel 1999). In this period, moisture transfer in such porous food material involves a complex mechanism which undergoes simultaneous vapor diffusion in the void pores due to the vapor pressure gradient and the outward liquid movement due to capillary action (Geankoplis 1993). The contribution of each mechanism to overall moisture diffusion is hard to estimate and therefore an average moisture diffusivity is obtained by the theoretical approach of solving Fick's second law of diffusion (Datta 2007a and Datta 2007b). This approach has been applied for the modeling drying process of several food products (Djaeni and Sari 2015; Kurozawa et al. 2012; Pancharia et al. 2002). It is a second-order partial differential equation that describes the heat and mass transfer in a medium as a function of position and time (Welty et al. 2008). It is also applicable either in the glassy or rubbery state. Near the transition state, the fluid behaves in a non-Fickian way (Singh et al. 2004; Takhar 2008) due to the additional time-dependent stress term. In this case, the more general form of Maxwell-Stefan equations are applicable (Taylor & Krishna 1993).

Fick's second law is considered in this study to model thin layer liquid-controlled diffusion as the drying occurred under the falling rate period and the shrinkage in the thickness of sugar kelp was infinitesimally small as compared to its superficial area. The solution of Fick's law for planar geometry at constant temperature and diffusion along the thickness is an infinite series equation and is given below (Crank 1975).

$$MR = \left[\frac{X_t - X_{eqb}}{X_o - X_{eqb}}\right] = \left\{\frac{8}{\pi^2}\sum_{n=0}^{\infty}\frac{1}{(2n+1)}\exp\left[-(2n+1)^2\frac{\pi^2 D_{ef}}{4L^2}t\right]\right\} \quad (3.6)$$

Expanding the above equation and neglecting higher-order terms

For n = 0, we obtain the following equation

$$MR = \left[\frac{X_t - X_{eqb}}{X_o - X_{eqb}}\right] = \left\{\frac{8}{\pi^2}\exp\left[-\frac{\pi^2 D_{ef}}{4L^2}t\right]\right\} \quad (3.7)$$

Taking natural logarithm on both sides gives an equation of a straight line

$$\ln(MR) = \ln\left[\frac{X_t - X_{eqb}}{X_o - X_{eqb}}\right] = \ln\frac{8}{\pi^2} - \frac{\pi^2 D_{ef}}{4L^2}t \quad (3.8)$$

The natural log of the moisture ratio (ln MR) is plotted on the Y-axis against time on the X-axis. Effective diffusivity (D_{ef}) is calculated from the slope of the above obtained graph.

The drying rate was estimated by the empirical model approach using Newton (Vega et al. 2007), Page and Henderson & Pabis (Doymaz 2007) kinetic models, as shown in **Table 3.1**. Where MR is the dimensionless moisture ratio; k is the drying rate constant (s^{-1}); a is Henderson & Pabis model constant and t is drying time (s). Model constants k, n and a are estimated using non-linear optimization in Microsoft Excel, 2016. The empirical approach is easy to handle compared to the analytical approach due to lower computational requirements and its representation of pure kinetics of the physical process. The

disadvantage of using the empirical model over the analytical approach is that it doesn't provide necessary information regarding the state variables when the process control changes, and it is applicable only for particular processing conditions.

Table 3.1. Models applied for estimating drying kinetics

Drying Kinetic Model	
Newton	$MR = \exp(-kt)$
Page	$MR = \exp(-kt^n)$
Henderson & Pabis	$MR = a\exp(-kt)$

3.2.6 Shrinkage

Triplicates of circular (2-inch diameter φ) shaped freshly harvested sugar kelp blades were dried at temperatures of 40°C and 70°C in an oven (VWR, VWR International, Radnor, PA, USA). Each sample was placed on a standard white background of size 10 x 10 cm^2 and was photographed using a digital camera Nikon-3300 DSLR (Nikon Inc., Melville, NY, USA) at regular intervals. For studying the plasticization effect of water during shrinkage, an image processing algorithm based on pixel thresholding was developed in MATLAB. Superficial area of the image was calculated based on the following steps: (1) conversion of color image to binary (black & white) image (**Fig. 3.1a**, and **3.1b**), (2) computing the total pixels in the white region of the image, and (3) comparing the number of pixels in white region with the pixels in the standard white background. Shrinkage data of the samples were fitted to the model proposed by Suzuki et al. (1976). This model correlates the relative superficial area reduction with the sample moisture content measured on a dry basis.

$$\frac{A_t}{A_o} = [a X_t + c]^n \tag{3.9}$$

$$a = \frac{\rho_o}{(X_0 + 1)} \tag{3.10}$$

$$c = 1 + a - \rho_o \tag{3.11}$$

The model constant n is the coefficient of shrinkage and it is estimated using non-linear optimization technique in Microsoft Excel, 2016.

3.2.7 Statistical Analysis

All the models fitted to the experimental data were evaluated using the determination coefficient (R^2), Sum squared error (SSE) and Root mean squared error (RMSE).

$$SSE = \frac{1}{N}\sum_{i=1}^{N}[X_{\text{mod}} - X_{\text{exp}}]^2 \tag{3.12}$$

$$RMSE = \left[\frac{1}{N}\sum_{i=1}^{N}[X_{\text{mod}} - X_{\text{exp}}]^2\right]^{1/2} \tag{3.13}$$

Where, N is sample size or no. of data points

Fig. 3.1. Shrinkage analysis of oven-dried sugar kelp (2-inch diameter). Superficial area of dried kelp was calculated based on an image processing algorithm developed in MATLAB. a) Conversion of color image, and b) binary image using pixel thresholding algorithm.

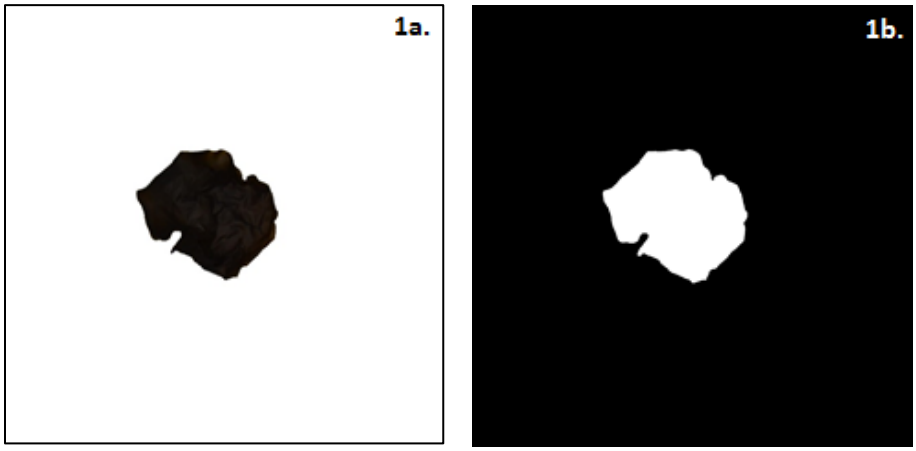

3.3 Results and Discussion

3.3.1 Proximate Analysis

Proximate analysis data of freeze-dried sugar kelp are summarized in **Table 3.2**. Carbohydrate content was highest (53.35 %) followed by crude protein (6.87 %) and fat (1.98 %) in the freeze-dried samples. Total soluble solids (TSS) of the samples were found to be 50.33 ^{o}Bx. TSS showed a linear relationship with the moisture content of the sample and can be given as Y = -58.766 X + 54.503, where Y is the TSS in (^{o}Bx) and X is the moisture content of the sample (kg H_2O / kg sample) with correlation coefficient (R^2 = 0.994) (**Fig 3.2**). The composition data of freeze-dried samples were compared with the composition of fresh sugar kelp reported by Schiener et al. (2015) (**Table 3.2**). The freeze-dried data showed comparable composition to the fresh sugar kelp.

Table 3.2. Proximate Composition

Analysis	Freeze-dried sugar kelp	Fresh sugar kelp (Schiener et al. 2015)
Moisture	5.58 ± 0.015% (wb)	84.90±2.9% (wb)
Crude Fat	1.98±0.053% (db)	N.A
Crude Protein	6.87±0.040% (db)	7.10±1.7% (db)
Ash	37.79±0.202% (db)	31.70±7.6% (db)
Carbohydrates	53.36±0.295% (db)	63.10±11.4% (db)
TSS	50.33±0.577 (^{o}Brix)	N.A

The mean values and standard deviations are for three replicates but crude protein. Duplicate analysis was performed for crude protein. db: dry basis; wb: wet basis

N.A = Not Available

3.3.2 Moisture Sorption Isotherm

The moisture sorption isotherm (MSI) of freeze-dried sugar kelp at 20^{o}C exhibited a typical type III behavior based on the Van der Waal's classification (Brunauer et al. 1940) (**Fig. 3.3**). The sugar content of freeze-dried sugar kelp in terms of TSS was 50.33 ^{o}Bx. The two major carbohydrates present in sugar kelp are alginates and mannitol (Scheiner et al. 2015). Alginates are extremely hygroscopic due to their ability to form hydrogen bonds with water molecule, whereas mannitol is low hygroscopic in nature (Tiwari & Troy 2015). A steep increase in the absorption of moisture by powdered sugar kelp was observed when it was subjected to water activity higher than 0.543. This might be due to the increase of

interaction via hydrogen bonds between water, hydroxyl and carboxyl groups of sugar resulting in solubilizing the high amount of sugars and polysaccharides present in sugar kelp at high water activity. This is commonly observed in seaweeds which contains high amount of sugars and polysaccharides such as *Gelidium sesquipedale* (Ait-Mohamed et al. 2005) *Gracilaria chilensis* (Lemus et al. 2008), *Bifurcaria bifurcata* (Moreira et al. 2016a), *Fucus vesiculosus* (Moreira et al. 2016b) and *Macrocystis Pyrifera* (Vega-Galvez et al. 2008). These sugars exist in amorphous forms and are hygroscopic at low moisture. They absorb relatively low moisture at lower humidity (< 50%) levels but show a steep rise in absorbed moisture at higher humidity (> 50%) due to sugar dissolution (Hubinger et al. 1992; Moraga G. et al. 2006; Tsami et al. 1990; Vasquez G. et al. 1999).

Fig. 3.2. Plot of experimental TSS (^{o}Bx) vs moisture content (kg H_2O/ kg wet sample).

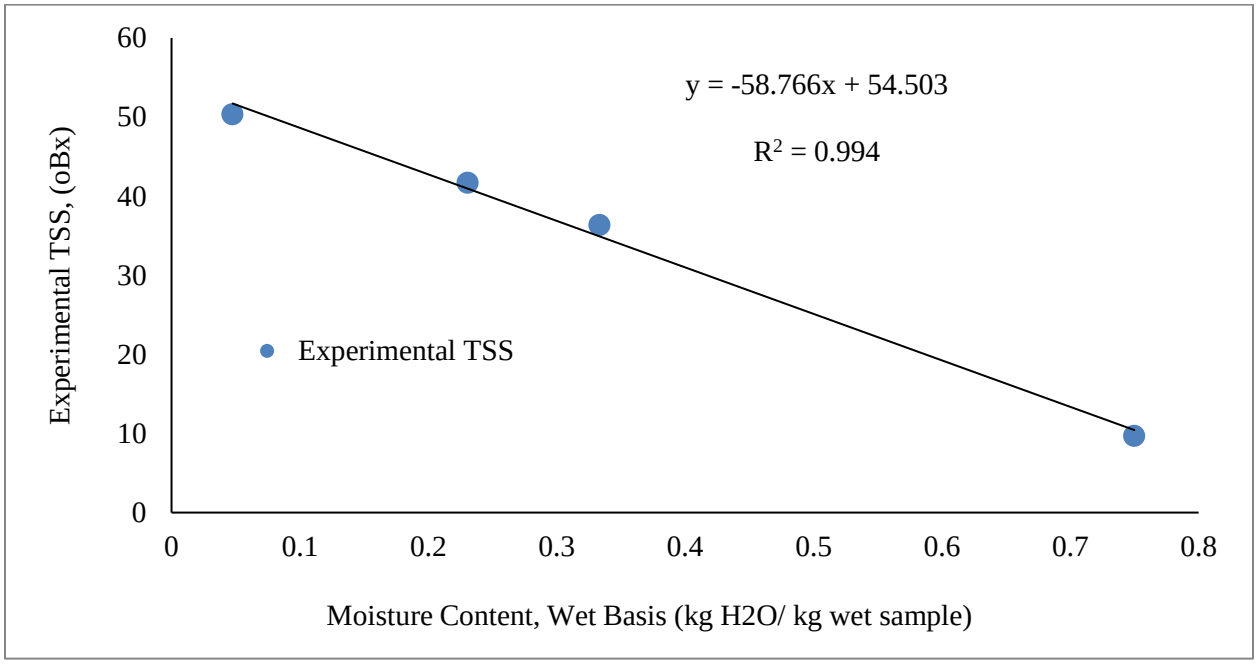

Fig. 3.3. Moisture sorption isotherm of freeze-dried sugar kelp at 20°C

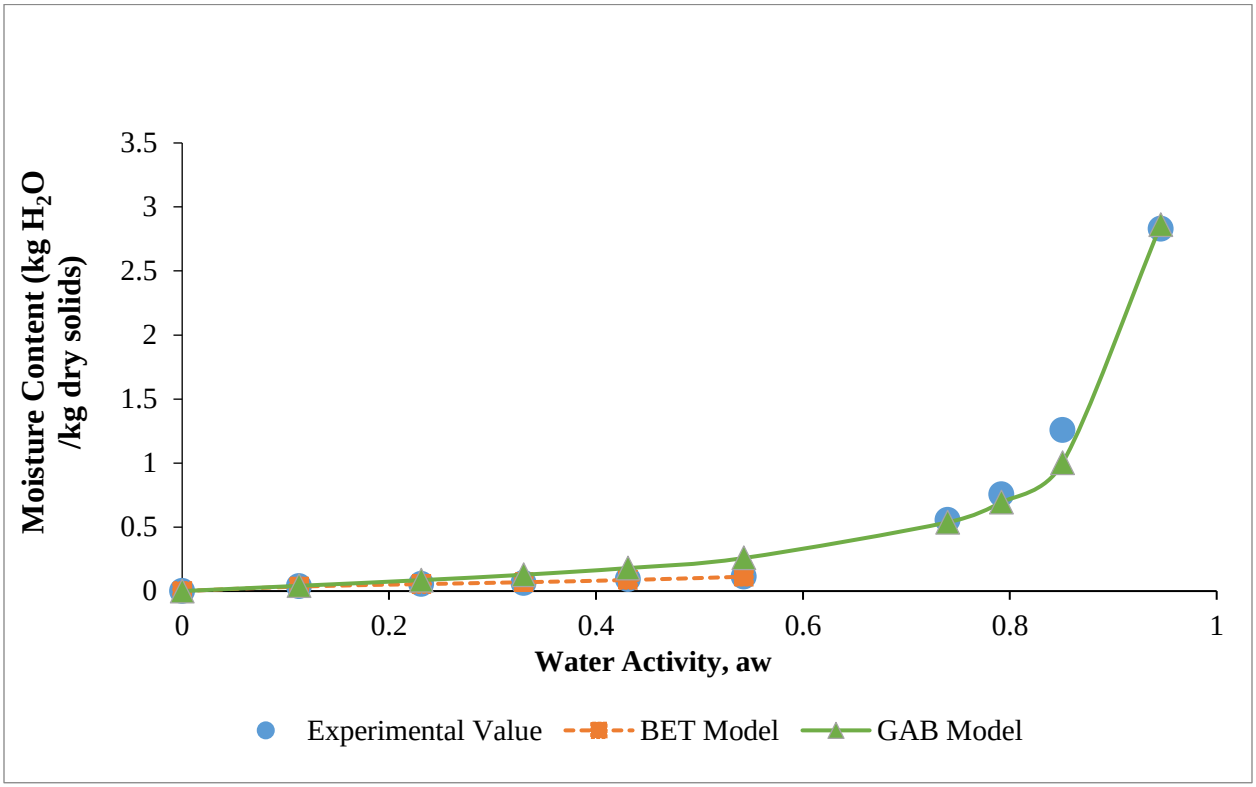

The MSI was fitted to the BET and GAB models. The BET model is a monolayer based model and considers the amount of water required to cover the entire surface of food with a single layer of water molecules. It is applicable in low water activity range (0.05 – 0.45) (Rahman 1995). However, the BET equation becomes insignificant at higher water activity level when the dissolution of sugars and polysaccharides become more significant than surface sorption. The GAB model is an extended version of the BET model which considers moisture sorption in multilayer and is applicable over a wide range of water activity (0.05 – 0.9).

The model coefficients of the BET and GAB models obtained using non-linear optimization are listed in **Table 3.3**. Based on BET constant C, the following isotherm in the lower water activity levels can be classified as Type II as the calculated constant C is greater than 2 (Brunauer et al. 1940). Sugar kelp, being a brown seaweed, contains high amounts of polysaccharides and showed a similar trend as

observed for red seaweed *Gracilaria* (Lemus et al. 2008). The goodness of fit of the GAB and BET models were evaluated using R^2, SSE and RMSE (**Table 3.3**).

Table 3.3. Model constants and fitness statistics

Model	Fresh-red alga (*Gracilaria*)[a]	Freeze-dried sugar kelp
BET Model		
M_b	0.071 kg H_2O/kg dry solids	0.055 kg H_2O/kg dry solids
B	25.843	10.18
R^2	0.998	0.990
SSE	0.0011	.00007
RMSE	0.0979	0.002
GAB Model		
M_g	N.A	0.162 kg H_2O/kg dry solids
C	N.A	2.14
K	N.A	0.998
R^2	N.A	0.986
SSE	N.A	0.104
RMSE	N.A	0.102

[a] Coefficients from (Lemus et al. 2008)

N.A = Not Available

3.3.3 Glass Transition

The glass transition curves of sugar kelp powders were obtained from a differential scanning calorimeter (DSC). Thermograms of prepared samples having a moisture content of less than 0.3 kg H_2O/ kg dry solids revealed the existence of one glass transition with no ice formation (**Fig. 3.4a**). Similar behavior was earlier reported for terrestrially grown foods including strawberry (Roos 1987), pineapple (Telis and Sobral 2001), tomato (Telis and Sobral 2002), kiwi (Wang et al. 2008b), raspberry (Syamaladevi et al. 2009) and rice (Sablani et al. 2009). The sugar kelp samples were scanned at three different scanning rates of 2°C/min, 5°C/min and 10°C/min. The scan rates of 5°C/min and 10°C/min have been commonly used for observing the glass transition in foods (Rahman 2004; Syamaladevi et al. 2009; Sablani et al. 2009; Wang et al. 2008b). In this study a scan rate of 2°C/min was considered optimal since the glass transition was more clearly observed at this rate compared to scan rates of 5°C/min and 10°C/min. This can be explained by a non-uniform heating of samples resulting from delayed temperature

response between the heater and the samples (Tang et al. 1991). The glass transition for a sample of moisture content 0.15 kg H_2O/ kg dry solids at the three scan rates (2°C/min, 5°C/min and 10°C/min) is shown in **Fig. 3.4**. Thermograms of prepared sugar kelp samples of different moisture content scanned at 2°C/min are shown in **Fig. 3.5**.

The glass transition is primarily a function of moisture content and molecular weight of the solids present in the sample and occurs over a wide range of temperatures (Rahman 2006). The initial T_{gi}, mid-point T_{gm}, and end-point T_{gf} of glass transitions are shown in **Table 3.4**. The plasticizing effect of water due to the water – carbohydrate interactions via hydrogen bonding and the changes in the free matrix volume were observed as the glass transition decreased from 2.01°C to -49.84°C as the moisture content was increased from 0.05 to 0.5 kg H_2O/ kg dry solids. The TSS of sugar kelp decreased linearly from 50.33 °Bx to 36.33 °Bx when the moisture content was increased from 0.05 to 0.5 kg H_2O/ kg dry solids, this suggests that the T_g of sugar kelp is associated with the soluble solid fraction present in the aqueous phase (Moraga et al. 2006; Zhao et al. 2015). Sugar kelp contains a high amount of total soluble solids in the form of water-soluble carbohydrates such as sodium alginate, laminarin and mannitol (Zvyagintsevaa et al. 1999). The glass transition lines were fitted non-linearly in the Gordon-Taylor (GT) equation (Gordon and Taylor 1952). The model constants in the GT model were T_{gs} = 30.44°C and k = 1.97. The glass transition of solids (T_{gs}) 30.44°C computed from GT model is close to the initial T_{gi} 34.16°C of pure solids.

Fig. 3.4. Glass transition curves of freeze-dried sugar kelp for moisture content (0.15 kg H_2O/ kg dry solids) determined by a differential scanning calorimeter at scan rate of (a) 2°C/min, (b) 5°C/min and (c) 10°C/min

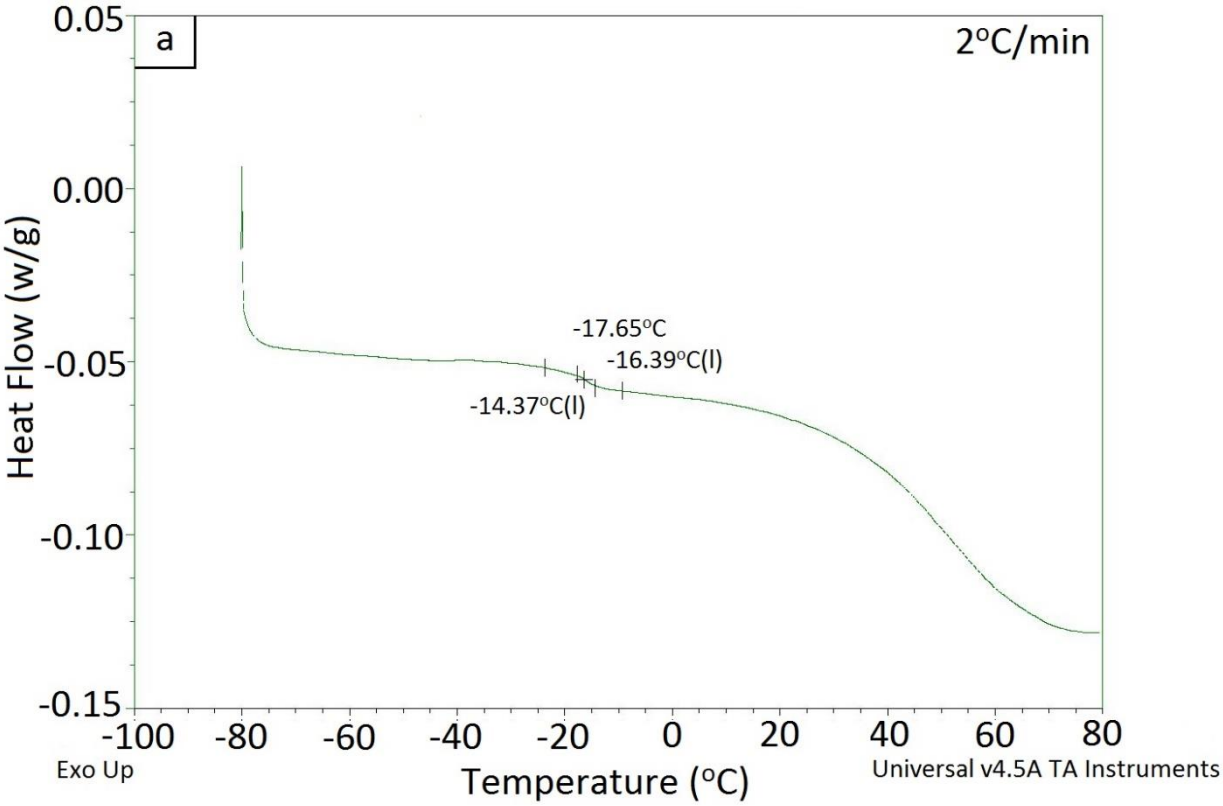

Fig. 3.4 continued

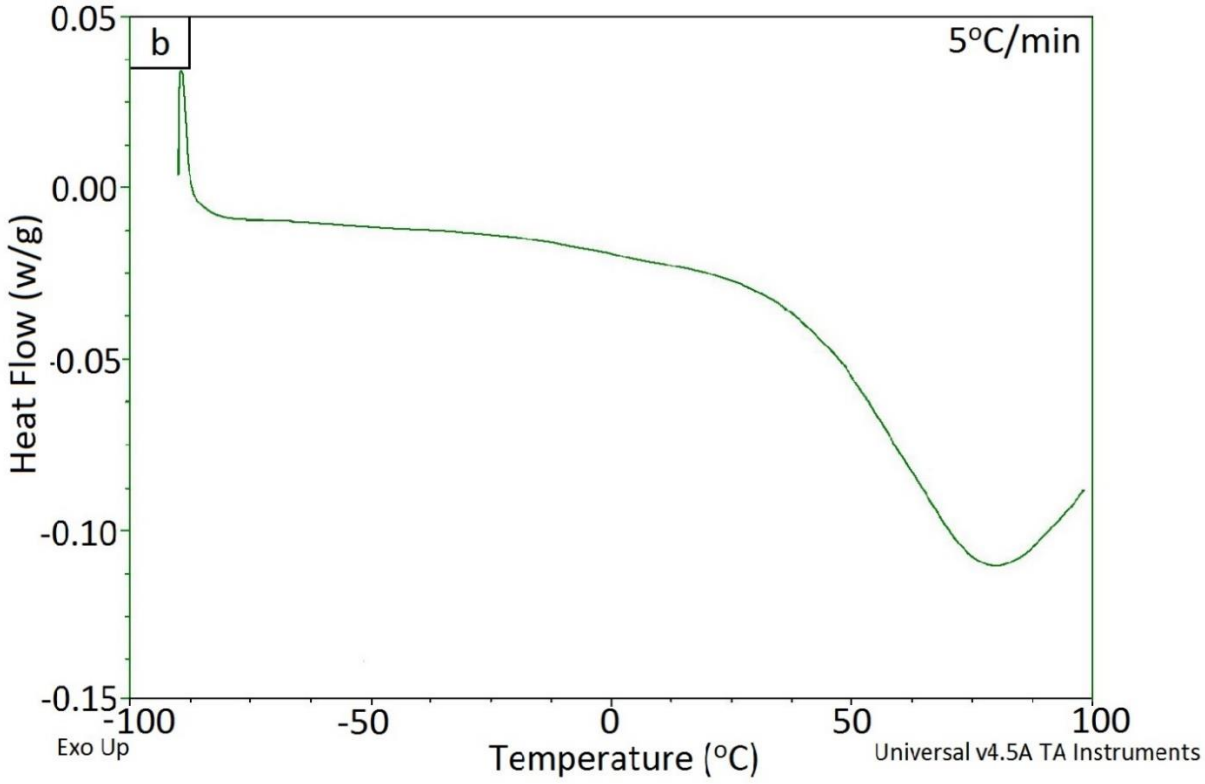

Table 3.4. Glass transition temperature of sugar kelp (at a scan rate of 2°C/min, no ice formation)

X, (kg H_2O/kg dry solids)	X_s, (kg solids/kg wet sample)	T_{gi}, (°C)	T_{gm}, (°C)	T_{gf}, (°C)
0	1.000	34.16 ± 2.317	47.02 ± 2.137	65.33 ± 4.172
0.05	0.952	00.96 ± 0.586	2.01 ± 0.303	03.14 ± 0.440
0.1	0.909	-04.92 ± 0.566	-06.78 ± 0.737	-07.84 ± 0.718
0.15	0.870	-17.31 ± 0.722	-15.74 ± 0.676	-13.71 ± 0.574
0.2	0.833	-18.79 ± 0.540	-17.28 ± 0.339	-15.69 ± 1.196
0.25	0.800	-20.02 ± 0.382	-19.12 ± 0.446	-18.00 ± 0.629

standard deviation of three replicates

Fig. 3.5. Thermograms of freeze-dried sugar kelp at moisture contents (a) 0.05, 0.10 and 0.15 kg H_2O/ kg dry solids, and (b) 0.20, 0.25 and 0.30 kg H_2O/ kg dry solids. The thermograms were generated using a Differential Scanning Calorimeter at a scan rate of 2°C/min

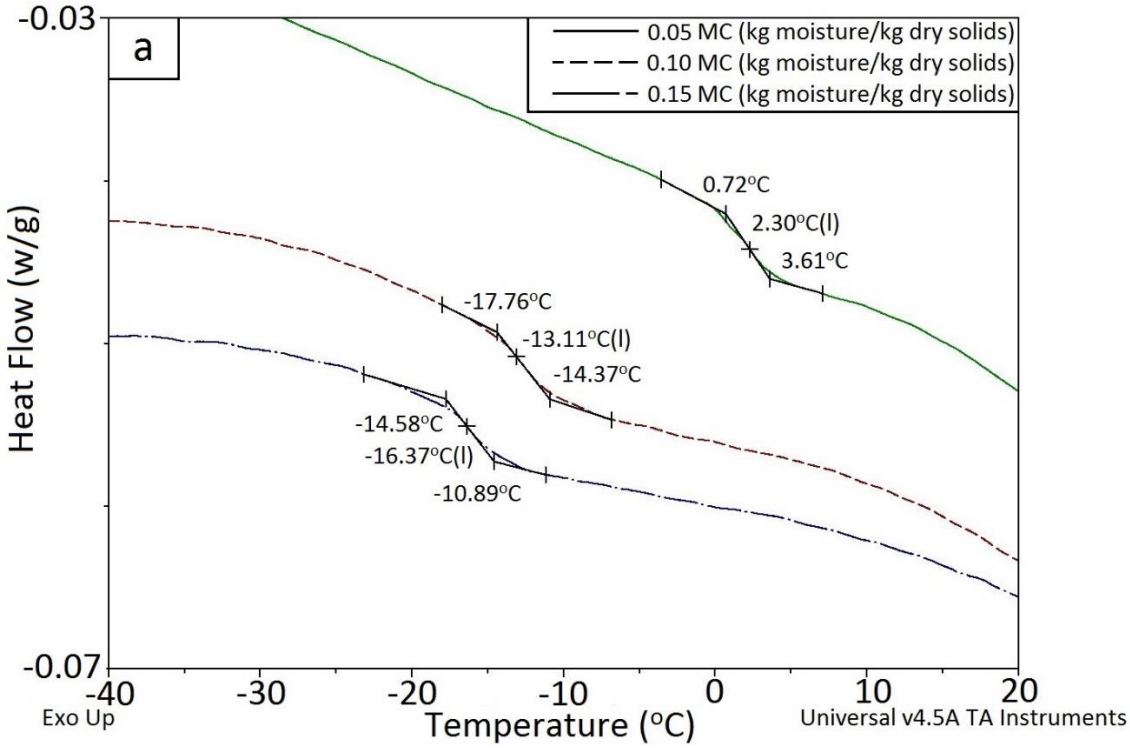

Fig. 3.5 continued

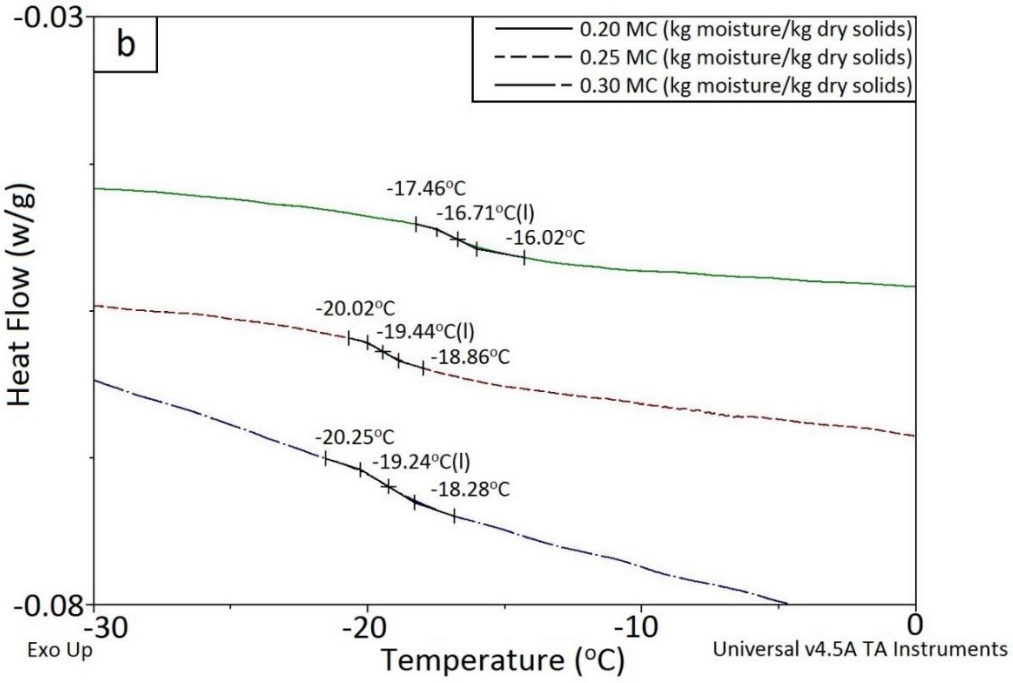

The glass transition of pure solids can be highly dependent on the chemical composition of the sugar kelp, especially the carbohydrates which comprise 53.36% of dry matter. The carbohydrates in sugar kelp exist in two forms: structural (alginates and cellulose) and storage (laminarin and mannitol) and vary depending on the harvest season and environmental conditions (Scheiner et al. 2015). Average values for alginate (28.5±3.9 % d.b), cellulose (11±1.4 % d.b), laminarin (8.2±5.3 % d.b) and mannitol (18.6±4.7 % d.b) in sugar kelp was reported by Scheiner et al. (2015). Each component of carbohydrate present in sugar kelp exhibits a different T_g in its pure state. Cellulose, sodium alginate and D-mannitol exhibit T_g of 220 °C (Szcześniak et al. 2008), 119 °C (Miura et al. 1999) and 11°C (Zhu et al. 2015), respectively. Several authors have shown that in binary polymer blends the T_g of the blend lies generally in between the T_g of pure components (Kalogeras and Brostow 2009; Kumar Naidu et al. 2005). The blending of carbohydrates may be a possible explanation in the case of sugar kelp as the T_{gs} of whole solids of sugar kelp (47.02 °C) lies in between of mannitol (11 °C) and alginate (119 °C). However, extrapolating this concept to more complex food systems would be oversimplified as interactions among the several different food components would likely deviate from the normal binary system behavior.

Sugar kelp samples of high moisture (> 0.3 kg H_2O/ kg dry solids) exhibited ice formation during DSC scans(**Fig. 3.6**). The prepared samples were initially scanned at a rate of 5°C/min from -80 °C to 22 °C without annealing for estimating the end-point of freezing point (T_m). Glass transitions were not detected for samples having moisture content higher than 0.5 H_2O/ kg dry solids as the transition endotherm was beyond the scanning range. For maximum freeze concentrated solid and ice formation the samples were scanned with annealing for 30 min at (T_m - 1) (**Fig. 3.6**). Depression in freezing point is a colligative property and depends on the concentration of total soluble solids and molecular weight of the solids. The initial freezing point (T_f) and T_m decreased from -3.4°C to -30.87°C and -17.78°C to -37.533°C, respectively as the moisture content was decreased from 3 to 0.3 kg H_2O/ kg dry solids due to the increase in the TSS from 41.67 °Bx to 9.67 °Bx. The freezing point of sugar kelp was found to be linearly dependent on the TSS of the samples and can be expressed as $Y = -0.8603 X + 6.2965$, where Y is the freezing point (°C) and X is the TSS (°Bx) and) with correlation coefficient ($R^2 = 0.984$). Several authors have reported the linear correlation between the depression of freezing point and the TSS of the samples (Wang et al. 2003; Zhao et al. 2015). The enthalpy of the ice melting endotherm (ΔH) was plotted linearly against the moisture content of the sample on a dry basis for determining the unfreezable water in sugar kelp. The unfreezable water determined by extending the line to zero ice melting enthalpy was 0.06 kg H_2O/ kg dry solids (**Fig. 3.7**). The initial freezing point (T_f), end-point of freezing (T_m) and ice melting enthalpy (ΔH) determined from the obtained thermograms are listed in **Table 3.5**.

Table 3.5. Initial freezing point (T_f), end-point of freezing (T_m) and ice melting enthalpy (ΔH) of Sugar kelp (with formation of ice and scan rate of 5 ^oC/min)

X, (kg H_2O/kg dry solids)	T_{gm},(^oC)	T_f, (^oC)	T_m, (^oC)	ΔH, (kJ/kg)
0.3	-20.30 ± 0.115[a]	-30.88 ± 0.632[a]	-37.53 ± 0.240[a]	00.609 ± 0.035[b]
0.5	-49.84 ± 4.970	-22.68 ± 0.542	-30.22 ± 0.387	011.74 ± 1.796
0.75	N.D	-17.72 ± 2.820	-25.12 ± 3.080	038.39 ± 20.43
1	N.D	-14.07 ± 0.684	-21.18 ± 1.390	084.71 ± 3.670
1.5	N.D	-11.10 ± 1.045	-18.17 ± 0.343	126.40 ± 6.500
2.5	N.D	-04.47 ± 0.517	-17.63 ± 0.145	148.83 ± 8.150
3	N.D	-03.40 ± 0.629	-17.78 ± 0.310	177.00 ± 9.050

[a] standard deviation of three replicates

[b] standard deviation of two replicates

N.D = Not detected

Fig. 3.6. Thermogram of freeze-dried sugar kelp at a moisture content 1.0 kg H_2O/ kg dry solids with annealing

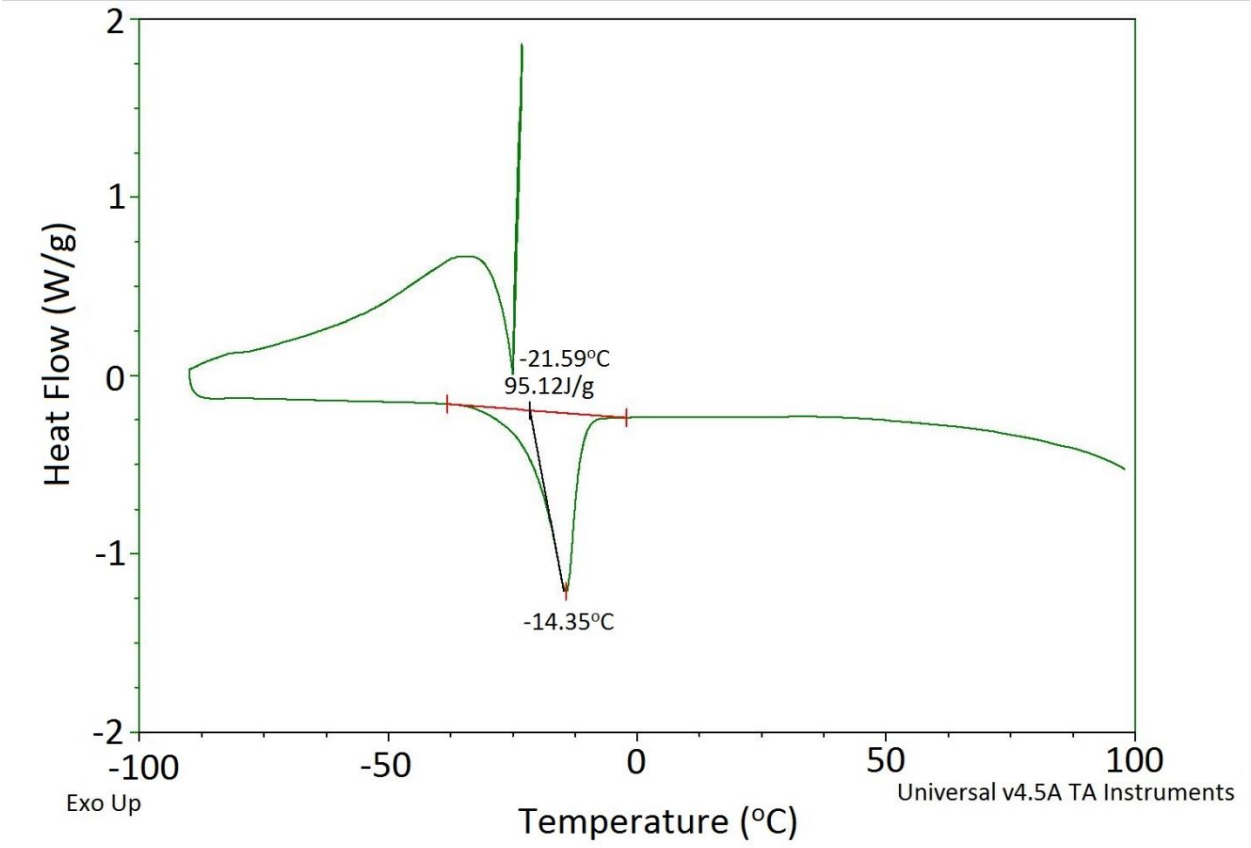

Fig. 3.7. Plot of ice-melting enthalpy vs moisture content (kg H_2O/ kg dry solids)

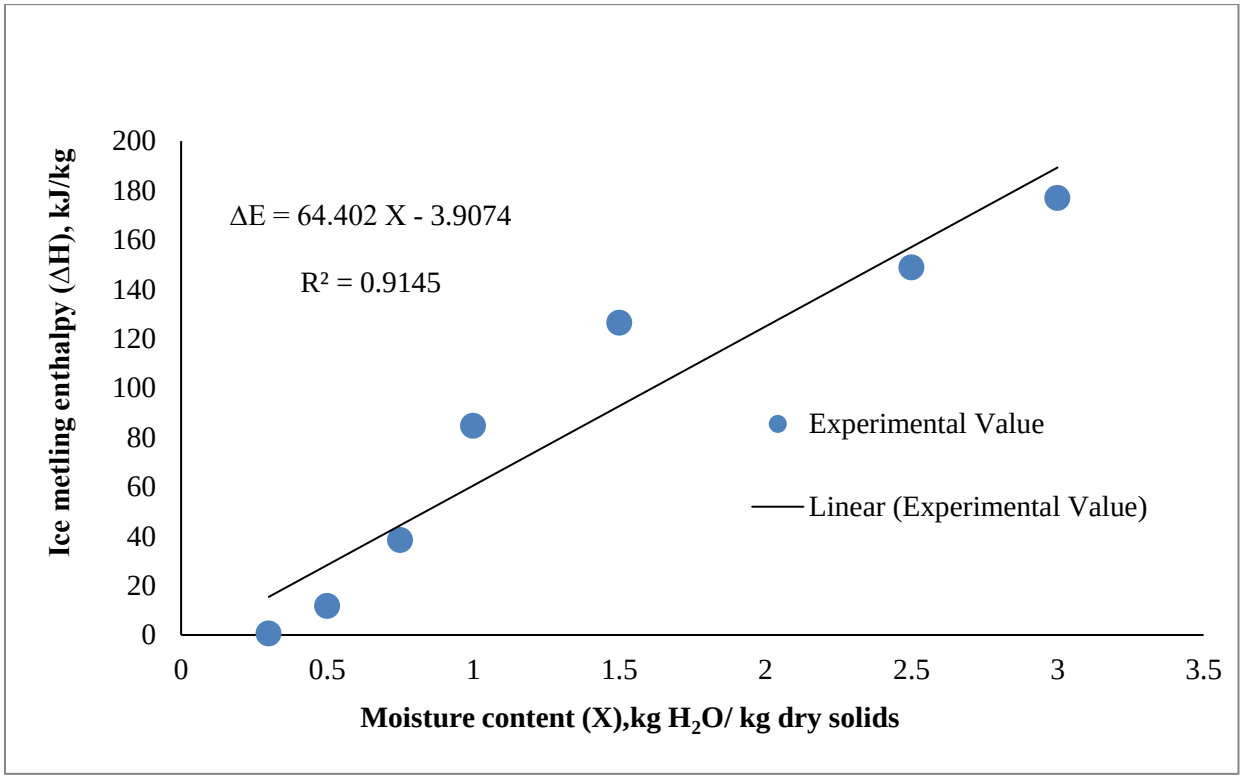

The freezing lines were modeled using modified Chen's equation. The parameters E in the equation were calculated using non-linear optimization as 0.099 after constraining B as 0.0592 kg H_2O/ kg dry solids, equal to the moisture content of the freeze-dried sample (0.0592 kg H_2O/ kg dry solids). The E values reported in the literature for apples (Bai et al. 2001), garlic (Rahman et al. 2005), kiwi (Wang et al. 2008b) and raspberries (Syamaladevi et al. 2009) are 0.238, 0.08, 0.101 and 0.064, respectively. The b value corresponds to the unfreezable water present in the sugar kelp and it is comparable to the unfreezable moisture data obtained from the enthalpy curve (0.06 kg H_2O/ kg dry solids). Bound water is the fraction of unfreezable water that is held firmly by the solid matrix and is unavailable for microbial growth and chemical reactions.

3.3.4 Drying Kinetics

Study of drying kinetics of seaweed was conducted in two stages. The first was designed to assess the effect of temperature and humidity levels on the drying rate in terms of overall effective moisture

diffusivity of the process and the second stage was employed to verify the application of Newton, Page and Henderson & Pabis models for describing the experimental drying curves obtained under the examined conditions. Moisture content variation of sugar kelp with respect to drying time for different values of drying parameters (temperature and relative humidity) has been determined. The effects of temperature and relative humidity on the reduction of moisture content as a function of time are shown in **Fig. 3.8**. It has been observed that with an increase in temperature the drying rate increases due to a higher convective heat transfer coefficient while decreasing relative humidity increases the drying rate due to a higher mass transfer coefficient.

Fig. 3.8. Effect of temperature and relative humidity on the moisture content of sugar kelp as a function of drying time at an air speed of 10 m/s

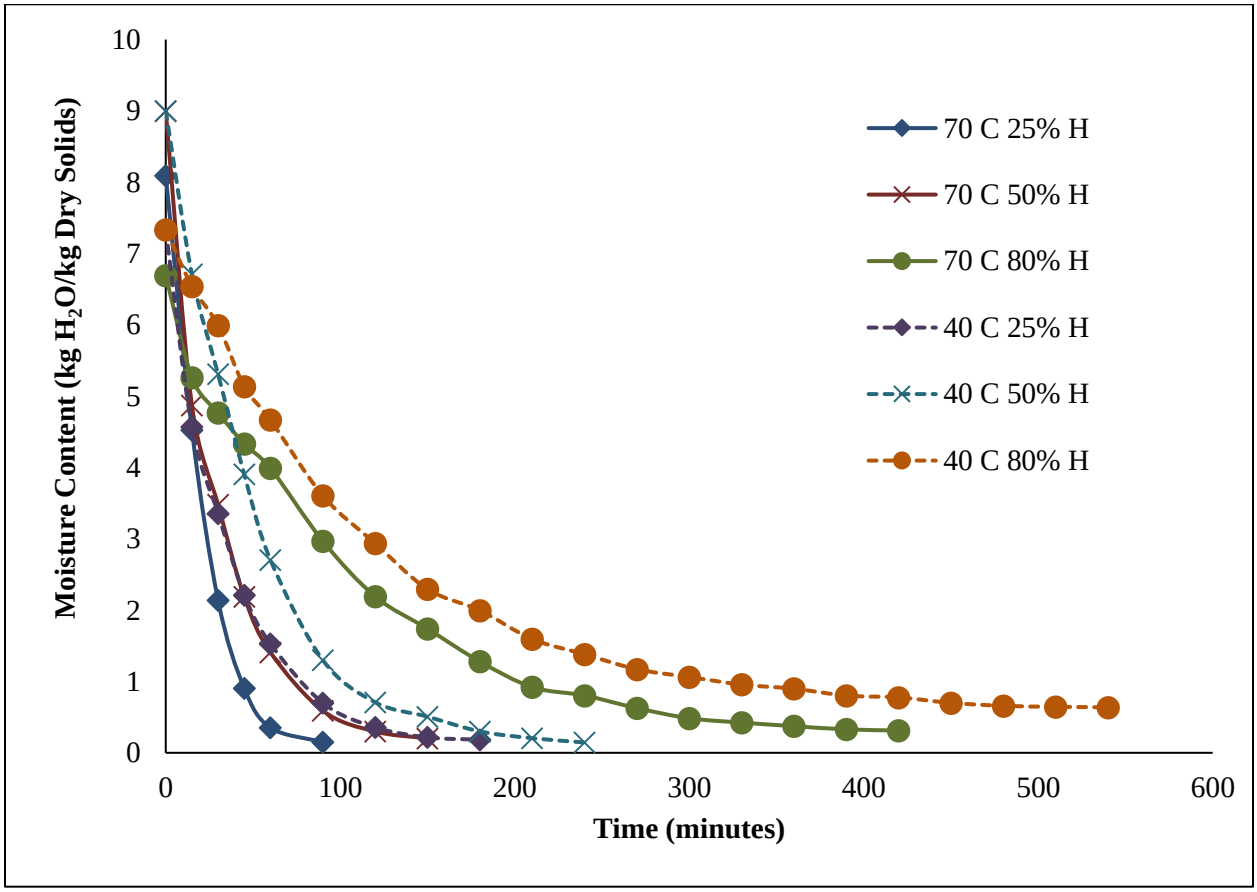

The EMC observed at the end of the drying process for 40°C and 70°C at humidity levels of 25%, 50% and 80% are listed in **Table 3.6**. The drying time sugar kelp taken to reach EMC at 40 °C and RH of 25%, 50% and 80% were 150 min, 240 min and 540 min respectively. At 70°C and RH of 25%, 50% and 80% the drying times were 90 min, 150 min and 420 min respectively. It was also observed that the whole drying process occurred in the falling rate period with no or negligible constant rate period. While drying food materials, the soluble solids migrate to the surface along with the moisture and form an impervious layer (case-hardening) creating a situation where the inner moisture is trapped by the hard-outer surface (Heldman 2003). This phenomenon is very common in foods which are dried at high temperature and contain a large amount of soluble solids. However, case hardening was not experienced while drying sugar kelp, which can be attributed to its thin profile allowing uniform diffusion. This behavior is similar to the findings reported in the literature for the drying of leafy plants like mint (Lebert et al. 1992), black tea (Temple and Van Boxtel 1999), bay leaves (Demir et al. 2004), and dill and parsley leaves (Doymaz 2006).

Table 3.6. Equilibrium moisture content

Temperature (°C)	Humidity (%)	X_{eqb} (kg H_2O/kg dry solids)
40	25	0.0926
	50	0.1259
	70	0.6024
70	25	0.0707
	50	0.1270
	70	0.2980

The natural logarithm of the moisture ratio (MR) was calculated and linearly plotted against drying time for both drying temperatures of 40°C and 70°C, as shown in **Fig. 3.9a** and **Fig. 3.9b**. Effective diffusivity of moisture during the drying process was calculated using the slope obtained from the above curve. The values of moisture diffusivity coefficient along with slope and R^2 of linear fit for different combinations of drying temperature and humidity are listed in the **Table 3.7**, where it can be seen that the

effective moisture diffusivity at 40 °C varied from 2.95 x 10^{-10} m^2/s to 0.74 x 10^{-10} m^2/s and 5.17 x 10^{-10} m^2/s to 1.47 x 10^{-10} m^2/s at 70 °C, corresponding to relative humidities of 25% and 80%. The application of Fick's diffusion law with the first term for modeling the drying process of sugar kelp can be justified since the R^2 values for a linear fit of the natural log of moisture ratio vs. time were in the range of 0.949 – 0.989. The obtained values of diffusivity coefficient are consistent with those existing in the literature for the leafy plants modeled based on Fick's thin layer moisture controlled diffusion such as 1.744 x 10^{-9} m^2/s - 4.992 x 10^{-9} m^2/s for nettle leaves and 1.975 x 10^{-10} m^2/s - 6.172 x 10^{-10} m^2/s for mint leaves (Kaya and Aydin 2009), 1.14 x 10^{-10} m^2/s - 2.98 x $10^{-10}$$m^2$/s for black tea (Pancharia et al. 2002) and 1.7 x 10^{-8} - 1.2 x 10^{-7} m^2/s for seaweed (*Eucheuma cottonii*) (Djaeni and Sari 2015).

Table 3.7. Moisture diffusivity at temperatures 40 °C and 70 °C

Temperature (°C)	Humidity (%)	Slope	Diffusivity Coefficient, D_{eff}, m^2/s X 10^{-10}	R^2
40	25	0.0004	2.95	0.9898
	50	0.0003	2.21	0.9850
	80	0.0001	0.74	0.9825
70	25	0.0007	5.17	0.9612
	50	0.0005	3.69	0.9792
	80	0.0002	1.47	0.9499

Fig. 3.9. a) ln(MR) vs time for a drying temperature of 40°C at different relative humidity levels **b)** ln(MR) vs time for a drying temperature of 70°C at different relative humidity levels

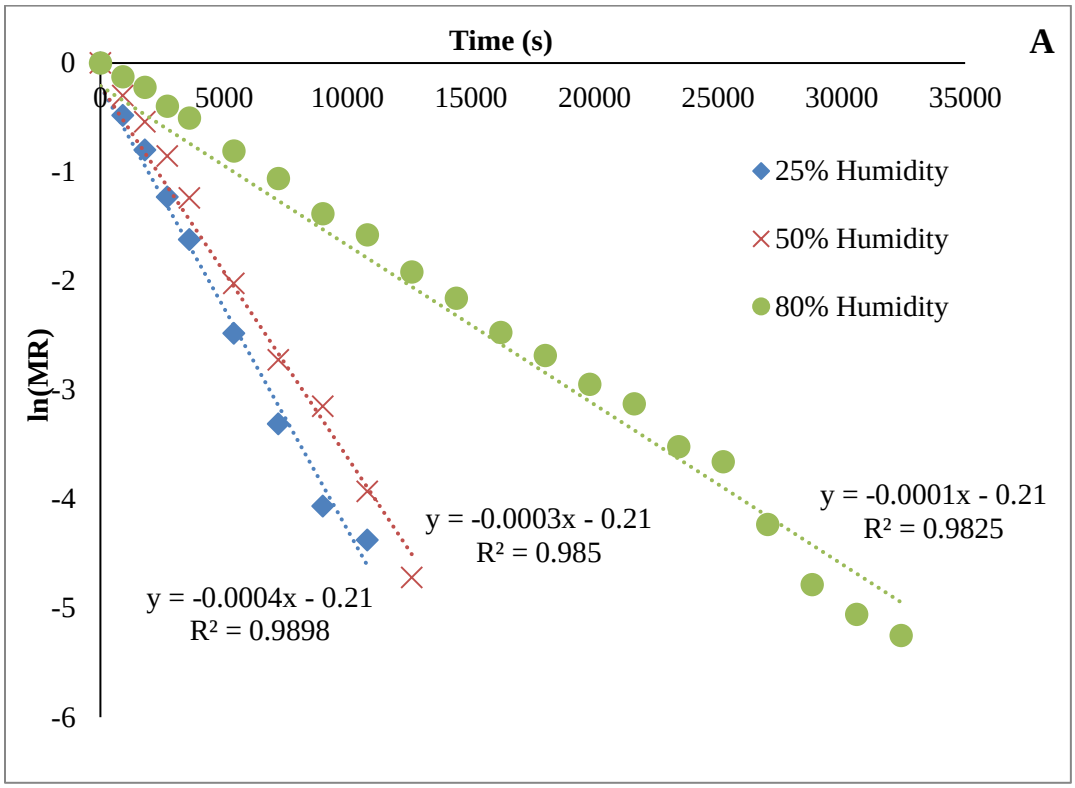

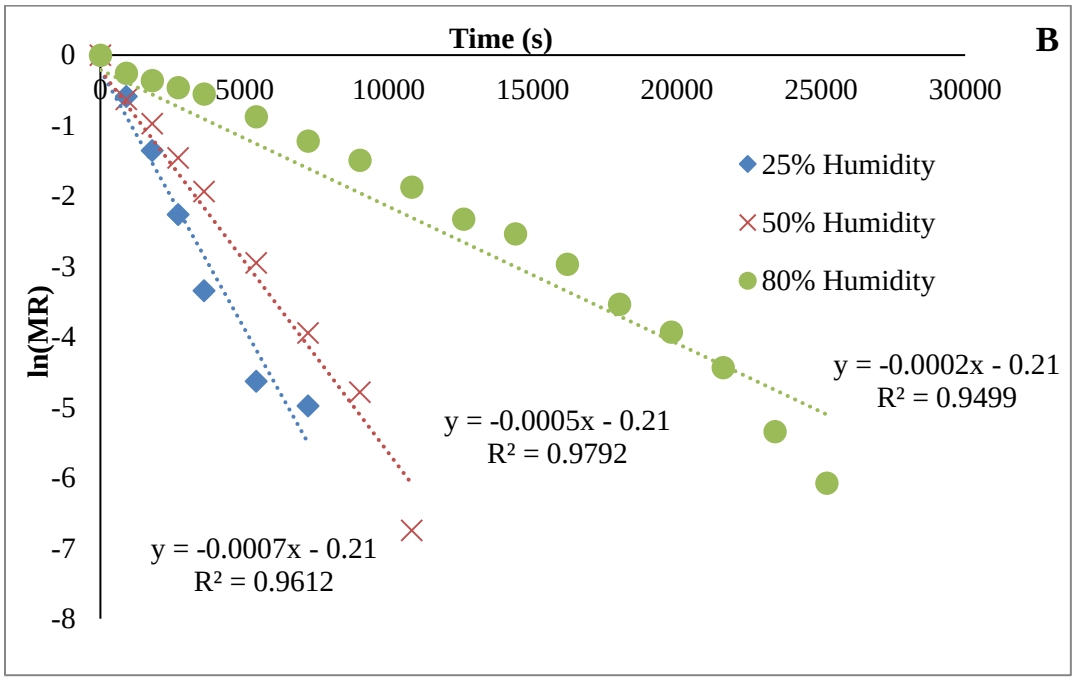

The drying data for sugar kelp drying were fitted to the kinetic models of Newton, Page, Henderson and Pabis for estimating the drying rate. The model constants were calculated using non-linear optimization by minimizing the SSE and are listed in **Table 3.8**. The SSE for the Page model was the lowest and gave better predictions than the other empirical models. The Page Model was also suggested for seaweed (*Eucheuma cottonii*) (Djaeni and Sari 2015) as it satisfactorily described the thin-layer drying under certain process conditions.

Table 3.8. Drying kinetic model constants at different temperatures

		Newton		Page			Henderson & Pabis		
Temperature (°C)	Humidity (%)	k, X 10^{-3} s^{-1}	SSE	k, X 10^{-3} s^{-1}	n	SSE	k, X 10^{-3} s^{-1}	a	SSE
40	25	0.462	0.002	0.802	0.929	0.0012	0.455	0.985	0.0018
	50	0.335	0.003	0.156	1.094	0.0016	0.340	1.013	0.0033
	80	0.147	0.002	0.162	0.907	0.0191	0.150	1.014	0.0014
70	25	0.746	0.004	0.138	1.227	0.0001	0.756	1.014	0.0037
	50	0.572	0.005	1.706	0.857	0.0019	0.559	0.978	0.0046
	80	0.173	0.011	0.212	0.976	0.0110	0.167	0.971	0.0095

3.3.5 Effect of Glass Transition on Shrinkage

The mid-point of glass transition (T_{gm}) of pure sugar kelp solids was observed at 47.02°C. Seaweeds are generally dried in the air temperature range of 30°C to 70°C (Djaeni and Sari 2015; Moreira et al. 2016). Drying temperatures of 40°C and 70°C were chosen to evaluate shrinkage as 40°C was lower than the observed T_{gm} while 70°C was higher. The sample thickness reduction was negligible and the volume reduction while drying was considered to be the same as the superficial area reduction. It was observed that the relative area shrinkage in the case of drying suhgar kelp at 70°C is more when compared to drying at 40°C. This suggests that the air temperature had a clear impact on the shrinkage of sugar kelp while drying. Levi and Karel 1995 showed that the rate of solid matrix mobility is directly proportional to the temperature difference between the product and its T_g at its specific moisture content. Drying at a higher temperature than the glass transition (T_g) keeps the product in a rubbery state, which allows a

higher shrinkage rate due to its mobile solid matrix. As the drying process progresses at lower moisture content, the glass transition temperature increases, resulting in lower rates of shrinkage due to the change in state from rubbery to glassy.

In **Fig. 3.10a** and **Fig. 3.10b**, the relative area during shrinkage while drying at 40°C and 70°C plotted against the moisture content (d.b) of the sample was fitted non-linearly to the Suzuki model (Suzuki 1976). The exponential constant (n) in the case of 40°C was n = 3.646; and in the case of 70°C, n = 4.665. Estimated model parameters a and b along with R^2 and SSE are listed in **Table 3.9.**

Fig 3.10. a) Relative area shrinkage at a drying temperature of 40 °C **b)** Relative area shrinkage at a drying temperature of 70°C

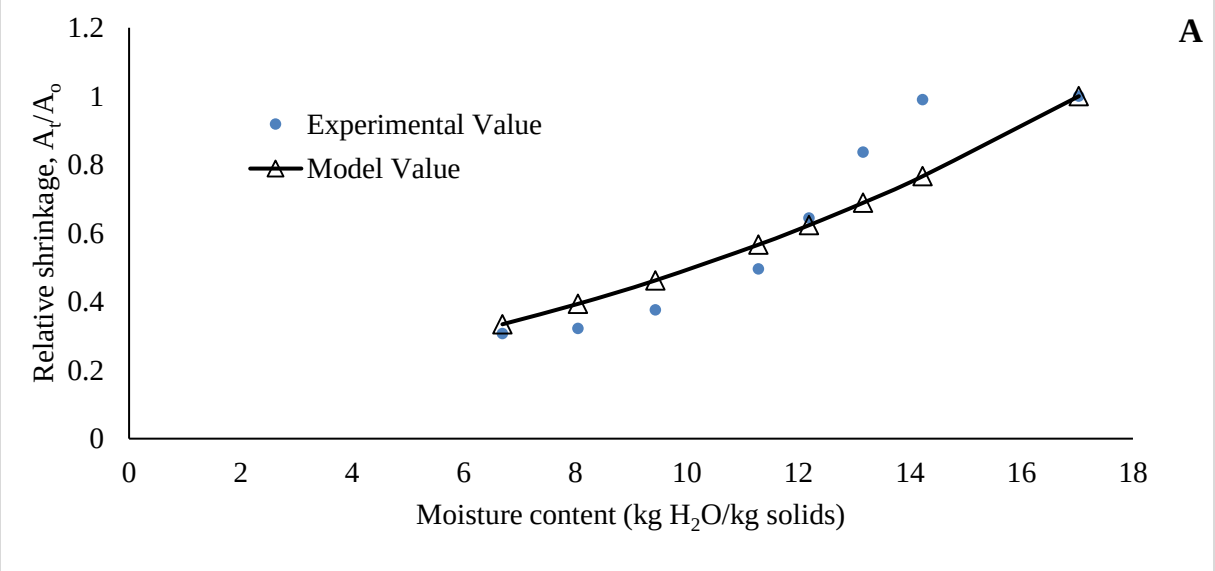

Fig. 3.10 continued

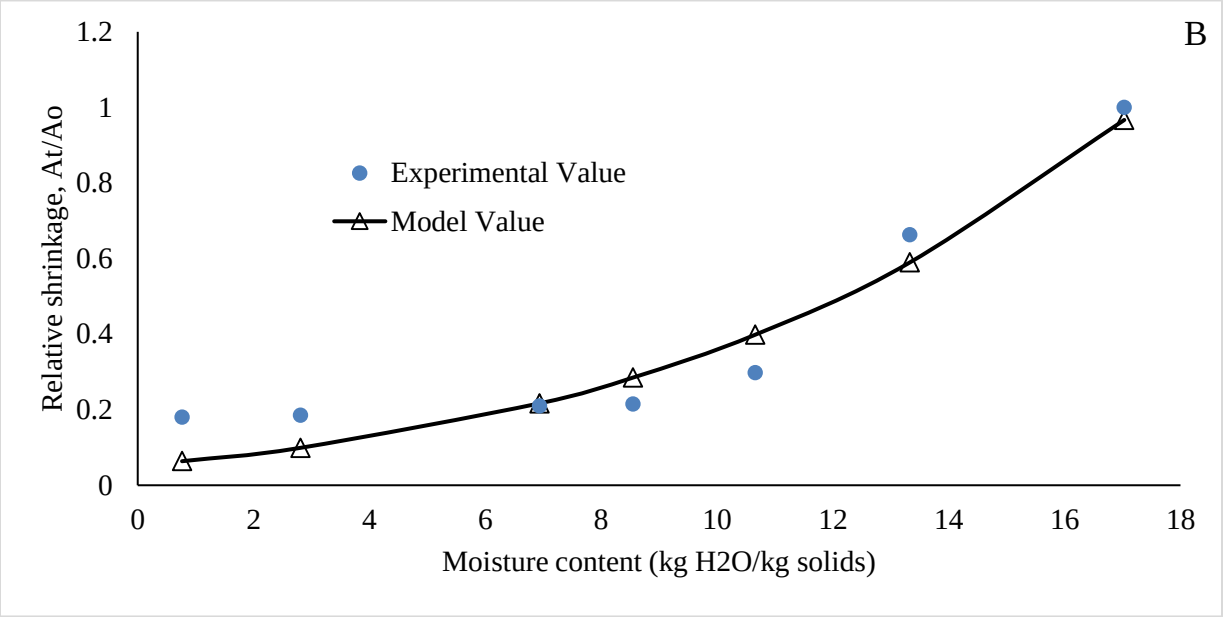

Table 3.9. Suzuki model parameters at different drying temperatures

Temperature, (°C)	n	a, g/cm^3	c, g/cm^3	R^2	SSE
40	3.646	0.0251	0.572	0.888	0.090
70	4.665	0.0269	0.533	0.934	0.042

For understanding the relationship between T_g and the relative shrinkage for sugar kelp, the data were plotted with respect to the moisture content of the samples (**Fig. 3.11**). The T_g of the dried seaweed while drying at 40°C and 70°C was in between -16°C and -20°C, corresponding to the final moisture content of dried samples (0.18- 0.22 kg H_2O/kg dry solids). So, the sugar kelp samples while drying never underwent the transition and were dried entirely in the rubbery state. While drying at 70°C, the temperature gradient between the sample and its T_g was always more than when dried at 40°C. Due to the higher temperature gradient, the samples drying at 70°C exhibited higher viscoelastic behavior, resulting in more relative shrinkage as compared to 40°C at any particular moisture content. The impact of state transition on shrinkage while drying low moisture samples can only be seen when the glass transition of pure solids (T_{gs}) is much higher than the air-drying temperatures and there is no shell formation (case-

hardening) (Kurozawa et al. 2012). The viscoelastic behavior of sugar kelp while drying can be explained using the concept of the temperature gradient between the air temperature and the T_g. However, this does not explain the controlling mechanism of material collapse which might be governed by surface tension, capillary forces and environment pressure (Rahman 2001).

Fig 3.11. Comparative plot of glass transition temperature (°C) and relative shrinkage of sugar kelp with respect to its moisture content (kg H_2O/kg solids)

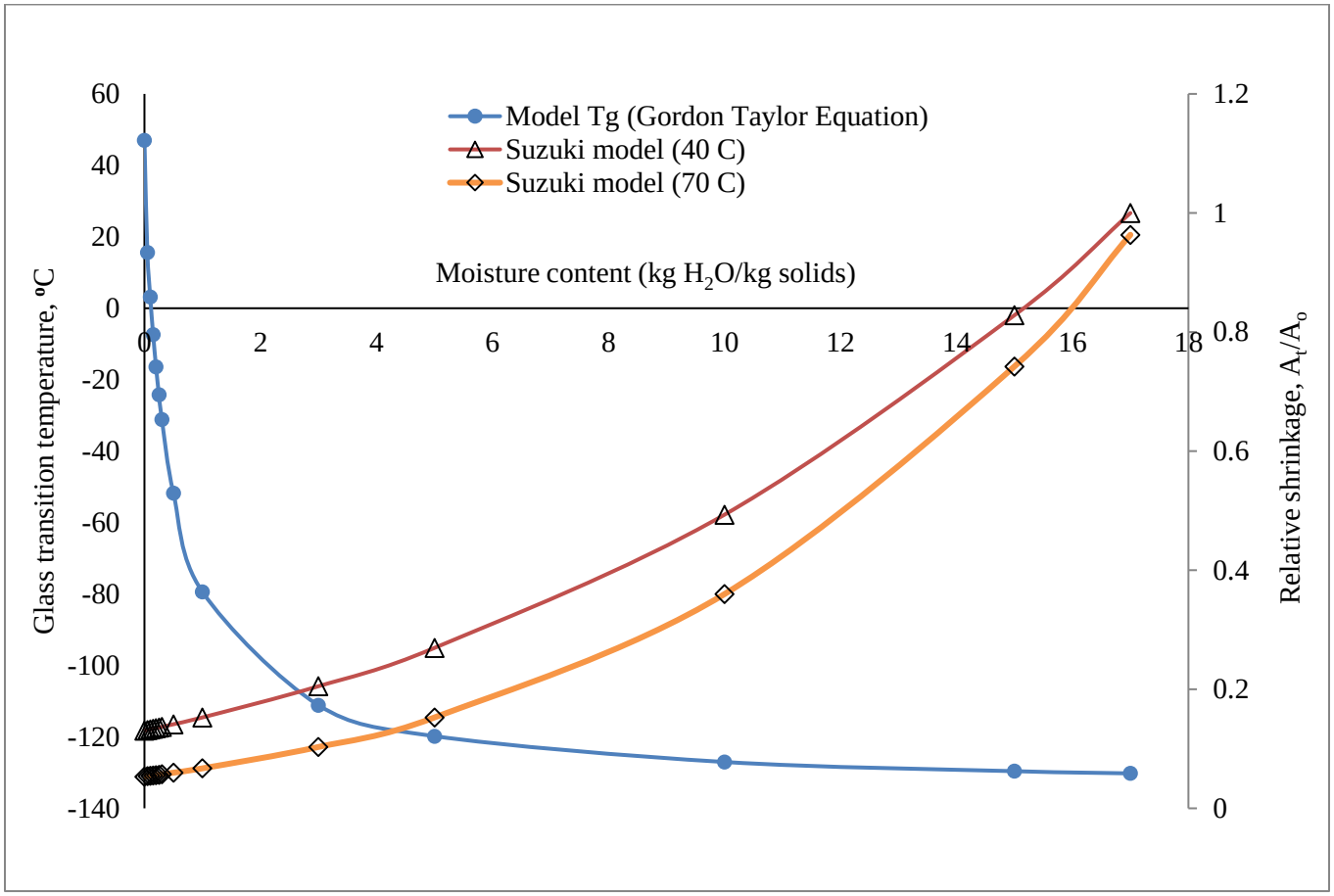

3.4 Conclusions

The temperature gradient between air temperature and glass transition temperature had a clear influence on the shrinkage rate of sugar kelp. Drying temperatures below T_g resulted in lower shrinkage rates as compared to higher drying temperatures. At higher drying temperatures, the amorphous form of water continued to stay in the rubbery state, exhibiting a more flexible solid matrix. As the drying was entirely in the rubbery state region, the diffusion mechanism did not deviate from ideal Fick's law, which can thus be applicable for modeling thin layer diffusion for the falling rate period. Subjecting seaweed to drying at high temperatures (> 40 ^{o}C) gives rapid removal of water but causes a higher rate of shrinkage that may negatively impact the textural quality. Case-hardening was not observed at high-temperature drying, even though sugar kelp contains a high amount of water-soluble sugars. Low-temperature drying can be used for retaining maximum nutrient profile and textural attributes, and when carried out at low humidity can result in rapid drying rates as compared to high temperature drying with high humidity. The glass transition temperature, initial and end-point of freezing point can be used for optimizing a freeze-drying method. Sugar kelp exhibited a type III moisture isotherm typically associated with foods that are highly porous, hygroscopic and contain high amounts of polysaccharides. A linear relationship was found between the TSS and the moisture content of the freeze-dried sugar kelp. Glass transition and freezing point are functions of TSS and can be predicted using the developed relationships. This information can be utilized to determine the storage parameters of both low and high moisture sugar kelp and for other species of seaweed.

CHAPTER 4

COMBINED EFFECTS OF SEASONAL VARIATION AND DRYING METHODS ON THE PHYSICO-CHEMICAL PROPERTIES AND ANTIOXIDANT ACTIVITY OF SUGAR KELP (*SACCHARINA LATISSIMA*)

4.1. Introduction

Seaweeds are a valuable source of bioactive agents and could potentially be introduced for the preparation of novel functional ingredients in pharmaceuticals and functional foods as an alternative approach for the treatment and or prevention of chronic diseases in humans. Commonly, seaweeds are dried to extend its shelf life under the sun or using hot air also known as convective drying and advanced drying systems attached with heat pumps to recover heat from exhaust air using a refrigerant and compression system. To retain the bioactive compounds and desired functional properties in dried kelp products, a detailed and simultaneous investigation of the seasonal variation and the effect of different drying methods and conditions (temperature, humidity) on the physicochemical properties, phenolic and antioxidant activity of sugar kelp is required. This comprehensive study was done over the harvesting period of sugar kelp to bridge the gap between the studies reported by other authors done earlier on the seasonal variation and the effect of the different drying methods on the physicochemical properties of the seaweeds. The objectives of this study were: (1) to determine the seasonal variation in the nutrient profile of the sugar kelp at the beginning and end of the harvesting period, and (2) to investigate the influence of different drying methods: freeze-drying, sun drying and heat pump drying (air temperature, relative humidity) on the physicochemical properties (moisture content, water activity, pH, color, fat content, ash content, crude protein, crude carbohydrate, water holding capacity, oil holding capacity, total soluble solids, vitamin C, total phenolic content and antioxidant activity) as compared to fresh sugar kelp. The results from this study will help in optimizing clean, energy-efficient heat pump drying systems for producing high-quality seaweed products for consumers.

4.2. Materials and Methods

4.2.1. Sample Preparation

For this study, fresh sugar kelp grown in Damariscotta bay, Maine (43°56'15.4"N; 69°34'53.0"W), was donated by Maine Fresh Sea Farms, Walpole, ME, USA and shipped to the University of Maine in the beginning of May 2017 for early season (S1) and end of June 2017 for late season (S2). Holdfasts were removed and the blades along with the stipes were washed under running water to remove any biofouling and surface salts. Raw sugar kelp was divided evenly into nine groups (1.2 kg each treatment: fresh, freeze-dried, sun-dried, 3 temperature (30 °C, 50 °C, and 70 °C) x 2 humidity (25% and 50%) levels) for physicochemical analysis classified as experimental groups, to provide uniform and representative samples (**Table 4.1**). The sun-dried sample was dried in the open air as one batch on a sunny and cloudless day at the University of Maine. The sun drying conditions for S1 and S2 were 19 °C, 40% relative humidity, 5 m s^{-1} wind speed and 7.2 UV index, and 25 °C, 70% relative humidity, 5 m s^{-1} wind speed and 9 UV index, respectively. Fresh sugar kelp was freeze-dried for 4 h at each temperature of -20 ºC, -10 ºC, 0 ºC, 10 ºC and 25 ºC using a freeze dryer (Virtis Ultra 35 EL, SP scientific, Warminster, PA, USA) with vacuum maintained at 20 Pa. Fresh sugar kelp samples of approximately 1 kg were dried at 3 levels of air temperature (30 °C, 50 °C, and 70 °C) with 2 levels of relative air humidity levels (25% and 50%) and air velocity of 1.0 m s^{-1} in a convective dryer (Cincinnati sub-zero, CSG, OH, USA). The drying time required for each level is reported in **Table 4.1**. After drying, the sugar kelp samples were ground into a fine powder using a food grinder (Magicbullet, Nutribullet LLC, Pacoima, CA, USA). The powdered samples were then sifted through a brass, multilevel sifter, and separated into two categories based on particle size: particles > 0.5 mm and particles < 0.5 mm. The final weight of the dried sugar kelp was measured and samples were kept in brown Nalgene bottles. These bottles were stored at room temperature (~22 ºC) in cardboard boxes to avoid any light interference until further analysis.

Table 4.1. Conditions (temperature, time and humidity) applied for producing dried sugar kelp during harvest season S1 (early May) and S2 (late June)

Treatment/Temperature	Drying time
Freeze drying (FD)	2 cycles of each temperature level (-20 ºC, -10 ºC, 0 ºC, 10 ºC and 25 ºC) for 4 h
Sun Drying (SD)	1 h under high air velocity (5 m s^{-1})
30°C and 25% Humidity	3.5 h
50°C and 25% Humidity	2.5 h
70°C and 25% Humidity	1.5 h
30°C and 50% Humidity	7.0 h
50°C and 50% Humidity	4.0 h
70°C and 50% Humidity	2.5 h

4.2.2. Physicochemical Analysis

4.2.2.1. Moisture Content

The moisture content of the dried sugar kelp was determined gravimetrically in triplicate according to the AOAC method (AOAC 1999). Briefly, 0.5 ± 0.002 g of powdered kelp was measured in a pre-weighed glass scintillation vial and kept in a natural convection air-oven at 105 ºC (VWR International, Radnor, PA). After 48 h, the hot vials were allowed to cool in a desiccator allowing them to reach room temperature. The moisture content of the samples was expressed in dry basis (D.B) as g H_2O $(100\ g)^{-1}$ dry solids.

4.2.2.2. Ash Content

Ash content was determined gravimetrically by heating the same glass scintillation vials containing the dried seaweed samples (after measuring moisture content) in a muffle furnace (Thermolyne Model F-A1730, Dubuque, IA, USA) at 550 °C for 7 h (AOAC 1999). The vials were cooled down to room temperature in a desiccator. The final weight of the vials plus sample ash was weighed. The ash content of the samples was calculated using formula (4.1).

$$Ash\ Content, \%\ (D.B) = \frac{W_{af}\ (g) - W_{sv}\ (g)}{W\ (g) - W_{sv}\ (g)} \times 100 \quad (4.1)$$

Where W represents the initial weight of dried sample and vial together (after calculating moisture content), W_{af} signifies the resulting weight of the vial plus the sample ash and W_{sv} is the weight of empty scintillation vial. The ash content of the samples was expressed as g ash $(100\ g)^{-1}$ dry solids.

4.2.2.3. Water Holding Capacity (WHC)

Water holding capacity (WHC) of the samples were measured in triplicate by a modified centrifugation method described by Suzuki et al. (1996). Briefly, 20 mL of de-ionized water was added to 50 mL centrifuge tube (CellTreat, Pepperell, MA, USA) containing 0.2 ± 0.001 g of dried kelp. The tubes were then shaken at a constant speed of 250 rpm using an agitator (Compact Digital Mini Rotator/Shaker, Thermo Scientific, Pittsburgh, PA, USA) for 24 h at room temperature (~ 22 ºC). The samples were then centrifuged (Beckman, Avanti J-25, Fullerton, CA, USA) at 14,000 x g for 15 min, the supernatant was collected, and the amount of the water absorbed by the pellet was determined by measuring the mass of the supernatant. The WHC of seaweed was calculated using formula (4.2) given below.

$$WHC\ (\%) = \frac{Water\ Added\ (g) - Water\ Decant(g)}{Dry\ Sample\ Weight\ (g)} \times 100 \qquad (4.2)$$

The WHC of the samples was expressed as the percentage mass of grams of water held by 1 g of sample dry weight (dried sample – remaining moisture content).

4.2.2.4. Oil Holding Capacity (OHC)

Oil holding capacity (OHC) of the samples were determined following the procedure of Caprez et al. (1986) with slight modifications. Corn oil (12 mL) (Hannaford, Scarborough, ME, USA) was added to 50 mL centrifuge tube (CellTreat, Pepperell, MA, USA) containing 3 ± 0.002 g of dried kelp. The tubes were vortexed using a high-speed vortexer (Vortex 2 Genie, VWR Scientific, Radnor, PA, USA) for 1 min per replicate to avoid any lump formation. The tubes were then shaken at a constant speed of 350 rpm using an agitator (Compact Digital Mini Rotator/Shaker, Thermo Scientific, Pittsburgh, PA, USA) for 30

min at room temperature (~ 22 ºC). After shaking, the mixture was centrifuged (Centrifuge 5430, Eppendorf NA, Hauppauge, NY, USA) at 2500 x g for 10 min. The excess oil supernatant was then removed and measured for its weight. Ten mL of oil was filled in 10 mL measuring cylinder and weighed for determining the density of the oil and the mass of oil absorbed. The density of the oil was found to be 0.92 g mL^{-1} at room temperature (~ 22 ºC). The OHC of dried seaweed was calculated using formula (4.3) given below.

$$OHC\ (\%) = \frac{Oil\ Added\ (g) - Oil\ Decant(g)}{Dry\ Sample\ Weight\ (g)} \times 100 \quad (4.3)$$

The OHC of the samples was expressed as the percentage mass of oil held by 1 g of dry sample.

4.2.2.5. Crude Fat Content

Crude fat/lipid content of the samples was determined using the acid hydrolysis method for seafoods (AOAC 2005). Ten mL of 8.1 N HCl was added to 2.5 g of dried sugar kelp and placed in a water bath (Julabo SW22, Allentown, PA, USA) for 90 min at 85 ºC, ensuring complete digestion of carbohydrates and proteins. Samples were allowed to reach room temperature. Once cooled, 7 mL of ethanol was added and then agitated vigorously for 30 sec. Three-stage solvent extractions were performed on each of the samples. For the first stage extraction, 25 mL of diethyl ether was added in the bottle and mixed moderately for 15 sec followed by rigrous agitation for 45 sec. The second step to the first extraction was to add 25 mL of petroleum ether to the above mixture, followed by 15 sec of slow to moderate agitation, then rigorous agitation for 45 sec. In the final step, the mixture was kept still for 30 min, allowing the digested sediments to settle out from the top floating layer consisting of a mixture of ether and lipids. This top layer was carefully extracted without disturbing the bottom sediments using a glass pipette and transferred to a pre-weighed beaker. The previous extraction steps were repeated two more times. For subsequent extractions, only 15 mL of diethyl ether and 15 mL of petroleum ether were used instead of 25 mL. The pooled mixture of ether and lipids was kept under the chemical hood

overnight allowing the ether to separate from lipids by volatilizing. This was followed by heating in the oven at 105 ºC for 15 min (VWR International, Radnor, PA) to remove any excess moisture and leaving behind only the lipids in the beaker. The fat content was calculated by reweighing the cooled beakers and using formula (4.4).

$$Crude\ Fat, \%\ (D.B) = \frac{[\ Beaker\ (g) + Fat/Lipid\ Weight\ (g)] - [\ Beaker(g)]}{Dry\ Sample\ Weight\ (g)} \times 100 \qquad (4.4)$$

Fat content was expressed as the g fat (100 g)$^{-1}$ dry solids.

4.2.2.6. pH

One gram sample of dried sugar kelp was weighed and placed in a 50 mL centrifuge tube (Celltreat, Pepperell, MA) to which 15 mL of de-ionized water was added. Contents were mixed using an agitator (Thermo Scientific Compact Digital Mini Rotator/Shaker, Pittsburgh, PA) for 1 min. The pH was then measured with a digital pH meter (Benchtop pH / MV Meter – 860031, Scottsdale, AZ) calibrated with standard pH buffer solutions of 4, 7 and 10.

4.2.2.7. Water Activity

The water activity was determined using a water activity meter (AquaLab Decagon, Pullman, WA) by weighing approximately 1 g of dried sugar kelp in disposable cups. The water activity meter was calibrated prior to taking sample reading with the standard salts solutions with a known water activity of 0.500 and 0.250.

4.2.2.8. Color Analysis

Color of the fresh and dried kelp was determined using a Hunter colorimeter (LabScan XE, Hunter Labs, Reston, VA) and expressed in L*a*b* values, in which: L* values are based on a scale of dark (0) to light (100); a* values are based on a scale of green (-) to red (+); and b* values are based on a

scale of blue (-) to yellow (+). Black and white ceramic standard plates were used to standardize the colorimeter before each use. An opening port size of 50.5 mm, area view of 44.5 mm, and D65 illumination of the colorimeter was used. A disc with 5.1 cm diameter hole was used. Approximately 1 g of dried kelp was placed in colorimeter cups for analysis. The overall change in the color (∆E) of the samples with respect to the fresh samples was calculated using the formula (4.5).

$$\Delta E = \sqrt{(L_0 - L^*)^2 + (a_0 - a^*)^2 + (b_0 - b^*)^2} \quad (4.5)$$

Where, L_0, a_0 and b_0 represents the L*, a* and b* of the fresh samples.

4.2.2.9 Crude Protein

The total nitrogen content was determined using a dry combustion analyzer (TruMac CNS, LECO Corporation, MI, USA) (AOAC 1990). The total crude protein was calculated using an average nitrogen-to-protein conversion factor of 5.3 for sugar kelp (Schiener et al. 2015).

4.2.2.10. Crude Carbohydrate

The crude carbohydrate was determined by the difference method (Merill and Watt 1973). It was expressed as g carbohydrate $(100\ g)^{-1}$ dry solids.

4.2.2.11. Total Soluble Solids (TSS)

Half-gram sample was homogenized (Polytron homogenizer, Brinkmann Instruments, Westbury, NY) in 9.5 mL of water (1:20 dilution) for 2 min and centrifuged (Centrifuge 5430, Eppendorf NA, Hauppauge, NY, USA) at 7000 x g for 10 min. The supernatant collected was used for measuring the total soluble solids (TSS) of the samples using a refractometer (Palette Digital Refractometers 0-45º, ATAGO U.S.A Inc., WA, USA).

4.2.2.12. Vitamin C

Vitamin C was determined by titrating dried sugar kelp extractions using 2,6-dichlorophenolindophenol dye method (AOAC 1968) (AOAC 1988). The precipitant solution was made by mixing equal amounts of solutions (A) and (B). The first solution (A) was made by dissolving 15 g of glacial metaphosphoric acid in 40 mL of glacial acetic acid and bringing it to 250 mL with distilled water. The second solution (B) was made by dissolving 0.9 g of ethylene diamine tetraacetic acid (EDTA) in 200 mL of de-ionized water and bringing it up to 250 mL. One gram of dried sugar kelp was homogenized for 2 min with 15 mL of cold precipitant solution using a polytron homogenizer (Brinkman Instruments, Westbury, NY). The solution was then centrifuged (Beckman, Avanti J-25, Fullerton, CA, USA) at 10,000 x g for 15 min at 25 ºC. Fifteen mL precipitant solution was again added to the suspended pellet and centrifuged again at the same specifications. Fifteen mL aliquots of sample extracts were titrated with the indophenol dye until the rose-pink endpoint lasted for 10 sec. The ascorbic acid concentration of the sample was calculated using formula (4.6).

$$Vitamin\ C, (mg\ ascorbic\ acid\ g^{-1} of\ sample\ weight) = C \times V \times \frac{DF}{WT} \quad (4.6)$$

Where C represents mg of ascorbic acid mL^{-1} of dye, V is mL of dye used for titration of the diluted sample (subtract blank volume first), DF is the dilution factor and WT is the weight of the dry sample (g).

4.2.3. Sugar Kelp Extraction for TPC, DPPH and FRAP Assay

Dried sugar kelp (2 ± 0.002 g) was mixed with 20 mL of 60% (v/v) methanol and agitated (Compact Digital Mini Rotator/Shaker, Thermo Scientific, Pittsburgh, PA, USA) at 210 rpm for 24 h at room temperature (~ 22 ºC). The solution was centrifuged at 2100 x g for 10 min at room temperature. The supernatant was collected and pellet wash was performed twice by adding 10 mL of 60% (v/v) methanol to the suspended pellet, followed by vortexing for 30 sec and centrifuge for 10 min at specifications described in the previous step. The decanted supernatant from both the extractions was

pooled together with the first extraction supernatant and was brought up to a final volume of 50 mL using de-ionized water followed by 30 s vortexing to ensure homogenization. The samples were stored at -80 ºC. The tubes were kept frozen at -80 ºC after dividing the final extract approximately in 3 equal parts to be used separately for TPC, DPPH and FRAP assay.

4.2.4. Total Phenolic Content (TPC)

The total phenolic content (TPC) in the methanolic sugar kelp extract was determined in duplicate using Folin-Ciocalteu's reagent method (Taga et al. 1984). The following solutions were prepared fresh on the day of the experiment: 0.2 N Folin-Ciocalteu's reagent, 6% w/v sodium bicarbonate solution and standard/stock 1000 µg/mL gallic acid solution. To prevent any light interference, all of the prepared solutions were kept in the round bottom flask covered with aluminum foil. The sample extract kept at -80 ºC was thawed at room temperature (~ 22 ºC). 750 µL of prepared Folin's reagent was added to the 100 µL aliquot of sample extract taken in a 3 mL glass cuvette. After 5 min, 750 µL of 6% (w/v) sodium bicarbonate was added vigorously. The glass cuvette was incubated in the dark for 1 h. 40% (v/v) methanol was used as a sample blank. The absorbance was determined at 725 nm using a UV-vis spectrophotometer (Beckman Du 530, Brea, CA). A linear calibration curve of the standard solution of gallic acid (0 – 200 µg/mL) was constructed to quantify the total phenolic content. The TPC of sugar kelp was expressed as mg gallic acid equivalents (GAE) g^{-1} of dry weight sample.

4.2.5. Ferric Reducing Antioxidant Power (FRAP)

The Ferric Reducing Antioxidant Power (FRAP) of the methanolic sugar kelp extract was determined in duplicate using the modified method described by Benzie and Strain (1999). The following solutions were prepared fresh on the day of the experiment: 300 mM sodium acetate buffer, 10 mM 2,4,6-tripyridyl-s-triazine (TPTZ) and 20 mM ferric chloride ($FeCl_3.6H_2O$) were added in the ratio (10:1:1) to make the FRAP reagent. This reagent was kept in a water bath maintained at 37 ºC. A timer set at 4 min was started as soon as 1.5 mL of prepared FRAP reagent was added to the 50 µL aliquot of sample extract

in a 3 mL glass cuvette. After 4 min, the absorbance was determined at 725 nm using a UV-vis spectrophotometer (Beckman Du 530, Brea, CA) maintaining the same speed and order of cuvettes. 40% methanol was used as a sample blank. A linear calibration curve of the standard solution of ferrous sulphate (50 – 500 µM) was constructed using a standard/stock solution of 1000 µM ferrous sulphate ($FeSO_4.7H_2O$). The FRAP value was expressed in µmol ferrous sulfate equivalents (FSE) g^{-1} of dry weight sample.

4.2.6. DPPH (α, α-diphenyl-β-picrylhydrazyl) Assay

DPPH radical scavenging activity of the methanolic sugar kelp extract was determined in duplicate using the modified method for 96-well microplate described by Blois (1958). 0.2 mM DPPH was prepared fresh on the day of the experiment by dissolving 78.8 mg of DPPH in 1000 mL of 100% (v/v) ethanol. Varying volumes of the sample (25 µL, 50 µL, 100 µL, 150 µL) were bought up to 150 µL with 40% (v/v) methanol. 150 µL of DPPH was added to the sample vigorously, ensuring uniform mixing in the microcell. Sample blank was prepared similarly to the sample except for 150 µL of DPPH, 150 µL of 100% (v/v) ethanol was added to account for the sample color. Equal volumes, 150 µL of 40% (v/v) methanol and DPPH solution are mixed to prepare the control. Control blank was made by mixing equal volumes, 150 µL, of 40% (v/v) methanol and 100% (v/v) ethanol each. The microplate was incubated in the dark for 30 min. The absorbance was determined at 517 nm using a 96-well microplate reader (Biotek Eon, Biotek Instruments, Winooski, VT). The following equation (4.7) is used for calculating the % DPPH inhibition (antioxidant activity).

$$\%\ DPPH\ inhibition = \frac{[(Control - Control\ Blank) - (Sample - Sample\ Blank)]}{[(Control - Control\ Blank)]} \times 100 \qquad (4.7)$$

The % DPPH inhibition of the samples was plotted against the varying volumes using MS excel (Microsoft Excel, 2013). Only an R^2 value greater than 0.95 was considered as linear. The concentration of the sample required for a 50% reduction of DPPH (EC_{50}) was calculated using the slope and constant

of the plotted line. The % DPPH inhibition of the sample were expressed as EC_{50} (mg mL^{-1}).

4.2.7. Statistical Analysis

Analyses for each experiment were performed in triplicate. All the quantitative results are reported as mean ± standard deviation. Multi-way ANOVA was used to determine any significant effects ($p \leq 0.05$) of the independent variables (temperature, humidity, drying time and season) at an individual level and the interaction effect (triple and double effect) on the response variable (physico-chemical properties). Tukey's honest significant difference (HSD) post hoc test was performed to identify any significant differences between the means of comparable treatment.

4.3. Results and Discussion

4.3.1. Moisture Content

The final MC on a dry basis of the obtained kelp with respect to their drying conditions (temperature and humidity), and the period of harvest are listed in **Table 4.2** as mean ± S.D. Results show that the MC of dried sugar kelp was, as expected, less than 20% for dried kelp from both harvest periods and different drying conditions. The drying temperature and harvest season significantly ($p < 0.05$) affected the final MC. As expected, for samples from both seasons, the MC decreased as the temperatures increases. For both the seasons, MC for freeze-dryed (FD) samples was significantly lower ($p < 0.05$) than any of the sun-dried (SD) and heat pump dried (HPD) sugar kelp at 25% and 50% humidity. This is because freeze drying works on the principle of sublimation under vacuum and removes the freezable water, while the HPD depends on the temperature, humidity and the air velocity inside the drying chamber. Even though the drying time and the MC of the fresh sugar kelp in both seasons were similar, statistically, the MC of the S2 dried kelp was significantly ($p < 0.05$) higher than S1. Overall, the lower drying temperature and high relative air humidity increases the MC of dried sugar kelp and requires longer drying time.

Table 4.2. Proximate composition of sugar kelp harvested in season S1 (early May) and S2 (late June)

	Season 1 (S1)					Season 2 (S2)				
Drying condition/ Treatment	Moisture (g (100 g)$^{-1}$ dry solids)	Ash (g (100 g)$^{-1}$ dry solids)	Fat (g (100 g)$^{-1}$ dry solids)	Crude protein (g (100 g)$^{-1}$ dry solids)	Crude carbohydrate (g (100 g)$^{-1}$ dry solids)	Moisture (g (100 g)$^{-1}$ dry solids)	Ash (g (100 g)$^{-1}$ dry solids)	Fat (g (100 g)$^{-1}$ dry solids)	Crude protein (g (100 g)$^{-1}$ dry solids)	Crude carbohydrate (g (100 g)$^{-1}$ dry solids)
FD	5.30 ± 0.1 aA	29.4 ± 0.2 a	1.6 ± 0.1 A	10.8 ± 0.1 aA	58.2 ± 0.0 aA	8.0 ± 2.1 aB	27.4 ± 0.8 a	2.3 ± 0.1 B	9.3 ± 0.0 aB	61.1 ± 0.8 aB
SD	16.4 ± 1.8 bA	29.6 ± 0.4 b	1.7 ± 0.1 A	10.9 ± 0.5 aA	57.8 ± 0.9 bA	18.2 ± 0.8 bB	29.4 ± 0.5 b	2.2 ± 0.2 B	9.2 ± 0.5 aB	59.2 ± 0.3 bB
30°C, 25%	13.2 ± 1.5 cA	28.5 ± 0.4 bx	1.7 ± 0.1 A	10.4 ± 0.6 abA	59.4 ± 0.6 baA	15.0 ± 0.4 cB	33.0 ± 0.9 bx	2.0 ± 0.5 B	8.4 ± 0.6 abB	56.7 ± 0.8 baB
50°C, 25%	11.1 ± 0.7 cA	29.8 ± 0.3 cx	1.8 ± 0.0 A	10.4 ± 0.2 bA	58.1 ± 0.4 cA	12.5 ± 0.4 cB	28.1 ± 0.8 cx	2.2 ± 0.2 B	7.8 ± 0.2 bB	62.0 ± 1.0 cB
70°C, 25%	13.6 ± 0.3 cA	22.9 ± 0.2 dx	2.2 ± 0.4 A	11.5 ± 0.5 bA	63.5 ± 0.3 dA	19.5 ± 1.2 cB	27.4 ± 0.3 dx	2.1 ± 0.2 B	7.4 ± 0.5 bB	63.1 ± 0.3 dB
30°C, 50%	14.5 ± 0.4 cA	28.9 ± 0.2 by	1.7 ± 0.0 A	10.5 ± 0.1 abA	58.9 ± 0.2 baA	16.6 ± 0.9 cB	27.6 ± 0.3 by	1.8 ± 0.0 B	9.3 ± 0.8 abB	61.3 ± 1.1 baB
50°C, 50%	13.1 ± 0.2 cA	28.0 ± 0.1 cy	1.7 ± 0.3 A	09.9 ± 0.5 bA	60.4 ± 0.6 cA	18.0 ± 1.1 cB	26.8 ± 0.3 cy	2.0 ± 0.1 B	9.7 ± 0.1 bB	61.5 ± 0.5 cB
70°C, 50%	10.7 ± 0.1 cA	27.9 ± 0.1 dy	1.8 ± 0.1 A	10.4 ± 0.2 bA	60.0 ± 0.2 dA	15.8 ± 1.6 cB	27.4 ± 1.0 dy	2.3 ± 0.1 B	7.7 ± 0.5 bB	62.6 ± 1.4 dB
Fresh	806.4 ± 31.4 dA	-	-	-	-	998.7 ± 49.1 dB	-	-	-	-

Results are mean ± standard deviation of triplicate for each sample (n = 3). Significant differences between the values are measured at $p < 0.05$.
Small letter (a, b): denotes row-wise comparison between treatments or with air drying temperatures.
Capital letter (A, B): denotes comparison between harvesting seasons, S1 and S2.
x/y: denotes comparison between the drying humidity

4.3.2. Ash Content

The ash content of the sugar kelp ranged from 22.85 ± 0.23 to 29.79 ± 0.31 g (100 g)$^{-1}$ dry solids and 26.78 ± 0.34 to 33.03 ± 0.90 g (100 g)$^{-1}$ dry solids for S1 and S2, respectively (**Table 4.2**). Manns et al. (2017) and Scheiner et al. (2015) reported that the average ash content of S. *latissima* is 21 - 38 g (100 g)$^{-1}$ dry solids, which is very similar to the values found in our study. In addition, the mean percentage of ash found in the dried kelp was comparable to those found in other species i.e., *Hypnea japonica* (22.1 ± 0.72 g (100 g)$^{-1}$ dry solids), *Undaria pinnatifida* (26.58 ± 4.24 g (100 g)$^{-1}$ dry solids) and *Sargassum wightii* (25 ± 2 g (100 g)$^{-1}$ dry solids) (Dawczynski et al. 2007; Smith et al. 2010; Syad et al. 2013). Moreover, other literature showed that the ash content in seaweed varies from 8 - 40 g (100 g)$^{-1}$ dry solids (Indegaard and Ostgaard 1991; Mabeau and Fleurence 1993) and this variation in ash content depends on seaweed species, composition of their cell walls, geographical origins, physiological stress, pH, the salinity of water and other environmental changes and method of mineralization (Astorga-España et al. 2015; Davis et al. 2003; Kumar et al. 2008; Mišurcová et al. 2011; Nisizawa 1987; Rao et al. 2007; Sánchez-Machado DI et al. 2004). Sugar kelp accumulates the highest amount of minerals during the winter period of sporulation followed by a decline in the summer and autumn months (Chapman 1987). During this winter period, the storage carbohydrate laminarin is at its lowest level, having been consumed to maintain growth during the freezing water temperatures and scanty sunshine by synthesizing more protein, lipid, and minerals (Black and Dewar 1949; Chapman and Craigie 1997; Chapman and Craigie 1978; Scheiner et al. 2015).In this study, the ash content showed that the harvesting seasons, S1 and S2 did not have a significant effect ($p > 0.05$). Similarly, there was no change observed in the ash content of sugar kelp for both wild-harvested and cultivated specimens in Danish waters, as reported by Manns et al. (2017) over the period of May-June.

4.3.3. Crude Fat Content

The average values of fat/lipid content measured in the sugar kelp were 1.78 ± 0.24 g $(100\ g)^{-1}$ dry solids and 2.11 ± 0.23 g $(100\ g)^{-1}$ dry solids for S1 and S2, respectively (**Table 4.2**). In general, the total mean fat/lipid content in Phaeophyceae was reported to be 3 g $(100\ g)^{-1}$ dry solids, varying from the lowest value of 0.1 g $(100\ g)^{-1}$ dry solids found in *Leathesia marina* to the highest value of 20 g $(100\ g)^{-1}$ dry solids in *Dictyota sandvicensis* (McDermid and Stuercke 2003; Renaud and Luong-Van 2006). Several factors such as algal life cycle, physiological state, seasonal and environmental factors including water depth, pH, salinity, temperature, availability of nutrients and sunlight contribute to the varying degrees of total fats in seaweeds (Guschina and Harwood 2006; Khotimchenko and Kulikova 2000; Melo et al. 2015). A significant difference was not found ($p > 0.05$) in the total fat content due to the drying conditions (temperature and humidity). This suggests that during drying, the fats present were not lost by dripping out of the porous structure or by converting into volatile oxidized compounds due to drying temperatures (Akonor et al. 2016; Tir et al. 2017).

The fat content values for the early season, S1 were significantly ($p < 0.05$) lower than the late season, S2. Several authors have reported that the seaweeds contain the highest amount of fat/lipid during the period of winter through spring and the minimum during summer (El Maghraby and Fakhry 2015; Nomura et al. 2013; Scheiner et al. 2015). For our study, contrasting results were observed as there was an increase in the levels of lipids from S1 to S2. Olofsson et al. (2012) attributed these variations in lipid content to the seaweed growth cycle, water temperature and availability of light. In the above study on microalgae, it was found that the presence of abundant light and high-water temperature resulted in higher lipid accumulation due to extended photosynthetic rate and overall lower energy cell demand. A study conducted on *Pavlova virdis*, also a marine microalga, revealed that water temperature affected the fatty acid profile, where at higher temperature, the polyunsaturated fatty acids decreased, while the saturated fatty acids increased keeping the overall fat content unchanged (Hu et al. 2008). In Maine, US, the effective day length and the light intensity increases faster than the water temperature between May and

June. This relative increase in the available sunshine and approximately the same water temperature could result in a higher photosynthetic rate and accretion of a high amount of fatty acids without change in its profile. Overall, drying conditions did not change the total crude fat in the sugar kelp, however, more studies on seaweeds are required to understand the possible impact of different drying conditions on the fatty acid profile.

4.3.4. Crude Protein

Traditionally, the crude protein content is calculated using a nitrogen-to-protein conversion factor also known as Jones' factor of 6.25 (Jones 1931), based on the assumption that all the nitrogen exists as proteins in the sample. However, corrected conversion factors have been reported based on the considered species and their respective phylum. Consequently, Lourenço et al. (2002) reported a conversion factor of 5.38 ± 0.50 for brown seaweeds, which corrected for the overestimated amounts due to non-protein nitrogen in the sample. Moreover, the studies performed by Manns et al. (2017) and Scheiner et al. (2015), also indicated seasonal variation in the Jones' factor observed within the same species of some brown seaweeds. For this study, an average Jones' factor of 5.3 was considered for calculating the crude protein content in sugar kelp (Scheiner et al. 2015).

The average nitrogen content in the dried kelp was not affected ($p > 0.05$) by the applied drying conditions (temperature and humidity) (**Table 4.2**). However, seasonal effects were significant ($p < 0.05$) and the average nitrogen values were found to be 2.01 ± 0.10 g $(100\ g)^{-1}$ dry solids and 1.64 ± 0.16 g $(100\ g)^{-1}$ dry solids, for S1 and S2, respectively (**Table 4.2**). These values are comparable with the average nitrogen content of 1.5 ± 0.5 g $(100\ g)^{-1}$ dry solids, reported for sugar kelp (Scheiner et al. 2015). As a result, the protein content (10.65 ± 0.53 g $(100\ g)^{-1}$ dry solids) was found to be higher in S1 as compared to the protein content (8.69 ± 0.85 g $(100\ g)^{-1}$ dry solids) in S2. Similar observations were also found in some studies, where the maximum value was observed during spring followed by the decline in protein content to a minimum during the summer (Kumar et al. 2015; Manns et al. 2017; Scheiner et al. 2015).

Like other chemical constituents, protein content can also fluctuate depending on several factors such as species, plant maturity, geographical locations, environmental conditions (water temperature, salinity, nutrient availability) and growing season (Fleurence 1999; Ito and Hori 1989). Irradiation has been identified as a major contributing factor to the varying amount of nutrient accumulation. During summer, the presence of high-intensity light activates the nitrogen metabolism. It induces higher nitrogen demand within the cell causing faster degradation rates of nitrogen, resulting in overall lower protein content.

4.3.5. Crude Carbohydrate

In this study, the carbohydrate content in sugar kelp comprised the major part of algal biomass (> 55 g (100 g)$^{-1}$ dry solids) and was found to be higher than the values reported earlier for sugar kelp ranging from 20 - 44 g (100 g)$^{-1}$ dry solids (Vilg et al. 2015). Statistical analysis indicated a significant difference ($p < 0.05$) in the carbohydrate levels for the temperature parameter, which may be explained by the sum of responses of other components to temperature, since in this study the total carbohydrates were determined by difference (100 – rest of the components) (**Table 4.2**). However, no significant change in the total carbohydrates content ($p > 0.05$) due to the drying humidity parameter was observed (**Table 4.2**).

Seasonal variability was significant ($p < 0.05$) as a higher carbohydrate content was observed in S2 than S1 (**Table 4.2**). The higher values during S2 can be possibly explained by higher levels of alginates that were found in brown seaweeds during summer, which made up almost 40% of the biomass (Rosell and Srivastava 1984). In addition to alginates, the storage levels of carbohydrates laminarin and mannitol have also increased due to the rise in the water temperature and irradiation during the summer. These can be used during cold winters as reserve carbohydrates to promote algal tissue growth (Adams et al. 2011; Black 1950). As a result, the elevated levels of carbohydrates in kelp were also accompanied by the lower levels of ash and crude protein content during S2. The corresponding r-values suggest a strong negative correlation between the carbohydrate and ash content of the sugar kelp for S1 and S2 and were r = -0.953 and r = -0.901, respectively, confirming the inverse relationship. Also, the carbohydrate content

of the sugar kelp was found to be linearly dependent with negative slope on the ash content and can be expressed as Y = -0.8803 X + 85.005, where Y is the crude carbohydrate value (g (100 g)$^{-1}$ dry solids) and X is the ash content (g (100 g)$^{-1}$ dry solids) with correlation coefficient (R^2 = 0718) (**Fig. 4.1**).

Fig.4.1 Correlation between crude carbohydrate and ash content of the sugar kelp samples dried under sun, freeze dryer and heat pump dryer for both the seasons, early May (S1) and late June (S2)

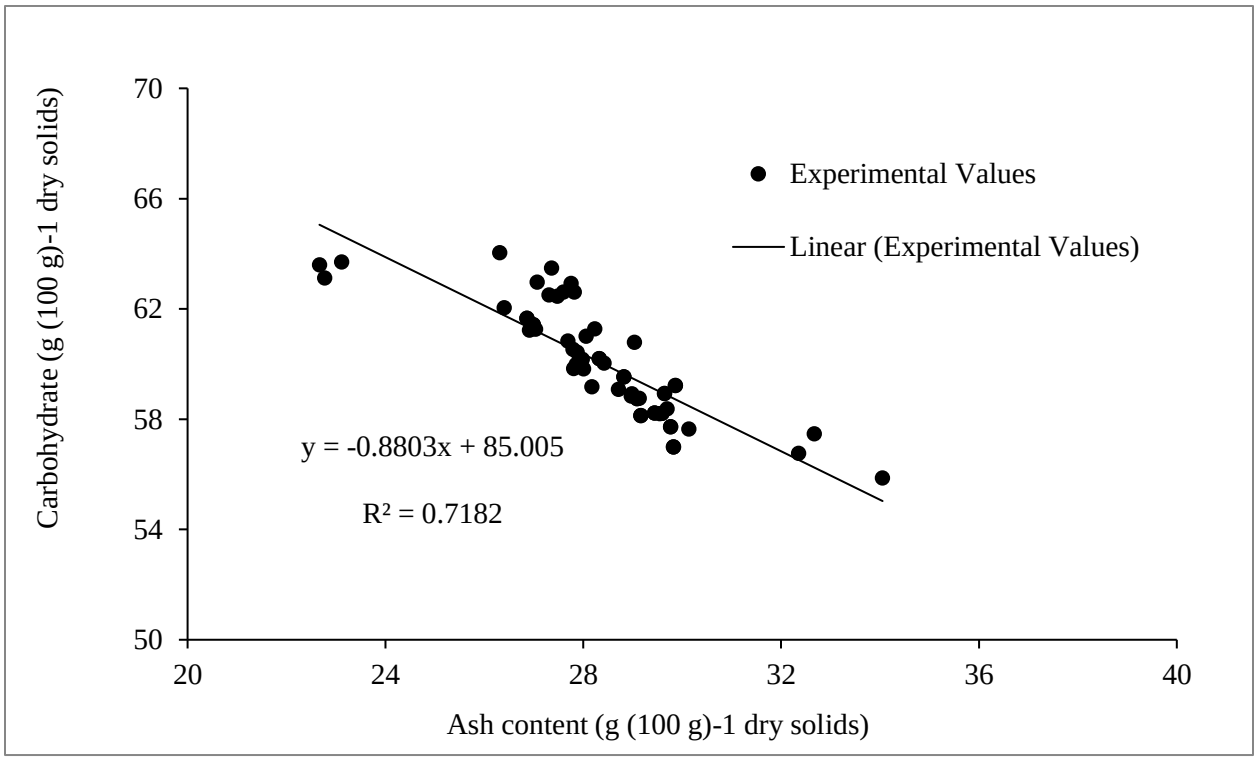

4.3.6. Water Holding Capacity (WHC)

The WHC of sugar kelp was higher than the three *Sargassum* species reported to be in the range of 506 – 1140 % (Wong and Cheung 2001). The statistical results indicated a significant effect ($p < 0.05$) of the drying conditions (temperature and humidity) on the WHC of dried sugar kelp (**Table 4.3)**. The WHC was the lowest for SD and FD kelp, and no significant difference ($p > 0.05$) was observed between them. The low values of WHC in FD kelp could be caused by slow freezing rates during the initial phase

of cooling, resulting in the formation of large ice crystals in the extracellular space between the cells, inflicting textural damage (Martino et al. 1998). Similar observations were also seen in the protein isolates of cowpea and bambara beans and carbohydrate-protein gum from durian fruit seed, where the WHC of the FD was less than the conventionally dried (Mirhosseini and Amid 2013; Mune and Sogi 2016). Case hardening is very common in foods that are dried at a faster rate and contain substantial amounts of soluble solids. This might have affected the kelp dried under the sun, where drying at a faster rate might have caused the soluble solids to migrate to the surface along with the moisture to form an impervious layer, creating a situation where the inner moisture was trapped by the hard-outer surface, resulting in poor WHC in SD kelp (Heldman 2013). The highest WHC values are seen among the significantly similar ($p > 0.05$) kelp dried at 70 °C, 50 °C and 30 °C, for both the seasons S1 and S2. This suggests that the textural properties of the sugar kelp were not dependent on the drying temperature. Furthermore, these results also support findings from our previous study reporting the relationship between the glass transition temperature (T_g) and the shrinkage rates of sugar kelp. The amorphous form of water, bound to the solid matrix in kelp, never transitioned from the initial rubbery to glassy states as the T_g of sugar kelp solids (47.02 °C) was never achieved (Sappati et al. 2017). Similar observations were also reported by Moreira et al. 2017, where they also found no significant differences between the shrinkage and the air-drying temperature in *Fucus vesiculosus*. There was a significant difference ($p < 0.05$) in the WHC of the dried kelp with respect to drying humidity (**Table 4.3**). The kelp dried at 25% humidity showed higher WHC compared to those dried at 50% humidity. Drying at 50% humidity at the same temperature might have damaged the porous structure due to shrinkage at the intracellular level, resulting in overall lower WHC (Kurozawa et al. 2012; Russo et al. 2012).

Table 4.3. Water holding capacity (WHC %) and oil holding capacity (OHC %) of sugar kelp harvested in season S1 (early May) and S2 (late June)

Humidity (%)	Treatment/ Temperature (°C)	Season 1 (S1)		Season 2 (S2)	
		WHC (%)	OHC (%)	WHC (%)	OHC (%)
25	30	2368.8 ± 48.1 bxA	235.4 ± 1.6 axA	1800.4 ± 50.2 bxB	219.1 ± 3.7 axB
	50	2289.4 ± 47.6 bxA	248.2 ± 3.5 axA	1872.4 ± 45.0 bxB	229.1 ± 5.1 axB
	70	2764.6 ± 4.8 bxA	220.3 ± 0.6 bxA	1766.6 ± 39.3 bxB	150.1 ± 8.0 bxB
50	30	2245.7 ± 48.2 byA	201.9 ± 8.7 ayA	1655.2 ± 20.5 byB	168.2 ± 2.8 ayB
	50	2295.8 ± 111.6 byA	217.1 ± 1.5 ayA	1585.3 ± 42.3 byB	153.6 ± 4.5 ayB
	70	2147.7 ± 30.9 byA	221.2 ± 5.6 byA	1633.5 ± 14.9 byB	190.3 ± 5.2 byB
N/A	FD	2061.6 ± 13.7 aA	225.7 ± 1.2 aA	1712.1 ± 60.0 aB	190.1 ± 2.9 aB
	SD	2095.5 ± 126.0 aA	205.9 ± 1.2 bA	1559.5 ± 20.0 aB	175.6 ± 1.9 bB

Results are mean ± standard deviation of triplicate for each sample (n = 3) for WHC and duplicate for each sample (n = 2) for OHC. Significant differences between the values are measured at $p < 0.05$. Small letter (a, b): denotes row-wise comparison between treatments or with air drying temperatures.
Capital letter (A, B): denotes comparison between harvesting seasons, S1 and S2.
x/y: denotes comparison between the drying humidity
FD: Freeze dried samples
SD: Sun dried samples

Irrespective of temperature and humidity, sugar kelp harvested during S1 exhibited significantly ($p < 0.05$) higher WHC as compared to S2 (**Table 4.3**). Alginates consist of GG, MM and GMGM sequenced blocks depending on the species, source and time of harvest (Lee and Mooney 2012). The G-blocks of alginate are responsible for hydrogel forming activity in the presence of cations such as Ca^{2+} by intermolecular cross-linking (George and Abraham, 2006). The water holding ability and gel formation activity of alginates depends on the quantity and the length of the G blocks present in the alginate chain, hence low M/G ratios in alginates are associated with higher gel strength and WHC. Manns et al. (2017) have reported the seasonal variation of M/G ratio present in sugar kelp with respect to the harvesting period. According to their data, the M/G ratio during the month of May was 1.80, which increased to 2.34 at the end of June. This supports our observation of higher WHC in S1 samples. Furthermore, dietary fibers are present at around 33-50 g $(100\ g)^{-1}$ dry solids in seaweeds and are mostly in the soluble form (Jiménez-Escrig and Cambrodon 1999; Rupérez and Saura-Calixto 2001). These soluble fibers exhibit a significant amount of water binding capacities and are prone to alteration due to processing methods such as grinding, drying, heating or extrusion (Camire and Flint 1991; Thibault et al. 1992). In *Sargassum horneri*, the dietary fiber content was found to be highest (6.68 g $(100\ g)^{-1}$ sample) in the month of March followed by gradual decline (Murakami et al. 2011). Also, the protein content can also impart certain desired functional characteristics in the food, especially emulsification, water/oil binding and foaming (Kinsella and Melachouris 2009). The polar groups present in protein can form hydrogen bonds with the water and enhance the hydration in the dried seaweeds (Ahmedna et al. 1999). In our study we found the corresponding r-value between the nitrogen content and WHC of the dried kelp was $r = 0.676$, suggesting higher protein in dried kelp may result in higher WHC. Finally, this suggests that the low M/G ratio, high % of dietary fibers and protein content in the sugar kelp belonging to S1, may all have contributed in varying degrees to the higher WHC as compared to S2.

4.3.7. Oil Holding Capacity (OHC)

Dried sheets of seaweeds are commonly consumed through use in soups or as sushi wraps.

However, some seaweed dishes and snacks are prepared by frying the sheets in oil. So, low OHC can also be one of the quantitative parameters in dried kelp of interest to consumers who are trending towards low-fat containing products (Dana and Saguy 2006). In contrast, high OHC in some of the food ingredients imparts certain desirable functional properties such as stabilization of food emulsions, flavor entrapment and lipid binding (Brewer et al. 2016). This suggests that, depending on its functional properties, dried kelp can be practically used in wide applications of food formulations.

The OHCs of dried sugar kelp were found to be higher than the 84% reported for three *Sargassum* species (Wong and Cheung, 2001). The results from this study indicated that the drying conditions (temperature and humidity) significantly ($p < 0.05$) influenced the capacity for oil absorption (OHC) in the dried sugar kelp (**Table 4.3**). The highest average OHCs were seen among the significantly similar ($p > 0.05$) kelp dried at FD, 50 °C and 30 °C conditions. Slow initial freezing rate might have ruptured the cell walls resulting in more void space and overall increase in the pore surface area of the FD kelp (Setiady et al. 2009). On the other hand, surface tension within the capillaries of the food matrix may also play a vital role in the oil absorption process (Kinsella and Melachouris 2009). Therefore, the FD kelp showed the highest oil absorption due to an increase in the porosity caused by the bursting of the cell wall. This also may have leached out the water binding components, such as dietary fiber, into the rehydration water, indicating lower WHC. The OHC was the lowest for the SD and 70 °C and no significant difference ($p > 0.05$) was observed among them. Again, case hardening due to faster drying rates might have formed an impervious layer, resulting in poor OHC in these samples. Furthermore, the OHC of the kelp harvested during S1 exhibited significantly ($p < 0.05$) higher OHC as compared to S2, irrespective of the drying conditions (**Table 4.3**). It is also believed that in addition to oil absorption through capillary action, interactions between oil and the hydrophobic components, especially the lipid and protein content in the food, also binds the oil (Hayta et al. 2002). The major fatty acids present in the corn oil used for testing OHC are palmitic acid (16:0), oleic acid (18:1) and linoleic acid (18:2) (Baur and Brown 1945). As a result, the non-polar side chains of the lipids and protein present in the seaweed might have attracted to

the fatty acids present in the corn oil and contributed towards the OHC of the food (Mirhosseini and Amid 2013). The correlation between the nitrogen content and OHC of the dried kelp was r = 0.444, suggesting higher protein content might have resulted in higher OHC. In our study, we also found higher lipid content and nitrogen content in the sugar kelp harvested during S1, possibly leading towards overall higher OHC.

4.3.8. Color

The change in color (∆E) along with the colorimetric coordinates L* (black-white), a* (green-red) and b* (blue-yellow) for the fresh and the dried sugar kelp are presented in **Table 4.4**. The L*, a* and b* values for the fresh sugar kelp were 19.39 ± 1.44, 0.71 ± 0.26 and 8.99 ± 0.89, respectively for S1 and 19.18 ± 0.72, 0.68 ± 0.17 and 10.06 ± 0.78, respectively for S2. From **Table 4.4**, all the treatment values for ΔE were significantly higher than 6.0 (p <0.05), showing a strong effect of the drying conditions (temperature and humidity) on the overall change in color (Silva and Silva, 1999). In addition, the ∆E values were the lowest for sun-dried, 30 °C, and 50 °C, while the highest difference is seen in 70 °C and freeze-dried kelp, for both the seasons, S1 and S2. Furthermore, the change in color ∆E was found to be positively correlated to the total phenolic content and the FRAP activity, which is discussed in detail in their respective sections of TPC and FRAP, below.

Table 4.4. Color analysis of sugar kelp harvested in season S1 (early May) and S2 (late June)

Humidity	Temperature/Treatment	Season 1 (S1)				Season 2 (S2)			
		L*	a*	b*	ΔE	L*	a*	b*	ΔE
25%	30°C	35.73 ± 1.04 axA	-0.34 ± 0.01 bxA	18.00 ± 0.20 cxA	18.7 ± 1.0 bxA	30.02 ± 0.58 axB	0.05 ± 0.05 bxB	14.54 ± 0.59 cxB	11.8 ± 0.3 bxB
	50°C	37.14 ± 1.30 axA	-0.80 ± 0.07 cxA	19.00 ± 0.42 bcxA	20.4 ± 1.1 bxA	28.23 ± 0.38 axB	0.63 ± 0.04 cxB	13.23 ± 0.16 bcxB	9.6 ± 0.4 bxB
	70°C	37.93 ± 1.31 bxA	-0.98 ± 0.02 axA	19.48 ± 0.69 bxA	21.4 ±1.2 axA	36.02 ± 0.34 bxB	1.17 ± 0.03 axB	16.43 ± 0.37 bxB	18.0 ± 0.2 axB
50%	30°C	39.39 ± 0.08 ayA	-0.48 ± 0.03 byA	18.71 ± 1.23 cyA	22.3 ± 0.5 byA	34.60 ± 0.52 ayB	0.11 ± 0.07 byB	15.96 ± 0.56 cyB	16.5 ± 0.3 byB
	50°C	39.07 ± 1.13 ayA	-0.28 ± 0.05 cyA	19.53 ± 1.29 bcyA	22.4 ± 0.4 byA	36.41 ± 0.19 ayB	0.87 ± 0.04 cyB	17.37 ± 0.26 bcyB	18.7 ± 0.1 byB
	70°C	40.88 ± 0.61 byA	1.09 ± 0.05 ayA	18.42 ± 1.30 byA	23.5 ± 1.1 ayA	36.11 ± 0.13 byB	2.37 ± 0.07 ayB	17.26 ± 0.19 byB	18.5 ± 0.1 ayB
N/A	FD	39.67 ± 0.96 aA	0.96 ± 0.05 aA	14.11 ± 0.29 aA	20.9 ± 1.0 aA	37.17 ± 2.48 aB	0.85 ± 0.19 aB	13.68 ± 0.33 aB	18.3 ± 2.5 aB
	SD	36.82 ± 0.45 bA	-0.55 ± 0.04 bA	18.80 ± 0.51 bcA	20.0 ± 0.4 bA	31.86 ± 0.64 bB	0.15 ± 0.11 bB	15.93 ± 0.11 bcB	14.0 ± 0.5 bB
	Fresh	19.39 ± 1.44 cA	0.71 ± 0.17 dA	8.99 ± 0.89 dA	-	19.18 ± 0.72 cB	0.68 ± 0.89 dB	10.06 ± 0.78 dB	-

Results are mean ± standard deviation of triplicate for each sample (n = 3). Significant differences between the values are measured at $p < 0.05$. Small letter (a, b, c, d): denotes row-wise comparison between treatments or with air drying temperatures.
Capital letter (A, B): denotes comparison between harvesting seasons, S1 and S2.
x/y: denotes comparison between the drying humidity

The observed L* and b* values increased for all the drying treatments as compared to the fresh sugar kelp, resulting in all the treated kelp being more light and yellowish. Elevated temperatures during drying can possibly induce the replacement of the central magnesium ion in chlorophyll a with two hydrogen ions, resulting in an undesirable olive brown color due to the formation of pheophytin (Turkmen et al. 2006). Potisate and Phoungchandang (2010) found that the concentration of chlorophyll a was reduced by high drying temperature in ivy gourd leaf using a heat pump based drying system. Fucoxanthin, a major carotenoid in brown seaweeds, is quite stable as compared to chlorophyll a in the presence of organic solvents, high temperature, oxygen, and light. Thermal processing such as blanching, boiling, steaming and sterilizing increased the free fucoxanthin content in *Sargassum ilicifolium* (Eko Susanto et al. 2017). A higher amount of available fucoxanthin content was also reported in dried *Undaria pinnatifida* while storing at 50 °C for 210 days and during baking at a temperature of 190 °C (Sugimura et al. 2012). Moreover, chlorophyll a can also be easily degraded by the chlorophyllase enzyme at temperatures higher than 60 °C (Erge et al. 2008). The b* values of the freeze-dried kelp were the closest to the fresh sugar kelp, while the second least differences were seen in the sample dried at 50 °C and 25% humidity. This indicates that an increase in drying temperature and humidity resulted in a higher concentration of free fucoxanthin and formation of undesirable colored and volatile substances, due to the enzymatic or non- enzymatic degradation of chlorophyll a (Drążkiewicz and Krupa 1991; Maskan 2001).

Dried sugar kelp in S1 showed significantly ($p < 0.05$) higher values of L* and b* values compared to the sugar kelp from S2. It is speculated that the colder temperature coupled with lower radiation during S1 resulted in high production of fucoxanthin through the activated xanthophyll-cycle pathway, possibly a response due to overstressed conditions (Eonseon et al. 2003). A similar trend was also observed in the case of *Sargassum horneri* and *Undaria pinnatifida*, where the fucoxanthin content was higher in the winter and spring than in the summer (Campbell et al. 1999; Terasaki et al. 2017).

Finally, low concentration of fucoxanthin during S2 may have resulted in the overall lower values of L*, b* and ∆E, and less browning of the kelp dried under the same drying conditions.

4.3.9. Total Phenolic Content (TPC)

Phenolic compounds present in the seaweeds are highly heat-sensitive, and their chemical activity can be altered vastly due to the applied processing conditions (Dang et al. 2016; Randhir et al. 2007). In this study, the drying temperature and humidity had a significant effect ($p < 0.05$) on the TPC of the sugar kelp, where the levels dropped by approximately 10 fold as compared to the fresh kelp **(Table 4.5)**. The highest amount of phenolic activity was exhibited by the freeze-dried and lowest by the kelp dried at 70 °C. The highest values in the FD were possibly due to less oxidation at low temperature and in the presence of little air under vacuum while drying, resulting in overall higher values of phenolic compounds (Hossain et al. 2010). The TPC values were not significantly different ($p > 0.05$) for the kelp dried at 30 °C and 50 °C, or for the sundried and 50 °C. The heat treatment might have caused cellular damage, followed by the release of bound phenolic compounds, showing an increase in TPC activity until 50 °C. Further heating might have induced higher enzymatic activity and oxidative stress leading to thermal degradation of the phenolic compounds (Lim and Murtijaya 2007; Tomaino et al. 2005). In addition, phenolic compounds are bound within the carbohydrate, protein and fatty acid matrix of the food structure (Randhir et al. 2007). An increase in phenolic activity has been reported in *Himanthalia elongata* under hydrothermal processing at 95 °C for 15 mins (Rajauria et al. 2010) as the heat treatment released these bound phenolic compounds from the food matrix. Furthermore, some reports also suggested that oven drying is better than freeze-drying in retaining the phenolic compounds (Ling et al. 2015; Wong and Cheung 2001), however, in this study freeze-dried kelp exhibited overall higher phenolic activity. The kelp dried at 25% exhibited values higher ($p < 0.05$) than kelp dried at 50% humidity, suggesting the phenolic compounds may have deteriorated due to oxidative stress caused by longer drying times at the same temperature **(Table 4.5)**. Low humidity reduces the drying time due to the increase in mass transfer rates at the same temperature (Djaeni and Sari 2015; Sappati et al. 2017). A similar finding was also

reported by Dang et al. (2017), where drying at high temperature (60 °C) and low humidity (11.1%), resulted in better retention of nutrients in H. *banksii*.

The initial content of total phenolic compounds found in the methanolic extracts of sugar kelp was 3.58 ± 0.14 mg GAE g^{-1} dry solids and 4.84 ± 0.26 mg GAE g^{-1} dry solids, for S1 and S2, respectively **(Table 4.5)**. These values are in the range reported for other brown seaweeds such as *Sargassum marginatum* (0.29 mg GAE g^{-1} dry solids), *Padina tetrastomatica* (0.61 mg GAE g^{-1} dry solids) and *Turbinaria conoides* (0.86 mg GAE g^{-1} dry solids) and *Himanthalia elongata* (15.5 mg GAE g^{-1} dry solids) (Chandini et al. 2008; Rajauria et al. 2010). The highest levels of phenolic compounds in the fresh kelp were seen in the late harvest season S2, which are in agreement with the observations of Scheiner et al. (2015) and Vilg et al. (2015). The synthesis of phenolic compounds is shown to increase with the rise in water temperature and light intensity, resulting in higher observed values during S2 (Aquino-Bolaños and Mercado-Silva 2004; Pavia et al. 1997). According to Lann et al. (2012), the increase in solar radiation during summer results in the production of higher amounts of phlorotannin, primarily responsible for the phenolic activity. However, during summer, S2, the phenolic activity of the kelp dried under sunlight was reduced significantly ($p < 0.05$) as compared to the fresh sugar kelp **(Table 4.5)**. These findings can be possibly explained by the exposure to the higher intensity of the radiation (UVA-UVB, IR and Microwaves) causing faster deterioration rates and resulting in lower values of TPC (Klein and Kurilich 2000).

Table 4.5. Phenolic content and antioxidant activity (TPC, FRAP and DPPH) of sugar kelp harvested in season S1 (early May) and S2 (late June)

Humidity	Treatment/ Temperature	Season 1 (S1)			Season 2 (S2)		
		TPC (mg GAE g^{-1} dry solids)	FRAP (µmol FSE g^{-1} dry solids)	DPPH, EC_{50} (mg dry solids mL^{-1})	TPC (mg GAE g^{-1} dry solids)	FRAP (µmol FSE g^{-1} dry solids)	DPPH, EC_{50} (mg dry solids mL^{-1})
25%	30°C	0.775 ± 0.041 cxA	6.43 ± 0.00 axA	8.61 cxA	0.376 ± 0.014 cxB	5.08 ± 0.54 axB	17.32 cxB
	50°C	0.758 ± 0.036 bcxA	6.31 ± 0.14 axA	9.38 cxA	0.668 ± 0.032 bcxB	5.76 ± 0.33 axB	11.75 cxB
	70°C	0.536 ± 0.037 dxA	6.34 ± 0.29 bxA	13.76 dxA	0.265 ± 0.019 dxB	3.33 ± 0.21 bxB	25.58 dxB
50%	30°C	0.543 ± 0.014 cyA	5.40 ± 0.42 ayA	13.25 cyA	0.308 ± 0.014 cyB	3.79 ± 0.14 ayB	22.29 cyB
	50°C	0.495 ± 0.036 bcyA	5.39 ± 0.29 ayA	12.75 cyA	0.238 ± 0.024 bcyB	2.95 ± 0.14 ayB	28.43 cyB
	70°C	0.296 ± 0.018 dyA	3.41 ± 0.07 byA	20.60 dyA	0.220 ± 0.014 dyB	2.94 ± 0.20 byB	31.48 dyB
N/A	FD	0.565 ± 0.021 aA	4.54 ± 0.13 aA	11.05 aA	0.693 ± 0.043 aB	5.71 ± 0.70 aB	9.07 aB
	SD	0.823 ± 0.014 bA	6.83 ± 0.29 aA	8.59 bA	0.282 ± 0.010 bB	3.60 ± 0.21 aB	19.53 bB
	Fresh	3.580 ± 0.139 eA	31.36 ± 2.22 cA	1.71 eA	4.837 ± 0.265 eB	26.65 ± 2.22 cB	1.26 eB

Results are mean ± standard deviation of triplicate for each sample (n = 3) except DPPH, where absorption value of triplicates are used for calculating EC_{50} value. Significant differences are measured at $p < 0.05$. Small letter (a, b, c, d, e): denotes row-wise comparison between treatments or with air drying temperatures.
Capital letter (A, B): denotes comparison between harvesting seasons, S1 and S2.
x/y: denotes comparison between the drying humidity

4.3.10. Ferric Reducing Antioxidant Power (FRAP)

The FRAP method measures the ferric reducing ability of the methanolic extracts of the sugar kelp based on the redox reaction. Previously, several authors have conducted FRAP assay on the various extracts of red and brown seaweeds (Dang et al. 2016; Ling et al. 2015; Neoh et al. 2016; Rajauria et al. 2010). The antioxidants present in the seaweed act as electron donors and at low pH, the complex ferric - tripyridyltriazine (Fe^{III} - TPTZ) is reduced to the ferrous form (Fe^{II}), producing an intense blue color solution showing maximum absorption at 593 nm.

The initial FRAP values of the fresh sugar kelp were 31.36 ± 2.22 µmol FSE g^{-1} dry solids and 26.65 ± 2.22 µmol FSE g^{-1} dry solids, for S1 and S2, respectively. The reducing potential of the dried sugar kelp extracts was significantly lower ($p < 0.05$) than the fresh kelp, for all the treatments. The values were not significantly different ($p > 0.05$) for the SD, 30 °C, 50 °C and FD kelp **(Table 4.5)**. However, drying above 50 °C resulted in a significant loss of the reducing capacity, as the lowest value was observed at 70 °C. The kelp dried at 25% humidity exhibited higher values of FSE as compared to the 50% humidity, similar to the trend for TPC. The polyphenolic compounds derived from seaweeds can potentially act as antioxidants by forming metal complexes, reducers (electron donors), proton donors and free radical scavengers (Leopoldini et al. 2004). The reducing capacity of the sugar kelp was found to be linearly dependent on the phenolic content, and can be expressed as Y = 5.874 X + 1.928, where Y is the FRAP value (µmol FSE g^{-1} dry solids) and X is the TPC (mg GAE g^{-1} dry solids) with correlation coefficient ($R^2 = 0.857$) (**Fig. 4.2**). The positive correlation between the FRAP and TPC values can also be quantified with the Pearson correlation coefficient (r), the values for S1 and S2 were r = 0.857 and r = 0.936, respectively. The strong correlation between FRAP and TPC was also reported in several seaweeds such as *Hormosira banskii* (Dang et al. 2017), *Sargassum muticum* and *Bifurcaria bifurcata* (Lann et al. 2008). Furthermore, the Pearson correlation between the change in color, ∆E and TPC was -0.729 and -0.273, for S1 and S2, respectively. Similarly, the r-values between ∆E and TPC were found to be -0.546 and -0.433, for S1 and S2, respectively. These moderately negative correlations suggest that the change in

color ∆E is a direct reflection of the loss of TPC and the FRAP activity in the sugar kelp. Contrasting results were reported by Rajauria et al. (2010), where the increase in ∆E value was reflected in higher phenolic and antioxidant content. An explanation of these observations may be that short exposure to elevated temperatures might have inactivated the deteriorative enzymes in seaweeds and released more pigments in the form of carotenoids bound in the solid matrix, resulting in higher change in color and overall phenolic activity. In contrast, drying at lower temperatures for extended periods might not have inactivated the enzymes responsible for the oxidation of these phenolic compounds, resulting in higher change in color with low phenolic activity.

Fig. 4.2. Correlation of ferric reducing antioxidant power value (µmol FSE g^{-1} dry solids) and total phenolic content (mg GAE g^{-1} dry solids) of the sugar kelp samples dried under sun, freeze dryer and heat pump dryer for both the seasons, early May (S1) and late June (S2)

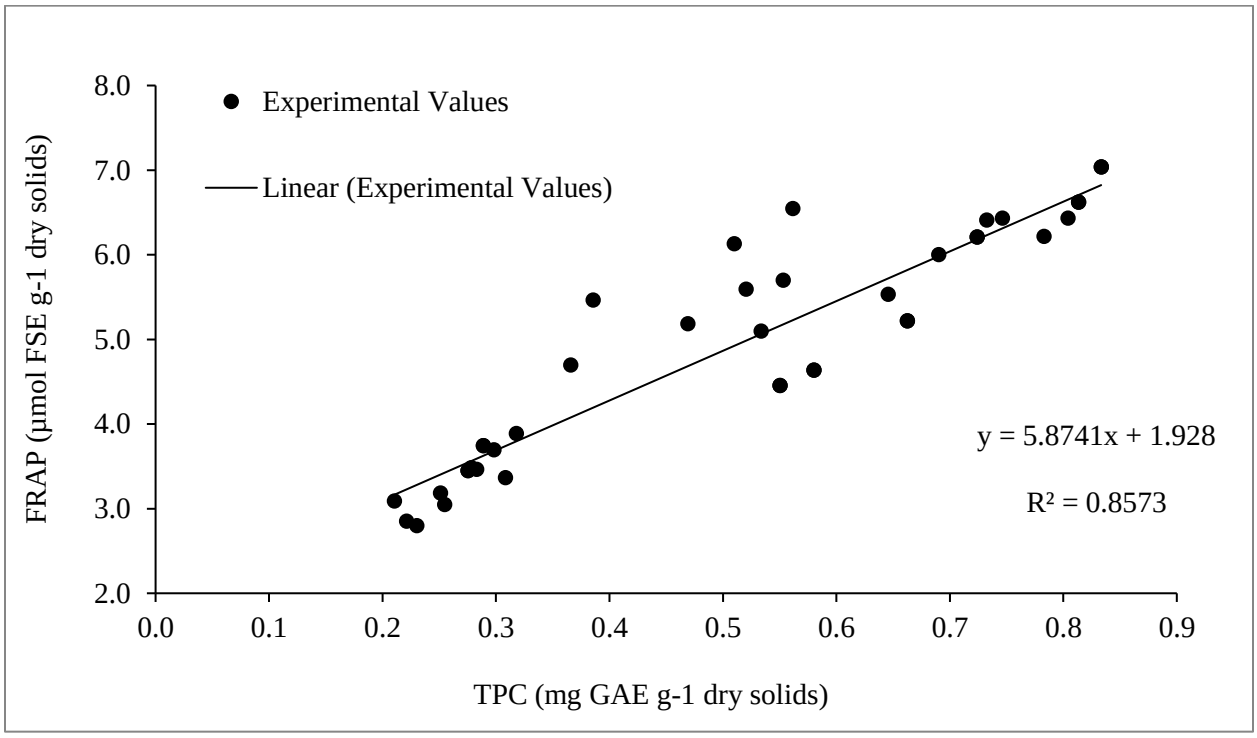

4.3.11. DPPH (α, α-diphenyl-β-picrylhydrazyl) Assay

DPPH is stable organic nitrogen-based radical exhibiting maximum absorption at 515 nm. The underlying mechanism for DPPH is believed to involve the transfer of a hydrogen atom. However, in the presence of strong hydrogen bond-forming solvents such as methanol and ethanol, the fast electron transfer process to DPPH dominates the very slow transfer of hydrogen atoms, hence becoming the rate-determining step for the kinetics (Foti et al. 2004). The FRAP and DPPH assays work on the same principle of electron transfer. In the case of DPPH, the electron-donating capacity of the compounds to quench free radicals is measured in a similar fashion to the electron transfer responsible for reducing the ferric Fe(III) to ferrous Fe(II) in the FRAP assay. The antioxidant activity measured using DPPH was expressed as EC_{50} value, defined as the concentration of substrate required to cause a 50% loss in the DPPH activity. Therefore, a higher value indicates weaker antioxidant activity.

The EC_{50} values for the fresh kelp were 1.71 mg dry solids mL^{-1} and 1.26 mg dry solids mL^{-1}, for S1 and S2, respectively **(Table 4.5)**. The effect of drying was observed on the EC_{50} as all the treatments significantly reduced ($p < 0.05$) the antioxidant capacity in the dried kelp **(Table 4.5)**. The antioxidant activity measured by DPPH showed a similar trend as the TPC values. The lowest values of EC_{50} were observed in the FD followed by the kelp dried under the sun, 30 °C, 50 °C and the highest at 70 °C. The antioxidant activity of the sugar kelp was also found to be linearly dependent with negative slope on the phenolic content and can be expressed as $Y = -30.576\ X + 31.184$, where Y is the EC_{50} value (mg dry solids mL^{-1}) and X is the TPC (mg GAE g^{-1} dry solids) with correlation coefficient ($R^2 = 0.835$) (**Fig. 4.3**). The corresponding correlations between the TPC and EC_{50} for S1 and S2 were, r = -0.925 and r = -0.910, respectively, suggesting a strong inverse relationship. The FRAP and DPPH also showed a strong negative correlation, r = -0.752 and r = -0.912, for S1 and S2, respectively, indicating that both the assays were able to capture all the potential antioxidant species in the sugar kelp. The kelp dried at 25% humidity exhibited lower values ($p < 0.05$) of EC_{50} as compared to 50% humidity at the same temperature (**Table 4.5**). These values are consistent with the trends observed in the TPC and FRAP data, where the

longer residence time at high humidity may have caused oxidative and thermal deterioration.

Fig. 4.3. Correlation of DPPH radical scavenging capacity, EC_{50} (mg dry solids/ ml) and total phenolic content (mg GAE/ g dry solids) of the sugar kelp samples dried under sun, freeze dryer and heat pump dryer for both the seasons, early May (S1) and late June (S2)

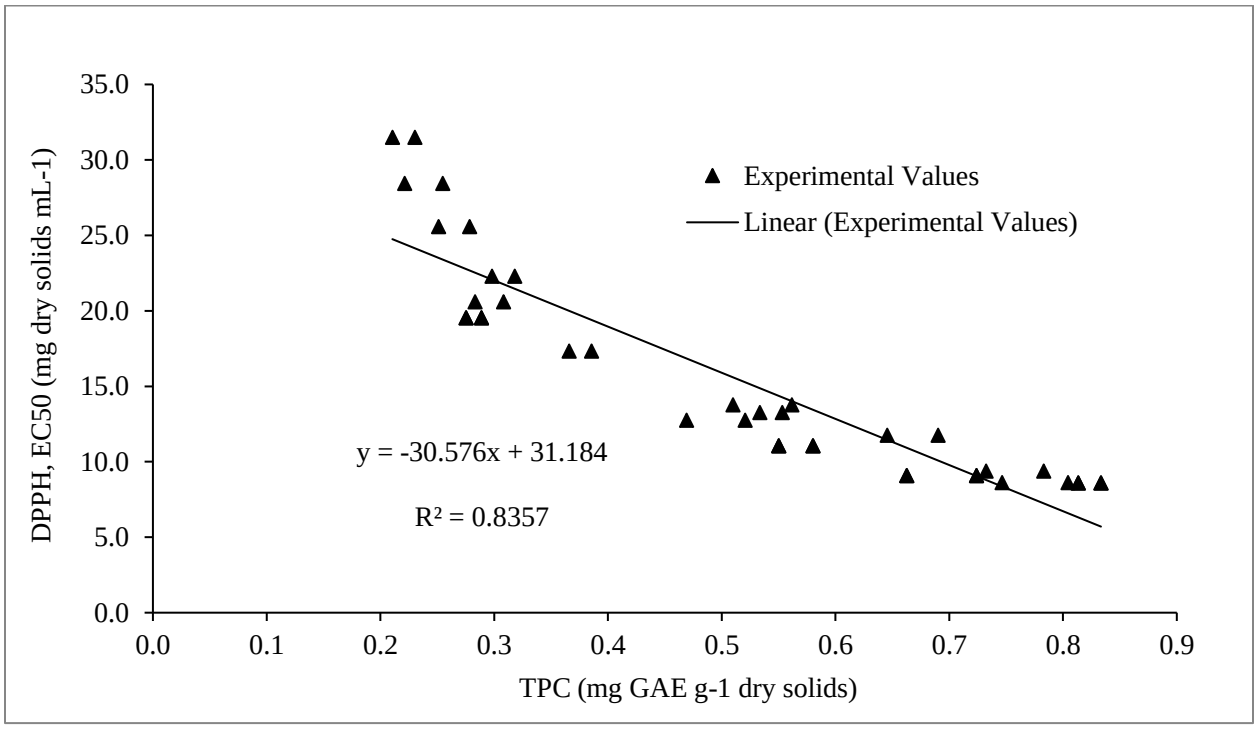

The dried S1 sugar kelp showed significantly ($p < 0.05$) lower values of EC_{50} compared to the dried S2 (**Table 4.5**). The primary compounds present in brown seaweeds responsible for free radical scavenging activity are phloroglucinol (polyphenol) and fucoxanthin (Airanthi et al. 2011). These compounds showed a positive correlation between the fucoxanthin content and the DPPH radical scavenging activity (Airanthi et al. 2011; Fariman et al. 2016). Moreover, winters in Maine, US, are characterized by low irradiation levels and higher nutrient availability compared to the other seasons. Higher availability of nutrient content is responsible for the accumulation of photosynthetic compounds, which also results in elevated levels of protein (Chopin et al. 1999; Harrison and Hurd 2001). Studies

have shown that under low light intensity, photosynthetic efficiency increases due to the higher production of light-harvesting molecules (Lüning 1990). Therefore, it can be assumed that the combination of cold-water temperature accompanied by elevated nutrients and lack of sunshine resulted in higher levels of fucoxanthin and lower level of phenolic compounds during S1 (Aquino-Bolaños and Mercado-Silva 2004; Lüning 1990; Pavia et al. 1997). As a result, low concentration of fucoxanthin and elevated polyphenols during S2, might have resulted in the lower values of TPC, FRAP and DPPH radical scavenging activity due to the enzymatic and non-enzymatic degradation of the compounds responsible for the antioxidant and phenolic activity.

4.3.12. Water Activity, pH, TSS and Vitamin C

The water activity of fresh kelp was found to be 0.929 ± 0.025. Drying decreases the water activity of the fresh kelp below the limiting water activity ($a_w < 0.6$), which results in reduced storage volume, prolonged shelf life by retarding microbial growth and preserving the chemical/physical properties (Gupta et al. 2011). The corresponding values of water activity of dried kelp under different drying conditions are listed in **Table 4.6**. The lowest value of a_w was exhibited by freeze-dried kelp for both season S1 and S2, with a_w of 0.154 ± 0.003 and 0.189 ± 0.013, respectively. The rest of the dried samples were in the range of 0.401 - 0.484 for S1 and 0.387 - 0.566 for S2. There was a significant difference ($p < 0.05$) in the a_w of the sugar kelp with different drying temperature, humidity or season. The Pearson correlation coefficient of water activity with respect to the moisture content of the sample was found to be r = 0.926. This shows the a_w of the dried seaweed was positively correlated to its moisture content, which is described appropriately by nonlinear behavior of moisture sorption isotherm at constant temperature (Lemus et al. 2008; Mohamed et al. 2005; Moreira et al. 2016; Moreira et al. 2017; Sappati et al. 2017; Vega-Gálvez et al. 2008). Overall, water activity values for the dried kelp were higher for S2 than for S1. Moreover, kelp dried at 50% humidity had higher water activity when compared to 25% humidity, as higher humidity increased the equilibrium moisture content of the sugar kelp. Therefore, this suggests that S2 dried kelp required a longer drying time due to higher free water in late

season kelp.

The pH of both fresh and dried kelp under different treatments are shown in **Table 4.6**. Even though significant differences were found between drying temperatures ($p < 0.05$), there were no major changes in the pH of dried kelp. The pH values were highest for fresh kelp followed by FD, 30 °C, 50 °C, 70 °C and SD in decreasing order and in the range of 6.39 ± 0.02 - 6.67 ± 0.02 and 6.06 ± 0.01 - 6.67 ± 0.16, for S1 and S2, respectively. A similar phenomenon of increasing acidity in sugar kelp was also seen in case of tomato and mango, where the rise in drying temperature resulted in increase of the titratable acidity predominantly due to the concentration of biomass due to moisture loss (Das Purkayastha et al. 2013; Kumar and Sagar 2014). The drop in pH of the dried kelp was significantly ($p < 0.05$) higher for the kelp harvested in S2 as compared to S1. Seasonal variations in several organic acids such as amino acids, fatty acids, alginic acid, and uronic acid might contribute to varying degrees towards the pH of the sugar kelp.

The effects of drying conditions on the total soluble solids (TSS) of the sugar kelp were significant ($p < 0.05$) (**Table 4.6**). The TSS represents the total soluble fraction present in the food which is present mostly in the form of soluble sugars. The TSS of the kelp was found to be in the range of 27.33 - 38.00 and 27.33 - 40.00, for S1 and S2, respectively, which is similar to the soluble dietary fibers present in some of the seaweeds (33-50 g $(100\ g)^{-1}$ dry solids) (Jiménez-Escrig and Cambrodon 1999; Rupérez and Saura-Calixto 2001). The presence of considerable amounts of water-soluble polysaccharides such as sodium alginate, laminarin, and mannitol in sugar kelp might be responsible for high water solubility (Zvyagintsevaa et al. 1999). The TSS of the sugar kelp showed a negative linear correlation with respect to its moisture content in our previous study, primarily due to the concentration of solids in dried kelp (Sappati et al. 2017). This relationship was also observed here as the correlation between the TSS and MC of the sugar kelp was r = -0.554 and r = -0.599, for S1 and S2, respectively. The lowest TSS values were found in the SD and 70 °C dried kelp. A faster drying rate might have caused the trapping of the soluble dietary fibers within the impervious layer (case-hardening), resulting in poor

solubility (Heldman 2013). The FD kelp showed the highest TSS values as the formation of ice crystals might have ruptured cell walls, which could result in leaching of the soluble dietary fiber into water. The kelp dried at 25% humidity exhibited TSS values higher ($p < 0.05$) than 50% humidity, possibly due to the low moisture content in the 25% humidity dried kelp. Again, it has been previously discussed in the WHC section that the presence of higher percent of dietary fibers in the kelp harvested in S1 might have resulted in significantly ($p < 0.05$) higher TSS as compared to S2.

The vitamin C content was studied to determine the effect of different drying temperatures and humidity on vitamin C in the sugar kelp. Vitamin C levels in fresh kelp were 0.452 ± 0.009 and 0.611 ± 0.074 mg ascorbic acid g^{-1} dry solids, for S1 and S2, respectively (**Table 4.6)**. In dried kelp, the vitamin C levels dropped approximately 5-10 fold as compared to fresh kelp (**Table 4.6**). There was no significant effect ($p < 0.05$) of the drying conditions (temperature and humidity) as well as the season. In this study, vitamin C content in sugar kelp was found to be much lower (0.052 mg g^{-1} wet sample) than in some other seaweeds such as *Eucheuma cottonii*, *Caulerpa lentillifera* and *Sargassum polycystum* (0.35 mg g^{-1} wet sample) (Matanjun et al. 2009).

Table 4.6. Physico-chemical properties (Water Activity, pH, TSS and Vitamin C) of sugar kelp harvested in season S1 (early May) and S2 (late June)

Humidity	Temperature/Treatment	Season 1 (S1)				Season 2 (S2)			
		a_w	pH	TSS (°Bx)	Vitamin C (mg ascorbic acid g^{-1} dry solids)	a_w	pH	TSS (°Bx)	Vitamin C (mg ascorbic acid g^{-1} dry solids)
25%	30°C	0.401 ± 0.002 cxA	6.56 ± 0.03 cA	37.33 ± 1.15 cxA	0.120 ± 0.022 a	0.456 ± 0.004 cxB	6.26 ± 0.01 cB	40.00 ± 2.00 cxB	0.130 ± 0.024 a
	50°C	0.352 ± 0.005 dxA	6.53 ± 0.02 cA	36.67 ± 1.15 cxA	0.100 ± 0.004 a	0.387 ± 0.001 dxB	6.24 ± 0.02 cB	30.00 ± 2.00 cxB	0.094 ± 0.010 a
	70°C	0.446 ± 0.001 bxA	6.44 ± 0.01 dA	27.33 ± 0.00 dxA	0.097 ± 0.049 a	0.566 ± 0.002 bxB	6.16 ± 0.04 dB	26.00 ± 1.15 dxB	0.102 ± 0.016 a
50%	30°C	0.484 ± 0.002 cyA	6.49 ± 0.04 cA	35.33 ± 1.15 cyA	0.094 ± 0.009 a	0.516 ± 0.000 cyB	6.20 ± 0.02 cB	27.33 ± 2.00 cyB	0.097 ± 0.023 a
	50°C	0.475 ± 0.001 dyA	6.51 ± 0.04 cA	38.00 ± 1.15 cyA	0.119 ± 0.010 a	0.561 ± 0.002 dyB	6.18 ± 0.01 cB	24.67 ± 1.15 cyB	0.076 ± 0.016 a
	70°C	0.431 ± 0.001 byA	6.39 ± 0.02 dA	36.00 ± 2.00 dyA	0.124 ± 0.022 a	0.533 ± 0.001 byB	6.12 ± 0.01 dB	26.67 ± 1.15 dyB	0.097 ± 0.008 a
N/A	FD	0.154 ± 0.003 aA	6.67 ± 0.02 aA	37.33 ± 1.15 aA	0.073 ± 0.115 a	0.189 ± 0.013 aB	6.35 ± 0.01 aB	36.67 ± 1.15 aB	0.115 ± 0.010 a
	SD	0.462 ± 0.001 bA	6.44 ± 0.01 bA	30.67 ± 1.15 bA	0.121 ± 0.012 a	0.530 ± 0.002 bB	3.06 ± 0.02 bB	31.33 ± 2.31 bB	0.098 ± 0.012 a
	Fresh	0.951 ± 0.001 eA	6.52 ± 0.08 eA	N/A	0.452 ± 0.009 b	0.907 ± 0.001 eB	6.67 ± 0.16 eB	N/A	0.611 ± 0.074 b

Results are mean ± standard deviation of triplicate for each sample (n = 3). Significant differences are measured at $p < 0.05$. Small letter (a, b, c, d, e): denotes row-wise comparison between treatments or with air drying temperatures.
Capital letter (A, B): denotes comparison between harvesting seasons, S1 and S2.
x/y: denotes comparison between the drying humidity

4.4. Conclusions

This is the first report comparing the effects of different drying methods (freeze drying (FD), sun drying (SD) and humidity and temperature-controlled drying (25% or 50% humidity and 30 °C, 50 °C or 70 °C) applied to sugar kelp on its physical and chemical properties. The increase in air drying temperature combined with low humidity increased the drying rate and decreased the total drying time. The final moisture content in the dried samples was less than 20% on a dry basis. As a result, the water activity was lower than the limiting water activity (0.6). The effects of seasonal harvesting time were very significant ($p < 0.05$) for moisture, fat, protein and carbohydrate content of the samples. In Maine, USA the relative increase in the availability of sunshine and water temperature in the month of June as compared to May resulted in a higher photosynthetic rate and accumulation of fats, carbohydrates, and moisture at the expense of protein in the later harvested kelp. After carbohydrates, the second most abundant component of the sugar kelp biomass was ash (~ 22 – 33 g (100 g)$^{-1}$ dry solids). In this study, ash contents were significantly similar ($p > 0.05$) for both the seasons S1 and S2. Results indicated the significant effect ($p < 0.05$) of the drying conditions (temperature and humidity) on the water and oil holding capacities (WHC and OHC) of dried sugar kelp. FD kelp exhibited the highest OHC and the lowest WHC likely due to bursting of cells and increased porosity, whereas SD performed poorly in both cases due to case hardening. Temperature-wise, the samples had similar WHC and OHC, however, at the lower humidity of 25%, the samples exhibited higher WHC and OHC. Seasonally, low mannuronic acid (M) and guluronic acid (G) (M/G) ratio in the alginate fraction, high % of dietary fibers and protein content in the samples belonging to S1 might be the possible reasons for higher values of WHC and OHC in S1. Change in color, ΔE, was also significantly affected ($p < 0.05$) by drying conditions and found to be negatively correlated to TPC and FRAP. Higher ΔE is thus an indicator of the loss of phenolic and antioxidant activity in the sugar kelp. Processing under any condition was found to reduce the TPC and FRAP values as compared to the fresh kelp. As expected, these values decreased with an increase in drying temperature and humidity. Also, drying below 50°C and at lower humidity were shown to be

preferable in terms of preserving the antioxidant and phenolic compounds as compared to FD. The pH and TSS values of the kelp were not affected by drying conditions and were similar to the fresh kelp. It can be concluded that the nutritional composition of sugar kelp is greatly affected by different drying methods and the harvesting period (**Table 4.7**). Moreover, the equipment and operating costs for freeze drying are higher and its drying capacity is much lower than that of customized HPD based drying systems. Hence an optimal drying strategy can be employed depending on economic factors and the way that the seaweeds will eventually be used.

Table 4.7. Summary of the effects of drying conditions on the physico-chemical properties of sugar kelp

Drying condition	Physico-Chemical Properties														
	MC	AC	Fat	Protein	Carbohydrate	WHC	OHC	ΔE	TPC	FRAP	DPPH	a_w	pH	TSS	Vit C
FD	a	a	a	a	a	a	a	a	a	a	a	a	a	a	a
SD	b	b	a	a	b	a	b	b	b	a	b	b	b	b	a
30°C, 25%	c	bx	a	ab	ab	bx	ax	bx	cx	ax	cx	cx	c	cx	a
50°C, 25%	c	cx	a	b	c	bx	ax	bx	bcx	ax	cx	dx	c	cx	a
70°C, 25%	c	dx	a	b	d	bx	bx	ax	dx	bx	dx	bx	d	dx	a
30°C, 50%	c	by	a	ab	ab	by	ay	by	cy	ay	cy	cy	c	cy	a
50°C, 50%	c	cy	a	b	c	by	ay	by	bcy	ay	cy	dy	c	cy	a
70°C, 50%	c	dy	a	b	d	by	by	ay	dy	by	dy	by	d	dy	a
Fresh	d	-	-	-	-	-	-	-	e	e	e	e	e	-	b

S1 and S2 had significant differences for every parameter in this table, and so are not shown here. The pattern of significance in the experimental design was identical for both seasons. Small letter (a, b, c, d, e): denotes row-wise comparison between treatments or with air drying temperatures.
x/y: denotes comparison between the drying humidity

CHAPTER 5

THERMOPHYSICAL PROPERTIES PREDICTION OF BROWN SEAWEED (*SACCHARINA LATISSIMA*) USING ARTIFICIAL NEURAL NETWORKS (ANNs) AND EMPIRICAL MODELS

5.1. Introduction

Knowing the thermal properties (thermal conductivity (k), thermal diffusivity (D), specific heat capacity (C)) of sugar kelp is important for predicting the influence of drying rate under different drying conditions on the overall chemical profile affecting the nutritional, functional and bioactive properties of the dried seaweeds. Furthermore, this information can also help optimize the design parameters of large-scale dryers to obtain uniform product quality. Although several research articles have reported the physicochemical properties of seaweeds and their variation with season and processing conditions, very limited information is available on the thermophysical properties of any type of seaweed based on its proximate constituents as compared to fruits, vegetables, and meat products. Fresh sugar kelp is a thin leafy sea vegetable which can be characterized as a continuous material with low porosity. Moreover, the glass transition temperature (T_g) of the kelp while air drying is always lower than the air temperature (Sappati et al. 2017). Consequently, the volume shrinkage during drying can be completely attributed to the volume lost due to moisture removal without creating any void space for air as the whole process of drying occurs completely in the rubbery phase above its T_g. However continuous monitoring of thermophysical properties while drying sugar kelp using dual needle probe can be experimentally challenging due to following reasons: 1) Due to its thin structure multiple blades of kelp need to be stacked along the heating needle 2) While drying, sugar kelp blade undergoes irregular shrinkage and might create inconsistent contact surface with the heating needle, and 3) Dried kelp becomes brittle and might break while stacking along the heating needle. Therefore, the granulated powder of kelp can be rehydrated to different moisture contents and packed in a cylindrical tube to measure the thermophysical properties of sugar kelp with respect to its moisture content, temperature, and porosity. This study has

been done on a variety of brown seaweed, sugar kelp (*Saccharina latissima*) to evaluate the effect of the moisture content and the temperature of the sample on its thermophysical properties.

Artificial neural networks (ANN), are models designed to function as a biological human brain, based on a progressive learning system. An ANN consists of a complex network of artificial neurons that perform in a function identical to biological neurons. The artificial neurons in one layer receive the input information and pass the activation value, calculated by subtracting the threshold value (bias) from the weighted input, through an activation function to the neurons connected in the next layer. The network training algorithm establishes a non-linear relationship between the input and output by adjusting the network weights and the threshold (bias) in order to minimize the error between the predicted value and training data set. Correspondingly, an ANN is capable of modeling complex nonlinear relationships due to its excellent fault tolerance, self-learning ability, and high computational capability as compared to traditional regression approaches based on individual food constituents. In recent years, ANNs have been applied across a wide range of problems in food science such as modeling microbial growth for food safety, interpreting spectroscopic data, process control and simulation, machine perception (electronic nose) and predicting physical, chemical, thermal and functional properties of food products during processing and storage (Hua et al. 2011; Huang et al. 2007; Topuz 2010).

The objectives of this study were: (1) to evaluate the thermophysical properties (thermal conductivity (k), thermal diffusivity (D), bulk density (ρ) and specific heat capacity (C) of sugar kelp considering porosity with respect to its moisture content and temperature, and (2) To compare the experimental thermophysical data with the Choi and Okos empirical model and the ANN model. The results from this study will help in optimizing the design parameters of large-scale dryers focused on clean, energy-efficient and closed drying systems for producing uniform and high-value products for consumers.

5.2. Materials and Methods

5.2.1. Sample Preparation

Fresh sugar kelp (*Saccharina latissima*) grown in Damariscotta bay, Maine (43°56'15.4"N; 69°34'53.0"W), was donated by Maine Fresh Sea Farms, Walpole, ME, USA and shipped to the University of Maine at the end of June 2017. Holdfasts were removed and the blades along with the stipes were washed under running water to remove any biofouling and surface salts. Fresh sugar kelp was then freeze-dried for 4 h at each temperature of -20 ºC, -10 ºC, 0 ºC, 10 ºC and 25 ºC using a freeze dryer (Virtis Ultra 35 EL, SP scientific, Warminster, PA, USA) with vacuum maintained at 20 Pa. After drying, the sugar kelp samples were ground into a fine powder using a food grinder (Magicbullet, Nutribullet LLC, Pacoima, CA, USA). The powdered samples were then sifted through a brass, multilevel sifter, and particles < 0.5 mm were kept in brown Nalgene bottles. These bottles were stored at room temperature (~22 ºC) in cardboard boxes to avoid exposure to light until further analysis.

5.2.2. Proximate Analysis

The moisture content of the dried sugar kelp was determined gravimetrically using the AOAC method. Briefly, 1.0 ± 0.002 g of powdered kelp was dried in an oven (VWR, VWR International, Radnor, PA, USA) at 105 ºC until there is no further change in weight ± 0.001 g (AOAC 1999). Ash content was determined gravimetrically by heating a glass scintillation vial containing the dried seaweed samples (after measuring moisture content) in a muffle furnace (Thermolyne Model F-A1730, Dubuque, IA, USA) at 550 °C for 7 h (AOAC 1999). Total nitrogen content was determined using a dry combustion analyzer (TruMac CNS, LECO Corporation, MI, USA) (AOAC 1990). The total crude protein was calculated using an average nitrogen-to-protein conversion factor of 5.3 for sugar kelp (Schiener et al. 2015). Crude fat/lipid content of the samples was measured using the acid hydrolysis method for seafoods (AOAC 2005). The total carbohydrate content was determined using the difference method (Merill and Watt 1973).

5.2.3. Thermal Properties

Sugar kelp samples of different moisture content (0.06, 0.10, 0.30, 0.50, 0.70 and 0.90 kg H_2O/ kg sample) were prepared by rehydrating the freeze-dried powder. Thermal conductivity (k) and thermal diffusivity (D) of the prepared samples were measured using a SH-1 dual needle of KD2 Pro thermal properties analyzer (Decagon Devices Inc., Pullman, WA, USA). The Dual-Needle sensor consists of two stainless steel parallel needles spaced 6 mm apart; one needle consists of a line-heating source while the temperature-monitoring thermocouple is enclosed in the other needle. Short duration heat pulses are applied to the heating needle and the temperature of the thermocouple needle is monitored during the heating phase and the cooling phase followed by the heating phase. The working principle of KD2 Pro is described using equation (5.1) for transient one-dimensional radial heat conduction equation for a long cylinder.

$$T - T_i = -\frac{q}{4\pi k} E_i \left(\frac{-r^2}{4Dt}\right) \quad (5.1)$$

where T is the final temperature (°C); T_i is the initial temperature (°C); q is the heat generated in the heating needle per unit length (W m^{-1}); k is the thermal conductivity of the medium (W m^{-1} K^{-1}); E_i is the elliptic integral function; t is heating time (s); r is the radial distance between the heating and the temperature monitoring probe (m); and D is the thermal diffusivity of the medium (m^2 s^{-1}). Equation (1) can also be expressed using an infinite power series considering initial terms as below.

$$T - T_i \cong \frac{q}{4\pi k}\left(\ln(t) - \gamma - \ln\left(\frac{r^2}{4D}\right)\right) \quad (5.2)$$

where γ is the Euler constant (0.5772). Sugar kelp samples were packed tightly inside the sample holder to avoid any air resistance during measurement and closed with a cap drilled with two holes (ϕ = 0.813 mm) spaced 6 mm apart to insert the SH-1 dual needle. After insertion, the space between the top of the cap and the needle head was sealed with non-wetting clay to avoid any moisture loss while heating the sample. The sample holder along with the inserted needle was held at room temperature for 15 min to

equilibrate with the surroundings. Before measurement, the sample holder was held by a clamp stand inside a water bath (Julabo SW22, Allentown, PA, USA) for 15 min to equilibrate and attain the required temperature at which the thermal properties were measured. The readings of k and D were recorded for six replicates at each temperature (30, 40, 50, 60, 70 °C) and moisture content (0.06, 0.10, 0.30, 0.50, 0.70, 0.90 kg H_2O/ kg sample) of the sample. The KD2 pro sensor was calibrated with the two-hole Delrin block provided by the manufacturer to verify its performance, before the measurements.

5.2.4. Particle Density, Bulk density and Porosity

The particle density of the sugar kelp samples of moisture content 0.06g water (g sample)$^{-1}$ was measured using liquid pycnometry (Bailey and Thomas 1912). Toluene was chosen as the working liquid due to its non-wettability, high boiling point and low specific gravity (Mohsenin 1986). In brief, the empty weight of the pycnometer was recorded along with its top head. After placing ~ 2 g sample in the glass flask of the pycnometer, toluene was poured in and stirred to remove the trapped air. The top head of the glass pycnometer was closed by the glass stopper with a capillary hole releasing the excess toluene. The particle density of the sample was calculated using formula (5.3).

$$\rho_S = \frac{W_S - W_E}{\left(V_P - \left(\frac{W_{ST} - W_S}{\rho_T}\right)\right)} \tag{5.3}$$

where, ρ_s is the particle density of the sample (kg m^{-3}) of moisture content 0.06 kg H_2O/ kg sample, W_S is the initial weight of the sample and the pycnometer together (kg), W_E is the weight of empty pycnometer (kg), V_P is the total volume of the empty pycnometer (m^3), W_{ST} is the initial weight of the sample plus poured toluene and the pycnometer together (kg) and ρ_T is the density of toluene at room temperature ~ 22 °C (867 kg m^{-3}).

The bulk density (ρ_T) of sugar kelp samples of moisture content (0.06, 0.10, 0.30, 0.50, 0.70, 0.90 g water (g sample)$^{-1}$) was measured by packing tightly in a glass cuvette of known volume. The porosity

(φ) of the samples was calculated assuming no excess volume due to interaction between added components and negligible air weight using formula (4).

$$\varphi = \frac{\left(V_C - \frac{M_S}{\rho_S} - \frac{M_W}{\rho_W}\right)}{(V_C)} \quad (5.4)$$

Where V_C is the total volume of the glass cuvette, M_S is the mass of the dry seaweed of moisture content 0.06 g water (g sample)$^{-1}$, ρ_s is the particle density of the sample (kg m^{-3}) of moisture content 0.06 g water (g sample)$^{-1}$, M_W is the amount of water added to bring the final moisture content in the sample, ρ_W is the density of water at room temperature ~ 22 °C (1000 kg m^{-3}).

5.2.5. Specific Heat

The specific heat capacity of the sugar kelp samples was calculated indirectly from the previously determined values of k, D and the ρ_T using the relationship (5).

$$C = \frac{k}{D\rho_T} \quad (5.5)$$

Where C is specific heat (J kg^{-1}K^{-1}); k is thermal conductivity (W m^{-1} K^{-1}); ρ_T is bulk density (kg m^{-3}); D is thermal diffusivity (m^2 s^{-1}) of the samples.

5.2.6. Empirical Models

The thermophysical properties were estimated by a predictive model approach based on the proximate content of the sugar kelp samples (**Table 5.1**) (Choi and Okos 1986). The empirical approach is easy to compute based on the proximate composition of the food samples. However, the major disadvantage of using the empirical model in estimating the thermal properties of sugar kelp is that these models were developed for specific land-based foods by studying the thermal properties of their proximate composition. It also does not provide necessary information regarding the geometric

arrangement of the major components of the food (perpendicular, parallel and dispersed), and it is very food-specific.

Table 5.1. Thermophysical properties calculated using Choi and Okos (1986) model based on the proximate content of food

Thermophysical Parameter	Equation
Thermal Conductivity (W m^{-1} °C^{-1})	$k = (0.57109 + 0.001762T - 6.7036 \times 10^{-6}T^2) X_w + (0.18071 - 0.0027604T - 1.7749 \times 10^{-7}T^2) X_f + (0.17881 + 0.001958T - 2.7178 \times 10^{-6}T^2) X_p + (0.20141 + 0.0013874T - 4.3312 \times 10^{-6}T^2) X_c + (0.32961 + 0.001401T - 2.9069 \times 10^{-6}T^2) X_a$
Specific Heat Capacity (J kg^{-1} °C^{-1})	$C = (4176.2 - 0.0909T + 0.0054T^2) X_w + (1984.2 + 1.4373T - 0.0048T^2) X_f + (2008.2 + 1.2089T - 0.0013T^2) X_p + (1548.8 + 1.9625T - 0.00594T^2) X_c + (1092.6 + 1.8896T - 0.00368T^2) X_a$
Density (kg m^{-3})	$\rho = (997.18 + 0.00314T - 0.00375T^2) X_w + (925.59 - 0.41757T) X_f + (1329.9 - 0.5184T) X_p + (1599.1 - 0.36589T) X_c + (2423.8 - 0.28063T) X_a$

Where X_i are the respective volume fractions of water, fats, protein, carbohydrate and ash present in each sample. T (°C) is the temperature of the sample. Thermal diffusivity of the samples is calculated using formula (5).

5.2.7. Artificial Neural Network (ANN) Model

The thermal properties of sugar kelp samples were fit into a two-layer feed-forward artificial neural network (ANN) programmed in MATLAB, 2017. In ANN, the processing of information occurs through multiple processing units called neurons. Each input parameter (I) passed through the neurons is multiplied by associated weights (W) of each neural connection to compute the net weighted input, followed by the addition of network bias (B). Subsequently, the output (O) of each neuron is calculated by applying a linear or non-linear transfer function (f) on its net weighted input. In this network, a sigmoid function was used for hidden layer neurons and a linear function was used in output layer neurons for function estimation. The network was trained with supervised Levenberg-Marquardt backpropagation algorithm. In this algorithm, the initial output parameter is computed by assigning random weights to each connection. Afterward, the network output is compared with the required target selected in the training dataset and the difference between target and output is propagated back to the

network in the form of mean square error (MSE). Consequently, the weights are adjusted until the produced output is close to the target by minimizing the MSE over the next iterations. The Levenberg-Marquardt method solves nonlinear least-squares between the function and the measured data points by combining two minimization methods: the gradient descent method and the Gauss-Newton method. There are three stages involved in designing the neural network: the training stage, the validation stage, and the testing stage. During the training stage, the network is presented with the data for adjusting the connection weights according to the MSE. The validation stage is used to avoid the network overtraining or overfitting by measuring and simultaneously improving the network generalization. The training ceases when the generalization stops improving, indicated by no further increase in the MSE. The testing of the network is performed by presenting a completely new independent data set after the training. Finally, the performance of this network in estimating the required target is measured using R^2 and MSE. In this study, 180 data points from 6 replicates at each temperature (30, 40, 50, 60, 70 °C) and moisture content (0.06, 0.10, 0.30, 0.50, 0.70, 0.90 g water (g sample)$^{-}$) were used for prediction of thermal properties of sugar kelp samples. The 180 data points were split randomly for training (70% of the data points), validation (15% of the data points) and testing (15% of the data points) of various network architecture. The network performance was tested for one hidden layer of neurons comprised 4,6,8,10,12 and 14 neurons to avoid complexity while choosing several architectural configurations. Out of 6 configurations, the one with minimized error parameters and higher R^2 value was selected as the optimum model and compared with the experimental and the empirical models.

5.2.8. Statistical Analysis

The thermophysical properties were modeled as a function of input parameters (temperature and moisture content). All the quantitative results are reported as mean ± standard deviation of six replicates. Multi-way ANOVA was used to determine any significant effects ($p \leq 0.05$) of the independent variables (temperature and moisture content) at an individual level and the interaction effect (double effect) on the response variable (thermophysical properties). Tukey's honest significant difference (HSD) post hoc test

was performed to identify any significant differences between the means of comparable treatment. Statistical software SAS Version 9.4 (SAS Institute, Cary, N.C, USA) was used for data analysis. Performance of different ANN configurations fitted to the experimental data was evaluated using the determination coefficient (R^2), mean absolute error (MAE), mean relative error (MRE) and the standard error (SE) of the thermophysical properties (Sablani et al. 2002).

5.3 Results and Discussion

5.3.1. Proximate Analysis

Carbohydrate content was highest (58.20 ± 0.4 g (100 g)$^{-1}$ dry solids) followed by ash content (29.4 ± 0.2 g (100 g)$^{-1}$ dry solids), crude protein (10.8 ± 0.1 g (100 g)$^{-1}$ dry solids), moisture content (5.3 ± 0.1 g (100 g)$^{-1}$ dry solids) and fat (1.6 ± 0.1 g (100 g)$^{-1}$ dry solids) in the freeze-dried samples. The fresh kelp was dried from 90 g moisture (100 g)$^{-1}$ sample to 6 g (100 g)$^{-1}$ sample to increase the shelf life by limiting the growth of bacteria, mold, yeast (Sappati et al. 2019). The composition of sugar kelp varies depending on several factors such as plant maturity, geographical locations, environmental conditions (water temperature, salinity, availability of nutrients, sunlight) and growing season (Schiener et al. 2015). The carbohydrates in sugar kelp exist in two forms: structural (alginates and cellulose) and storage (laminarin, mannitol, and fucoidan) (Schiener et al. 2015). In a previous study, the carbohydrate content in sugar kelp comprised more than 55 g (100 g)$^{-1}$ dry solids of algal biomass (Sappati et al. 2019). After carbohydrates, the second most abundant component of sugar kelp biomass is ash (~ 22 – 33 g (100 g)$^{-1}$ dry solids). Besides, the average protein content and fat content in the sugar kelp ranged from 9 - 11 g (100 g)$^{-1}$ dry solids) and 1.5 – 2 g (100 g)$^{-1}$ dry solids, respectively (Sappati et al. 2019).

5.3.2. Thermal Conductivity (k)

Thermal conductivity (k) of the food determines the rate of heat transfer through the food during thermal processing. In this study, the sample temperature and moisture content had a significant effect (p<0.05) on the thermal conductivity of the sugar kelp samples (**Table 5.3**). The k for the sugar kelp was

in the range of 0.147 ± 0.001 – 0.626 ± 0.072 W m^{-1} K^{-1} for a temperature range of 30 - 70 °C and moisture content varying from 6 to 90 g water (100 g sample)$^{-1}$. Balingasa and Elepaño reported the thermal conductivity of the red seaweed (*Kappaphycus spp.)* to vary from 0.221 to 0.304 W m^{-1} K^{-1} within a moisture content range of 90.7 to 31.9 g (100 g sample)$^{-1}$, which is within the range of the values observed in our study (Balingasa and Elepaño 2009). Additionally, the k of sugar kelp was also comparable to some of the terrestrially grown foods (**Table 5.2**). The k of water is higher than for other components present in foods. Therefore, the thermal conductivity of food is highly influenced by the moisture content rather than the other food proximate (carbohydrates, ash, protein, fats) (Minh et al. 1969). The obtained k of the sugar kelp samples was found to be in good agreement ($R^2 > 0.8$) with the Choi and Okos proximate content-based regression model (**Table 5.6**). Also, the Choi and Okos model predicted closer but significantly ($p<0.05$) different values of k of sugar kelp as compared to the experimental values (**Table 5.3**). This slight difference could be because the primary constituent groups in seaweeds are completely different from the land-based products resulting in different k values calculated based on the Choi and Okos model. For instance, the major carbohydrates present in sugar kelp (alginates, cellulose, laminarin, mannitol, and fucoidan) are more complex polysaccharides than the ones considered in the Choi and Okos model (dextrose, lactose, sucrose, starch). Only the linear effects of sample temperature and the moisture content on the k of sugar kelp were significant ($p<0.05$). The interaction effect (moisture content X sample temperature) was found to be insignificant ($p>0.05$) on the k value. The regression model ($R^2 = 0.9055$) developed based on the temperature and moisture content can be expressed as:

$$k = 0.01199 + 0.003387\ T + 0.004007\ MC \quad (5.6)$$

where T is the sample temperature (°C) and MC is the moisture content (g (100 g)$^{-1}$ sample).

Table 5.2. Thermophysical properties (k, D and C) of terrestrially grown foods

Thermophysical properties	Food	Temperature (°C)	Moisture (% wet basis)	Value	Reference
k (W m^{-1} K^{-1})	Potato	20	63-83	0.541	Rao 1975; Puttongsiri et al. 2012
	Strawberry	28	87	0.462	Delgado et al. 1997
	Spinach	21	93	0.347	Delgado et al. 1997
	Rice flour	30	18	0.130	Muramatsu et al. 2005
	Whole milk powder	30	3.8	0.091	Muramatsu et al. 2005
	Veal meat	30	70	0.507	Elansari and Hobani 2009
D (mm^2 s^{-1})	Apple	0-30	85	0.14	Bennett et al. 1969
	Potato	0-70	63-83	0.13	Minh et al. 1969
	Strawberry	5	92	0.13	Riedel 1969
	Beef chuck	40-65	66	0.12	Dickerson and Read 1975
C (J kg^{-1} $°C^{-1}$)	Gooseberry	N.A	88	3950	USDA 1996
	Lemon	N.A	87	3950	USDA 1996
	Strawberry	N.A	88	3940	USDA 1996
	Mango	N.A	82	3740	USDA 1996
	Veal meat	N.A	76	3650	USDA 1996

N.A Not available

Table 5.3. Thermal conductivity of sugar kelp measured using KD2 Pro and Choi and Okos model

Analysis	Sample Temperature	Moisture Content (g water (100 g sample)$^{-1}$)					
		6	10	30	50	70	90
Experimental Thermal Conductivity (W m^{-1} K^{-1})	30°C	0.147 ± 0.001 aAx	0.175 ± 0.004 aAx	0.226 ± 0.009 aBx	0.342 ± 0.008 aCx	0.421 ± 0.021 aDx	0.473 ± 0.011 aDx
	40°C	0.178 ± 0.005 bAx	0.205 ± 0.011 bAx	0.255 ± 0.014 bBx	0.374 ± 0.025 bCx	0.447 ± 0.025 bDx	0.497 ± 0.005 bDx
	50°C	0.200 ± 0.006 cAx	0.219 ± 0.004 cAx	0.260 ± 0.011 cBx	0.402 ± 0.057 cCx	0.508 ± 0.014 cDx	0.519 ± 0.025 cDx
	60°C	0.239 ± 0.016 dAx	0.252 ± 0.015 dAx	0.289 ± 0.019 dBx	0.444 ± 0.046 dCx	0.558 ± 0.048 dDx	0.543 ± 0.017 dDx
	70°C	0.349 ± 0.017 eAx	0.284 ± 0.021 eAx	0.329 ± 0.026 eBx	0.459 ± 0.030 eCx	0.626 ± 0.072 eDx	0.580 ± 0.067 eDx
Choi and Okos Model Thermal Conductivity (W m^{-1} K^{-1})	30°C	0.158 ± 0.000 aAy	0.165 ± 0.000 aBy	0.234 ± 0.000 aCy	0.356 ± 0.000 aDy	0.498 ± 0.000 aEy	0.562 ± 0.000 aFy
	40°C	0.164 ± 0.000 bAy	0.171 ± 0.000 bBy	0.241 ± 0.000 bCy	0.366 ± 0.000 bDy	0.510 ± 0.000 bEy	0.575 ± 0.000 bFy
	50°C	0.171 ± 0.000 cAy	0.177 ± 0.000 cBy	0.248 ± 0.000 cCy	0.375 ± 0.000 cDy	0.520 ± 0.001 cEy	0.589 ± 0.000 cFy
	60°C	0.176 ± 0.000 dAy	0.182 ± 0.000 dBy	0.254 ± 0.000 dCy	0.384 ± 0.000 dDy	0.533 ± 0.000 dEy	0.602 ± 0.000 dFy
	70°C	0.181 ± 0.000 eAy	0.187 ± 0.000 eBy	0.260 ± 0.000 eCy	0.391 ± 0.001 eDy	0.541 ± 0.001 eEy	0.611 ± 0.000 eFy

Results are mean ± standard deviation (n = 3)
Small letter (a, b, c, d, e): denotes row-wise significant difference between sample temperature
Capital letter (A, B, C, D, E, F): denotes significant difference between moisture content
x/y: denotes comparison between the experimental and model data

Table 5.4. Thermal diffusivity of sugar kelp measured using KD2 Pro and Choi and Okos model

Analysis	Sample Temperature	Moisture Content (g water (100 g sample)$^{-1}$)					
		6	10	30	50	70	90
Experimental Thermal Diffusivity ($mm^2 s^{-1}$)	30°C	0.244 ± 0.001 aAx	0.153 ± 0.018 aBx	0.135 ± 0.006 aCx	0.149 ± 0.009 aCx	0.144 ± 0.005 aBCx	0.152 ± 0.006 aBx
	40°C	0.181 ± 0.002 aAx	0.158 ± 0.007 aBx	0.141 ± 0.004 aCx	0.153 ± 0.006 aCx	0.157 ± 0.005 aBCx	0.156 ± 0.003 aBx
	50°C	0.171 ± 0.012 aAx	0.177 ± 0.013 aBx	0.149 ± 0.005 aCx	0.154 ± 0.006 aCx	0.166 ± 0.015 aBCx	0.173 ± 0.023 aBx
	60°C	0.198 ± 0.024 bAx	0.187 ± 0.015 bBx	0.166 ± 0.009 bCx	0.171 ± 0.016 bCx	0.175 ± 0.006 bBCx	0.190 ± 0.012 bBx
	70°C	0.213 ± 0.028 cAx	0.208 ± 0.009 cBx	0.189 ± 0.031 cCx	0.176 ± 0.022 cCx	0.188 ± 0.021 cBCx	0.188 ± 0.021 cBx
Choi and Okos Model Thermal Diffusivity ($mm^2 s^{-1}$)	30°C	0.138 ± 0.000 aAy	0.147 ± 0.000 aBy	0.162 ± 0.000 aCy	0.153 ± 0.000 aDy	0.143 ± 0.000 aEy	0.151 ± 0.000 aFy
	40°C	0.143 ± 0.000 bAy	0.152 ± 0.000 bBy	0.167 ± 0.000 bCy	0.157 ± 0.000 bDy	0.146 ± 0.000 bEy	0.154 ± 0.000 bFy
	50°C	0.148 ± 0.000 cAy	0.156 ± 0.000 cBy	0.171 ± 0.000 cCy	0.160 ± 0.000 cDy	0.149 ± 0.000 cEy	0.157 ± 0.000 cFy
	60°C	0.151 ± 0.000 dAy	0.160 ± 0.000 dBy	0.175 ± 0.000 dCy	0.163 ± 0.000 dDy	0.152 ± 0.000 dEy	0.160 ± 0.000 dFy
	70°C	0.155 ± 0.000 eAy	0.164 ± 0.000 eBy	0.178 ± 0.000 eCy	0.165 ± 0.000 eDy	0.153 ± 0.000 eEy	0.162 ± 0.000 eFy

Results are mean ± standard deviation (n = 3)
Small letter (a, b, c, d, e): denotes row-wise significant difference between sample temperature
Capital letter (A, B, C, D, E, F): denotes significant difference between moisture content
x/y: denotes comparison between the experimental and model data

5.3.3. Thermal Diffusivity (D)

Thermal diffusivity (D) is a material-specific property for describing the ability of the material to conduct heat energy relative to its ability to store heat energy. The D of sugar kelp was identical to red seaweed (*Kappaphycus spp.)* reported in the range of 0.089 – 0.184 $mm^2\ s^{-1}$ (Balingasa and Elepaño 2009). The statistical results indicated a significant effect (p<0.05) of the sample conditions (temperature and moisture content) on the D of sugar kelp (**Table 5.4)**. The D was lowest for samples held at 30 °C, 40 °C and 50 °C, and no significant difference (p>0.05) was observed between them. Additionally, the D of sugar kelp was also found comparable to some of the terrestrially grown foods (**Table 5.2**). However, the obtained D of the sugar kelp samples was found to be poorly correlated (R^2 < 0.8) with the Choi and Okos model (**Table 5.6**). Moreover, similar to thermal conductivity, the Choi and Okos model predicted significantly (p<0.05) different values of the thermal diffusivity of the sugar kelp as compared to the experimental values (**Table 5.3**). Both linear and quadratic effects of sample temperature and moisture content on thermal diffusivity of sugar kelp were significant (p<0.05). Also, the interaction effect (moisture content X sample temperature) was found significant (p<0.05) on the D value. The regression model (R^2 = 0.4689) developed based on the temperature and moisture content can be expressed as:

$$D = 0.2624 - 0.003219\ T - 0.001956\ MC + 3.599 \times 10^{-5}\ T^2 + 6.817 \times 10^{-6}\ T \times MC + 1.472 \times 10^{-5}\ MC^2 \quad (5.7)$$

where T is the sample temperature (°C) and MC is the moisture content (g (100 g)$^{-1}$ sample).

5.3.4. Particle Density, Bulk Density (ρ_T) and Porosity (φ)

Choi and Okos proposed an empirical equation to estimate densities of the main constituents of food and their temperature dependence (Choi and Okos 1986). However, in this study, the material density was considered to be independent of the sample temperature and only dependent on the moisture content. During the experiment, the sample was prepared and packed hermetically at room temperature in a sealed container leaving no space for thermal expansion. The particle density of 0.06 g water $(g)^{-1}$

sample was observed to be 1566 kg m^{-3}. The moisture content of the kelp has a significant effect (p<0.05) on its ρ_T **(Table 5.5).** The bulk density of the high moisture samples (0.70 and 0.90 g water $(g)^{-1}$ sample) was close to that of water with porosity equivalent to zero. This suggests that fresh sugar kelp can be characterized as continuous material with very low porosity. Zabalaga et al. reported that the porosity was increased as moisture content decreased during the early stage of banana drying, reaching a maximum value at a moisture content of 46 g water (100 g sample)$^{-1}$ (Zabalaga et al. 2016). Further drying decreased of porosity with reduction in moisture content resulted in a decrease of porosity of unripe banana. As the drying proceeds, previously occupied pores by water are either replaced by air or are collapsed due to shrinkage. Similar behavioral trends were also reported during drying of mango, banana slices and pineapple (Yan et al. 2008). In the case of fresh sugar kelp, the amorphous form of water always stays in the rubbery state as the T_g of kelp is below the air-drying temperature and therefore the volume shrinkage can be contributed to the volume of the water loss without creating any void fractions in the dried kelp (Sappati et al. 2017). Under this assumption, the thermophysical properties of the continuous thin matrix of kelp while drying can be estimated indirectly from granular rehydrated kelp without considering the porosity. At room temperature, the bulk densities of the samples varied non-linearly with the moisture content (**Table 5.5**). With the increase in the water content, the primary carbohydrate alginate in the presence of cations such as Ca^{2+} binds excess amounts of water by intermolecular cross-linking resulting in swelling and a decrease of density (George and Abraham 2006). Irrespective of the sample conditions, porosity values calculated using Choi and Okos model assuming no excess volume due to interaction and negligible air mass were found to be similar to the experimental values **(Table 5.5)**.

Table 5.5. Measured bulk density, calculated porosity and the Choi and Okos model porosity of sugar kelp

Moisture Content (g water/ 100g sample)	Measured Bulk Density (kg/m^3)	Calculated Porosity	Choi and Okos Model Porosity
6	806.00 ± 8.31 A	0.49 ± 0.01 A	0.51 A
10	756.23 ± 2.70 B	0.51 ± 0.00 A	0.52 A
30	753.85 ± 11.78 B	0.45 ± 0.01 B	0.46 B
50	896.22 ± 16.79 C	0.29 ± 0.01 C	0.29 C
70	1022.39 ± 38.71 D	0.11 ± 0.03 D	0.10 D
90	969.59 ± 13.55 E	0.09 ± 0.01 D	0.06 E

Results are mean ± standard deviation (n = 6)
Capital letter (A, B, C, D, E): denotes significant difference between moisture content

5.3.5. Specific Heat Capacity (C)

The C of sugar kelp was calculated indirectly from the values of k, ρ and D, and was in the range of 749.00 ± 5.11 – 3270.62 ± 219.35 J kg^{-1} $°C^{-1}$ for the temperature and moisture content varying from 30 to 70 °C and 6 to 90 g water (100 g sample)$^{-1}$, respectively (**Table 5.6**). The C of fresh sugar kelp was higher than for fresh Sargassum species (*Sargassum Natans*) at 50 °C (Wong and Cheung 2001). Furthermore, the C above the freezing point of terrestrially grown foods has similar values to sugar kelp (**Table 5.2**). Both linear and quadratic effects of moisture content on C of sugar kelp were significant ($p<0.05$), whereas only the linear effect of sample temperature was significant ($p<0.05$) (**Table 5.6**). The interaction effect (moisture content X sample temperature) was also found significant ($p<0.05$). The regression model ($R^2 = 0.8829$) developed based on the temperature and moisture content can be expressed as:

$$C = 297.6 + 17.73\ T + 52.94\ MC - 0.1986\ T \times MC - 0.2352\ MC^2 \quad (5.8)$$

where T is the sample temperature (°C) and MC is the moisture content (g (100 g)$^{-1}$ sample). The samples held at 30 °C and 6 g water (100 g sample)$^{-1}$ exhibited the lowest C and were significantly ($p<0.05$) lower as compared to the other conditions. The specific heat capacity is the measure of the ability of the material to store the thermal energy. As the temperature increases, the average kinetic

energy of the molecules increases contributing positively towards the net internal energy and thus raises the specific heat of the material. The experimental values of C of the sugar kelp samples were found to be in good agreement ($R^2 = 0.758$) and were significantly ($p<0.05$) different than the Choi and Okos model (**Table 5.6)**. On the other hand, the temperature had no significant effect ($p>0.05$) on the C as predicted by Choi and Okos model possibly due to less effect of temperature on C of individual food components in the considered range. Water has much higher specific heat capacity as compared to its counterparts present in the food, possibly resulting in higher specific heat capacity in samples containing high moisture.

Table 5.6. Specific heat capacity of sugar kelp measured using KD2 Pro and Choi and Okos model

Analysis	Sample Temperature	Moisture Content (g water (100 g sample)$^{-1}$)					
		6	10	30	50	70	90
Experimental Specific heat capacity (J kg^{-1} °C^{-1})	30°C	749.00 ± 5.11 aAx	1535.22 ± 180.33 aBx	2152.60 ± 155.98 aCx	2574.05 ± 149.43 aDx	2863.99 ± 166.46 aEx	3204.58 ± 89.72 aEx
	40°C	1218.84 ± 23.62 bAx	1720.60 ± 93.12 bBx	2343.27 ± 231.09 bCx	2722.60 ± 102.43 bDx	2787.38 ± 136.51 bEx	3287.35 ± 94.40 bEx
	50°C	1455.73 ± 112.73 bAx	1644.04 ± 109.82 bBx	2254.28 ± 146.76 bCx	2907.37 ± 310.37 bDx	3024.32 ± 301.54 bEx	3136.37 ± 401.44 bEx
	60°C	1507.96 ± 159.27 bAx	1783.08 ± 104.49 bBx	2253.20 ± 247.29 bCx	2902.34 ± 284.22 bDx	3116.27 ± 198.23 bEx	2963.44 ± 199.14 bEx
	70°C	2060.26 ± 260.60 cAx	1808.95 ± 98.98 cBx	2278.42 ± 278.73 cCx	2946.88 ± 443.30 cDx	3270.62 ± 219.35 cEx	3213.65 ± 418.20 cEx
Choi and Okos Model Specific heat capacity (J kg^{-1} °C^{-1})	30°C	1416.77 ± 0.04 Ay	1479.11 ± 0.41 By	1908.21 ± 0.33 Cy	2589.54 ± 0.24 Dy	3395.76 ± 0.31 Ey	3827.27 ± 0.62 Fy
	40°C	1423.79 ± 0.09 Ay	1486.03 ± 0.19 By	1915.72 ± 0.10 Cy	2599.05 ± 0.27 Dy	3407.15 ± 0.27 Ey	3858.52 ± 0.40 Fy
	50°C	1432.20 ± 0.41 Ay	1493.20 ± 0.17 By	1923.51 ± 0.31 Cy	2609.86 ± 0.44 Dy	3419.26 ± 1.44 Ey	3854.21 ± 1.11 Fy
	60°C	1438.66 ± 0.97 Ay	1500.04 ± 0.17 By	1932.81 ± 0.36 Cy	2622.52 ± 0.27 Dy	3437.83 ± 0.57 Ey	3874.19 ± 0.33 Fy
	70°C	1466.09 ± 0.77 Ay	1506.35 ± 0.19 By	1941.72 ± 0.72 Cy	2634.13 ± 2.12 Dy	3453.10 ± 2.89 Ey	3893.01 ± 0.38 Fy

Results are mean ± standard deviation (n = 3)
Small letter (a, b, c): denotes row-wise significant difference between sample temperature

5.3.6. Modeling with Artificial Neural Network (ANN)

In the current study, ANN was used as an alternate tool for estimating the thermophysical properties (k, D, C) of the sugar kelp based on the parameters of sample temperature and moisture content. After repeated network training, assessment and validation with one hidden layer of neurons comprised of 2, 4, 6, 8, 10, 12, 14 and 16 neurons, the model with the lowest error in terms of mean absolute error (MAE), mean relative error (MRE), standard error (SE) and highest R^2 value was selected as optimum (**Table 5.7**). Multiple hidden layers were not considered in this study as simple ANN configurations are a good predictor for the input dataset with an inherent variation. The output from the neural network with several configurations was obtained using a second data set consisting of similar size (180) input data points not used in the training. The best ANN configuration with maximum performance included ten, six and eight neurons in a hidden layer for predicting the k, D and C, respectively. **Fig. 5.1** demonstrates an excellent correlation fit between the experimental and predicted values by the ANN model. The corresponding network estimated the k with 0.019 W m^{-1} K^{-1} MAE, 0.049 MRE and 0.002 W m^{-1} K^{-1} (R^2 = 0.961), D with 0.010 mm^2 s^{-1} MRE, 0.054 MAE and 0.001 mm^2 s^{-1} (R^2 = 0.750) and C with 152.25 J kg^{-1} $°C^{-1}$ MAE, 0.060 MAE and 15.29 J kg^{-1} $°C^{-1}$ (R^2 = 0.920). Also, the optimum ANN model predicted the thermophysical properties with a higher coefficient of determination (R^2) as compared to the regression model and the Choi and Okos model (**Table 5.7**). The regression equation can be written as Y = B2 + LW tansig(B1 + IW (x)); where Y is the output parameter, X is the input matrix, B1 and B2 are bias value for layer 1 and 2 respectively, IW is the input weight matrix and LW is layer weight matrix. The matrix value of B1, B2, IW, and LW for the best ANN configuration to predict the thermophysical properties are given in **Table 5.8**. Lastly, the developed ANN model in this study was able to capture the effect of sample temperature and moisture content on the thermophysical properties of sugar kelp with high confidence.

Table 5.7. Prediction errors in the thermophysical properties with different ANN configurations and Choi and Okos Model

Thermophysical Properties	Model	Neurons	Performance measures			
			MAE	MRE	SE	R^2
Thermal Conductivity, k	ANN	2	0.024	0.065	0.002	0.945
		4	0.020	0.055	0.002	0.957
		6	0.019	0.049	0.002	0.960
		8	**0.019**	**0.049**	**0.002**	**0.961**
		10	0.019	0.051	0.002	0.960
		12	0.020	0.054	0.005	0.956
		14	0.023	0.060	0.002	0.935
		16	0.020	0.054	0.003	0.957
	Choi and Okos	NA	0.051	0.143	0.005	0.853
Thermal Diffusivity, D	ANN	2	0.012	0.070	0.001	0.640
		4	0.011	0.063	0.001	0.705
		6	0.013	0.077	0.001	0.576
		8	0.012	0.069	0.001	0.599
		10	0.012	0.067	0.001	0.619
		12	0.010	0.060	0.001	0.720
		14	**0.010**	**0.054**	**0.001**	**0.750**
		16	0.010	0.056	0.001	0.749
	Choi and Okos	NA	0.024	0.128	0.002	0.014
Specific Heat Capacity, C	ANN	2	194.232	0.092	18.550	0.884
		4	184.356	0.082	17.726	0.893
		6	156.648	0.066	15.880	0.915
		8	177.051	0.080	16.854	0.905
		10	**152.255**	**0.065**	**15.291**	**0.920**
		12	163.899	0.070	16.611	0.907
		14	176.824	0.087	16.877	0.903
		16	164.575	0.077	15.890	0.914
	Choi and Okos	NA	380.167	0.172	35.235	0.758

One hidden layer was considered and the neurons in that layer were listed in the table.
MAE, MRE, SE and R^2 are the mean absolute error, the mean relative error, the standard error and the coefficient of determination of thermophysical properties (thermal conductivity, thermal diffusivity, specific heat capacity) of sugar kelp.

Table 5.8. Regression parameters for predicting the thermophysical properties of sugar kelp with best ANN configuration

Thermal Conductivity, k for 8 neurons																	
IW		LW														B1	B2
1.60	-5.18	1.58	-0.19	-0.05	-0.44	-0.22	-0.09	-0.15	-0.23							-7.76	1.18
-4.60	-8.92															7.30	
6.93	-6.40															-3.22	
-0.98	-2.61															0.07	
-2.52	6.85															-4.88	
-2.45	-2.55															-2.41	
5.88	-3.41															5.31	
-1.39	-3.60															-5.01	
Thermal Diffusivity, D for 14 neurons																	
-4.12	-4.43	-0.63	-0.29	-0.56	-0.34	-0.04	-0.27	-0.19	-0.15	0.15	-0.12	-0.29	-0.23	0.72	-2.93	4.92	2.30
-4.39	2.36															4.83	
4.59	2.30															-3.98	
-3.52	2.68															2.59	
-1.39	-5.06															1.88	
-3.14	-4.04															1.27	
3.91	3.42															-0.47	
-0.65	-5.30															-0.21	
4.75	-2.16															1.50	
-3.03	4.14															-1.95	
4.75	-2.37															2.66	
-3.40	3.81															-3.86	
3.88	2.76															5.23	
1.90	4.91															6.74	
Specific Heat Capacity, C for 10 neurons																	
-5.08	8.04	0.35	-0.74	0.79	-0.22	2.04	-0.17	-1.19	0.24				0.24	-0.24		9.81	-0.96
4.16	1.05															-3.64	
8.48	2.12															-7.66	
5.95	-3.42															-2.83	
0.57	3.33															4.48	
-4.93	0.26															0.80	
-1.53	1.58															3.12	
-1.09	-3.13															3.93	
0.91	5.72															0.68	
0.21	-3.98															4.00	

Where Y is the output parameter, X is the input matrix, B1 and B2 are bias value for layer 1 and 2 respectively, IW is the input weight matrix and LW is layer weight matrix.

Fig. 5.1. Correlation of experimental versus neutral network values of thermophysical properties of sugar kelp with training data set (a) thermal conductivity, (b) specific heat capacity, (c) thermal diffusivity. The best ANN configuration included eight, ten and fourteen neurons in each layer for (a) thermal conductivity, (b) specific heat capacity, (c) thermal diffusivity, respectively

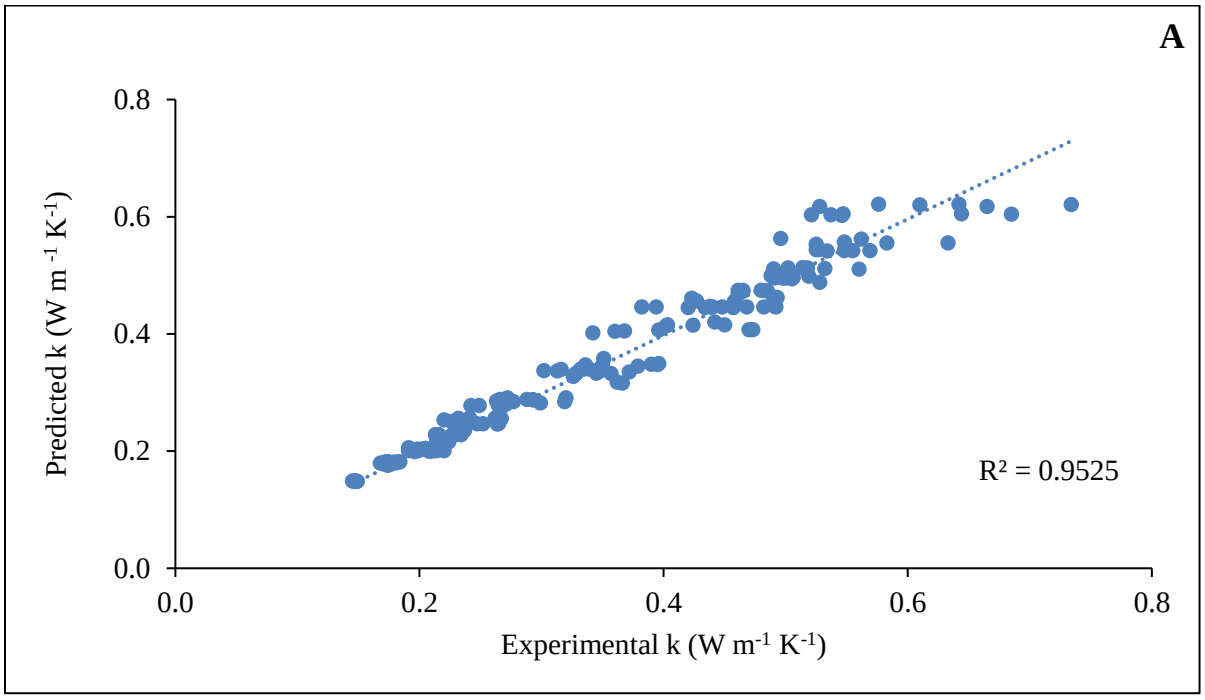

Fig. 5.1 continued

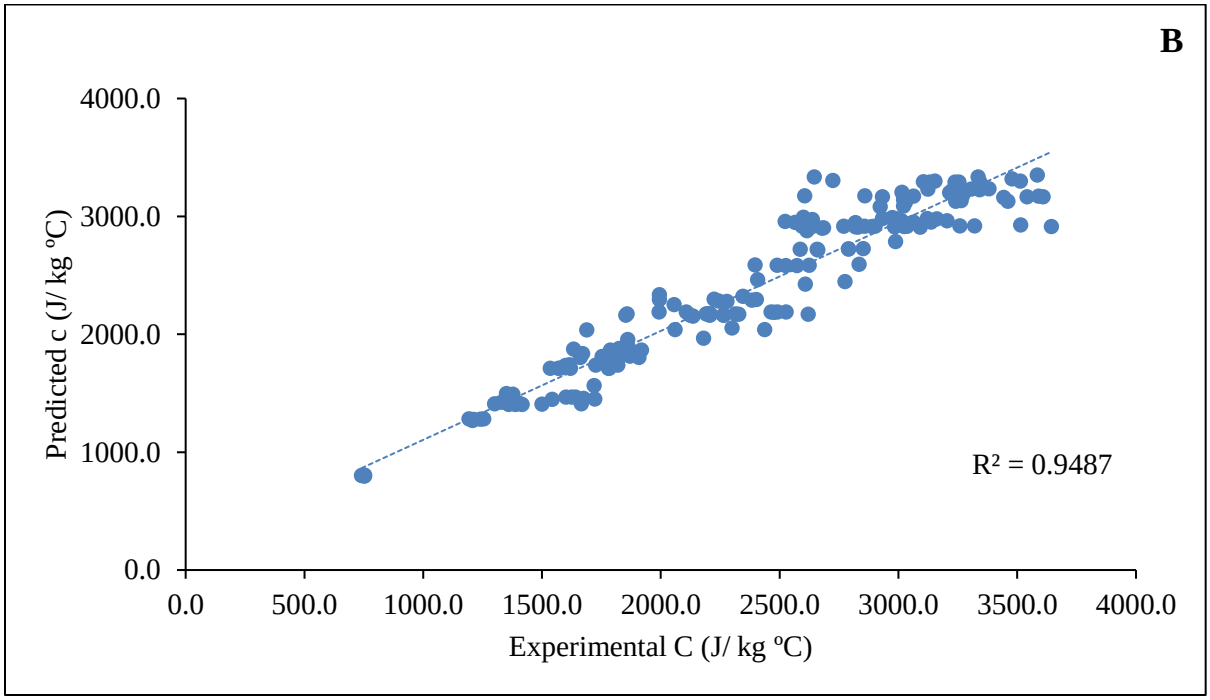

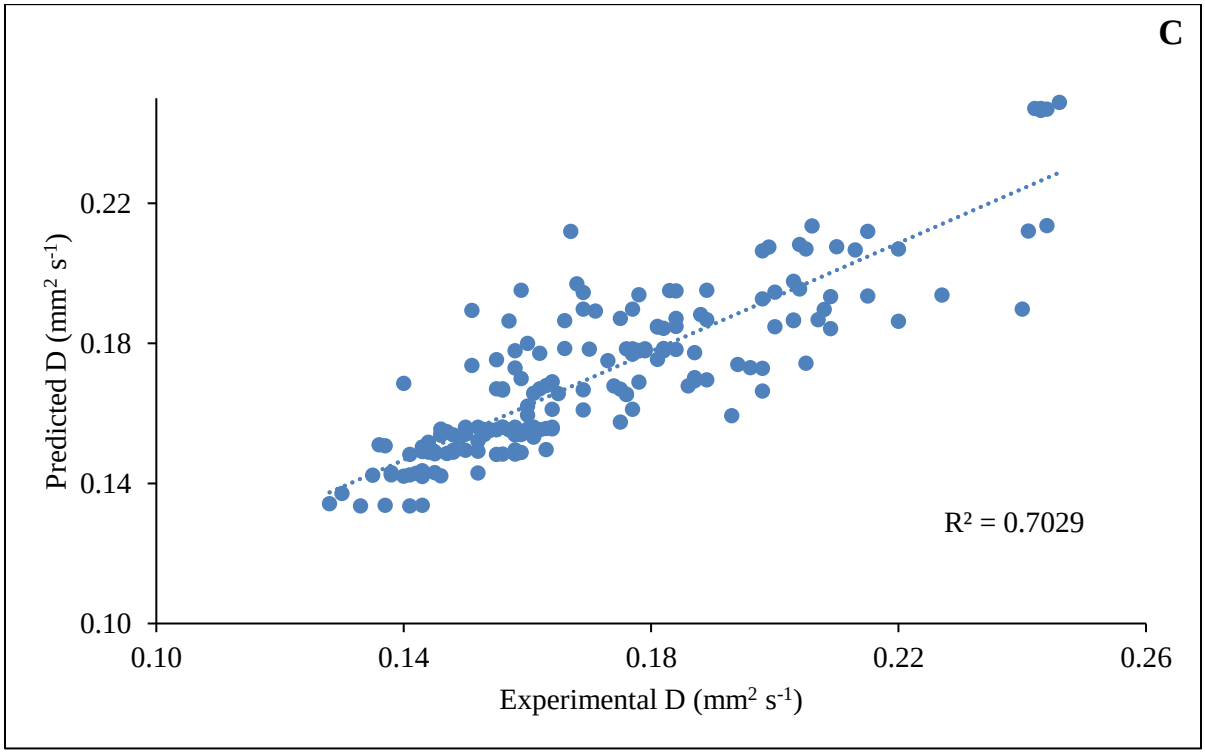

5.4 Conclusions

This is the first study reporting the effects of moisture content and the sample temperature of sugar kelp on its thermophysical properties (thermal conductivity, thermal diffusivity, material density, specific heat capacity). In the seaweed drying process, the thermophysical properties change continuously with the sample temperature and moisture content. A comparative study was performed between the regression analysis, Choi and Okos model and ANN model to estimate their ability to predict the thermophysical properties in a dynamic process of sugar kelp drying based on the sample temperature and moisture content. The bulk density of the kelp varied non-linearly with moisture content, whereas k, C and D were in the range of 0.147 – 0.626 W m^{-1} K^{-1}, 484.46 – 3954.26 J kg^{-1} $°C^{-1}$ and 0.135 – 0.244 mm^2 s^{-1}, respectively for a temperature range of 30 - 70 °C and moisture content varying from 6 to 90 g (100 g sample)$^{-1}$. Choi and Okos model calculated significantly ($p<0.05$) different values of thermophysical properties of sugar kelp based on its major composition including water, fats/lipids, carbohydrate, protein, ash content and air fraction. Above the freezing point, in high moisture samples (> 30 g (100 g)$^{-1}$ sample), water content significantly ($p<0.05$) influenced the specific heat capacity and the thermal conductivity of sugar kelp as compared to the other major food components. ANNs were proved to have the ability to learn from the training data set and model non-linear and complex relationships between inputs and outputs. Also, in this study, the optimum ANN model determined the thermophysical properties with less than 16 neurons in one hidden layer. The predicted values by the ANN model were in excellent correlation with the experimental values in terms of coefficient of determination (R^2) as compared to the regression model and the Choi and Okos model with relatively low MAE, MRE, and SE. It can be concluded that the thermophysical properties of fresh sugar kelp are greatly influenced by the moisture content as compared to other food components and will not be affected by the seasonal variation in proximate composition. These results will help in estimating the necessary drying times for sugar kelp depending on the thermophysical properties and drying conditions.

CHAPTER 6

MATHEMATICAL MODELING FOR PREDICTING DRYING TIME OF BROWN SEAWEED (*SACCHARINA LATISSIMA*) IN A PACKED BED HIGHLY TURBULENT HOT AIR CONVECTIVE DRYER

6.1. Introduction

For extending the shelf life of foods, water is removed through evaporation from the food product to the drying air. The process of drying is very energy-intensive (Sagar and Suresh 2010). Seaweeds are dried primarily using two methods: direct sunlight dryer and conventional hot air convective dryer. As seen in previous chapters, different dying methods and conditions highly influence the dried product quality in terms of chemical, physical, thermal and nutritional properties. Sun drying of seaweed is becoming more attractive in tropical and temperate zones due to its simple and low-cost design. However, in cold arctic zones, the use of conventional dryers is predominant. Even though the power consumption is relatively higher in conventional dryers, they give more control over sun drying in terms of selecting drying parameters and hence the final product properties.

High rates of drying are achieved in a fluidized bed for products especially grains, seeds and light agricultural produce drying due to uniform heat and mass transfer across the bed. Long blades of kelp are hung vertically with uniform space in a convective dryer and hot air is either blown horizontally or vertically across the bed of kelp to produce a final dried product with desired moisture content. Sugar kelp is long, skinny and has a thickness less than 2 mm across its blade. It has been also observed that the drying of sugar kelp primarily occurs in a falling drying period due to its significantly lower thickness as compared to its length and width (Sappati et al. 2017). In the falling period, the surface of the product is not saturated and the rate of drying falls consistently over the drying period. The rate of water movement to the surface is determined primarily due to two physical phenomena: diffusion and capillary movement. The mechanism of liquid diffusion was observed during the drying process of sugar kelp as the thickness of sugar kelp is comparatively very low as compared to its net surface area (Sappati et al. 2017). During

this period, the rate of drying is governed by the rate of diffusion rather than the rate of mass transfer of the liquid from the surface to the surrounding gas phase. Experimental drying data are usually preferred over mathematical equations to predict the drying rate. However, this approach is tedious and consumes a lot of energy and time. In this chapter, a mathematical model wass developed to simulate batch drying of vertically hanged sugar kelp in a hot air convective dryer. In the developed model the drying of material was considered to occur in a falling rate period and accompanied by simultaneous transfer of water vapor from the surface of kelp to the bulk air phase and heat transfer from the bulk air phase to the evaporating surface of kelp through convection. Also, the equations were derived considering no heat transfer by radiation from the surface of the dryer. The objectives of this study were: (1) to develop a mathematical model to simulate the drying process of sugar kelp hung vertically in hot air convective dryer, and (2) to investigate the influence of velocity, humidity and temperature of the inlet air on the drying time as compared to the experimental data. The results from this study will help in predicting the drying time and energy requirement in a packed bed setup for drying vertically hung kelp. The data can also be used to determine the inlet air condition for optimizing the energy consumption and the drying period for producing high-quality seaweed products for consumers.

6.2 Materials and Methods

6.2.1 Materials

Fresh sugar kelp (*Saccharina latissima*) grown in Damariscotta bay, Maine (43°56'15.4"N; 69°34'53.0"W), was donated by Maine Fresh Sea Farms, Walpole, ME, USA and shipped to the University of Maine at the beginning of May 2018. For this study, one batch of 28 kelp blades of approximately size 635 mm height, 152 mm width and 2 mm thickness is hot-air dried at 6 different combination of 3 temperatures (30 °C, 50 °C, and 70 °C) and 2 relative humidities (25% and 50%) for estimating the drying time.

6.2.2 Drying Process

The drying experiment was carried out in a hot air convective dryer of the cross-sectional area of 30 x 30 inch and bed length of 50 inches. Each sugar kelp blade wass weighed initially and hung uniformly along the four rows and seven columns in the dryer. The air velocity inside the dryer wass maintained at 1 m/s using the butterfly valve at the exhaust. The temperature and humidity of the inlet and outlet air were constantly measured at an interval of 20 s during the entire drying process using datalogger thermocouple (EL-USB-2 Lascar Humidity and Temperature USB Logger, LASCAR Electronics Inc., PA, USA). A total of nine data loggers were placed along the bed length of the dryer, three each on the inlet, mid-region and outlet. A schematic diagram of the drying setup is shown in **Fig. 6.1**. Initial and final moisture content of the samples was measured in triplicate according to the AOAC method (AOAC 1999).

Fig 6.1. 2D representation of the drying cabinet

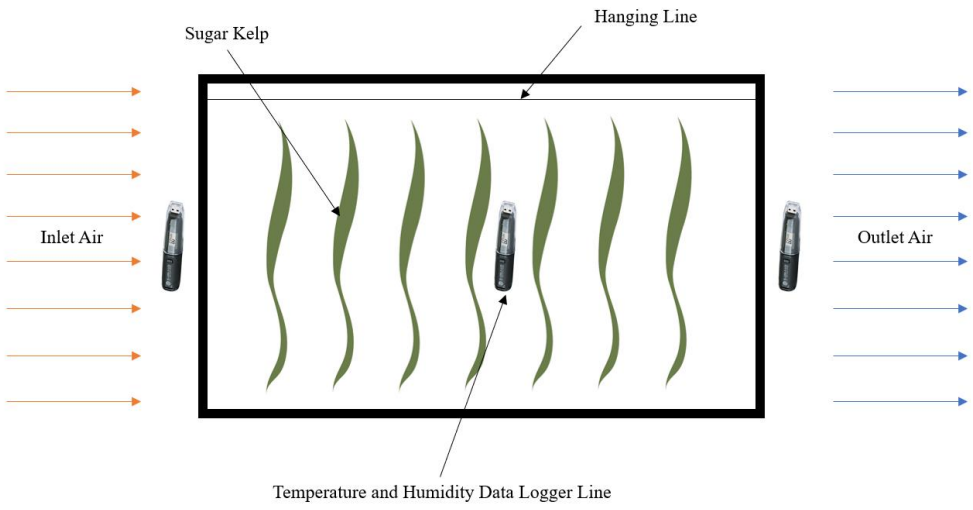

6.2.3 Mathematical Model

An adiabatic drying system was assumed with no heat transfer between the drying chamber and the surrounding air. The inlet air is entering at a temperature of T1 and humidity of H1 and leaves the bed with a temperature of T2 and humidity of H2. Hence, both the temperature and humidity will vary across the bed length. Now assuming a small cross-section of length dZ along the bed and balancing differential heat dQ across this small section,

$$dQ = -GC_s\,A\,dT \tag{6.1}$$

Where q is the heat-transfer rate (W), C_s is the humid heat of the air-water vapor mixture and G is the airflow rate (kg dry air m^{-2} s^{-1}) across the cross-sectional area A (m^2).

Also, over the small differential section, the convective heat transfer equation between the product and the air can be written as

$$dQ = h\,a\,A\,dZ\,(T - T_w) \tag{6.2}$$

Where h is the convective heat-transfer coefficient (W m^{-2} k^{-1}), a is the ratio of the surface area of the solids and bed volume (m^{-1}) and T_w is the wet-bulb temperature of the product. On equating, rearranging and integrating eq. (6.1) and (6.2) across the bed length from 0 to Z and the temperature from T1 to T2,

$$\frac{h\,a}{G\,C_s}\int_0^Z dZ = -\int_{T1}^{T2}\frac{dT}{T-T_w} \tag{6.3}$$

$$\frac{h\,a\,Z}{G\,C_s} = \ln\frac{T_1-T_w}{T_2-T_w} \tag{6.4}$$

Where Z is the bed length (m)

In the falling rate period, the rate of drying, R (kg H_2O s^{-1} m^{-2}) is given by

$$R = -\frac{L_s}{A}\frac{dX}{dt} \tag{6.5}$$

Where L_s is the initial dry solids present in the dryer (kg), A is the net surface area of drying (m^2), dX is the differential change in the moisture content (kg H_2O (kg dry solids)$^{-1}$) and dt is a small increment in time (s). It has been observed the rate of drying is directly proportional to the moisture content of the sugar kelp (Sappati et al. 2017) and therefore R can be written as,

$$R = mX \tag{6.6}$$

Where m is proportional constant. On equating, rearranging and integrating eq. (6.5) and (6.6) from initial to final moisture content over the period of t.

$$\int_0^t dt = -\frac{L_s}{m\,A} \int_{X_i}^{X_f} \frac{dX}{X} \tag{6.7}$$

$$t = \frac{L_s}{m\,A} \ln \frac{X_i}{X_f} \tag{6.8}$$

From eq. 6.6, m can be also written for an initial rate of drying and moisture content as

$$m = \frac{R_i}{X_i} \tag{6.9}$$

Where, Ri is the initial rate of drying (kg H_2O s^{-1} m^{-2}), X_i is the initial moisture content (kg H_2O (kg dry solids)$^{-1}$) and X_f is the final moisture content (kg H_2O (kg dry solids)$^{-1}$). Substituting the value of m from eq. 6.9 in 6.8 will result in

$$t = \frac{L_s}{A} \frac{X_i}{R_i} \ln \frac{X_i}{X_f} \tag{6.10}$$

At any given instance of time let's assume initially the air is at temperature T moving across the bed of solids at a temperature of wet bulb T_w.

The convective heat transfer equation between the product and the air can be written as

$$Q = h\ A\ (T - T_w) \tag{6.11}$$

The same amount of heat is also providing the latent heat of evaporation λ_w to evaporate the water from the surface of kelp at wet-bulb temperature T_w and the Q can also be written as

$$Q = R_i \ \lambda_w \ A \tag{6.12}$$

Equating 6.11 and 6.12 we get

$$Q = h \ A \ (T - T_w) = R_i \ \lambda_w \ A \tag{6.13}$$

$$\text{And, } R_i = \frac{h\,(T - T_w)}{\lambda_w} \tag{6.14}$$

$$\text{Also, } \frac{L_s}{A} = \frac{\rho_s}{a} \tag{6.15}$$

Where ρ_s is the bulk density of the dry solids in the dryer. Substituting the value of R_i and L_s/A from eq. 6.14 and 6.15 in 6.10 will give,

$$t = \frac{\rho_s}{a} \frac{X_i \lambda_w}{h\,(T - T_w)} \ln \frac{X_i}{X_f} \tag{6.16}$$

Eq. 6.16 hold only for one small section of the drying bed. As the air temperature is varied throughout the bed a log mean temperature difference can be used as an approximation for the whole bed in place of T - T_w and can be represented as

$$(T - T_w)_{LM} = \frac{T_1 - T_2}{\ln\left[\frac{T_1 - T_w}{T_2 - T_w}\right]} \tag{6.17}$$

Substituting T2 from eq. 6.4 and $(T - T_w)_{LM}$ from 6.17 in 6.16 will result in

$$t = \frac{\rho_s \lambda_w Z X_i}{G C_s (T_1 - T_w)} \ln \frac{X_i}{X_f} \left[\frac{1}{1 - e^{\frac{-haZ}{GC_s}}}\right] \tag{6.18}$$

Convective heat transfer coefficients can be estimated using the formula given below considering uniform circulation of air throughout the bed (Geankoplis, 1993)

$$h = 0.214 \frac{G_t^{0.59}}{D_p^{0.41}} \quad \text{if} \quad \frac{D_p G_t}{\mu} < 350 \tag{6.19}$$

or

$$h = 0.214 \frac{G_t^{0.49}}{D_p^{0.51}} \quad \text{if} \quad \frac{D_p G_t}{\mu} > 350 \tag{6.20}$$

Where D_p is diameter in m of a sphere having the same surface area as the kelp in the bed, G_t is the total mass velocity entering the bed (kg h^{-1} m^{-2}), and μ is the viscosity of the air (kg m^{-1} h^{-1}).

The geometry factor of bed (a), the ratio of the surface area of the solids and bed volume (m^{-1}) can be calculated using

$$a = \frac{6(1-\varepsilon)}{D_p} \tag{6.21}$$

Where ε is the void fraction of the kelp in the drying bed

6.3 Results and Discussion

The average weight of 28 sugar kelp blades was 94.18 ± 47.36 g. The initial run was tested with an inlet air temperature and relative humidity of 40 °C and 25 % in the drying cabinet with an air velocity of 1 m/s. The total drying time observed under these conditions was 3 hrs. The recorded relative humidity in the chamber was much higher than the setpoint of 25% for the first 60 minutes of drying time indicating that the dryer was working at the maximum saturated condition. After 60 minutes, due to the removal of significant moisture from the drying sample, the attached heat pump to the convective dryer was able to maintain the RH of 25% (**Fig. 6.2**). Throughout the run, the inlet air temperature was maintained at 40 ± 2 °C (**Fig. 6.3**). Using this given information, sample calculations for the following parameter of air and the products wre computed for this run from eq. 6.1-6.21.

Fig 6.2. Variation in the surrounding, inlet, center and outlet air relative humidity for an initial air temperature and relative humidity setpoint of 40 ℃ and 25 % in the drying cabinet

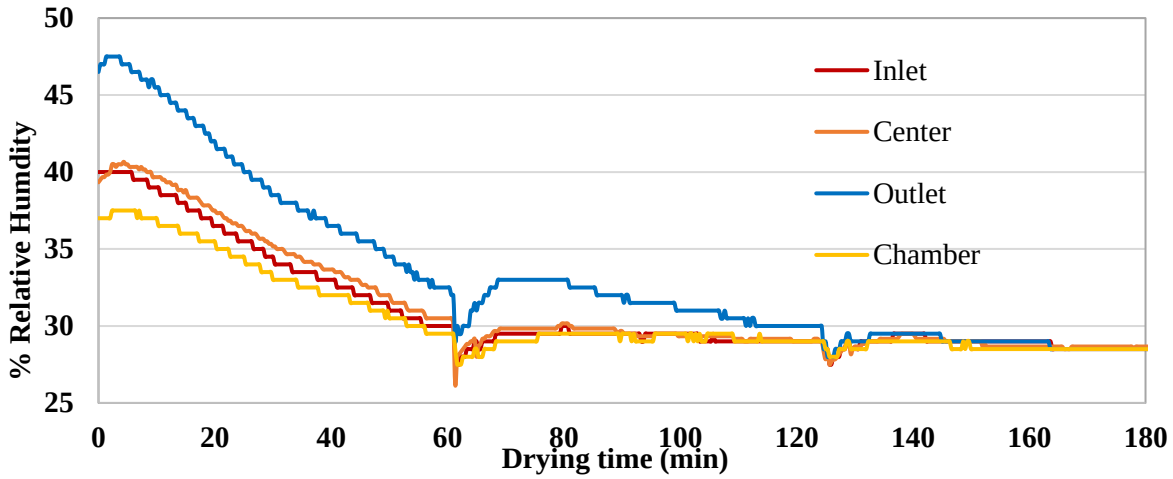

Fig 6.3. Variation in the surrounding, inlet, center and outlet air temperature for an initial air temperature and relative humidity setpoint of 40 ℃ and 25 % in the drying cabinet

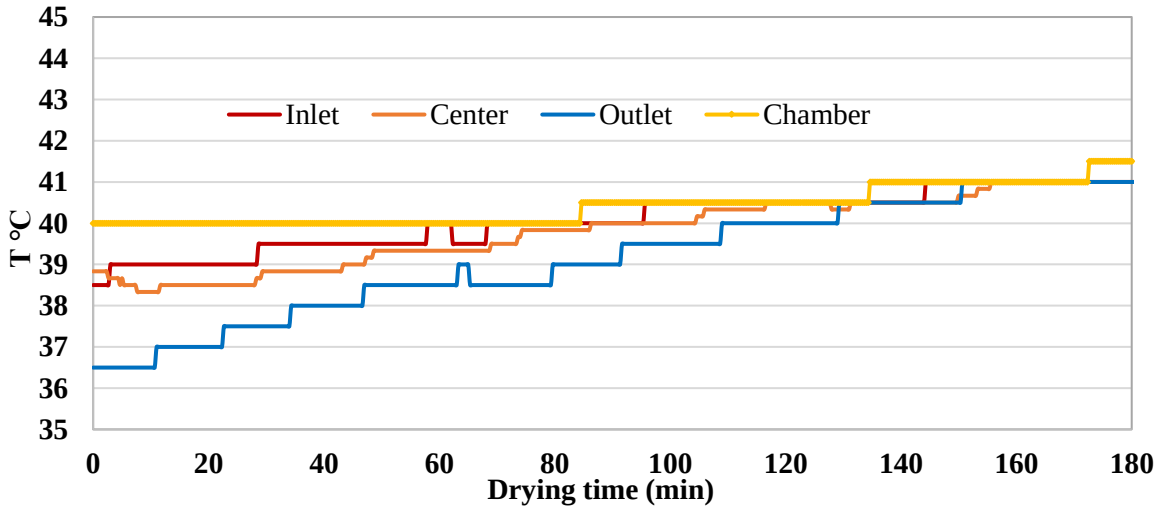

6.3.1 Inlet Air Absolute Humidity

Saturation vapor pressure is calculated using Benten's equation (6.22)

$$P_s(kPa) = 0.61078\, e^{\left(\frac{17.24\,T}{T+237.2}\right)} \quad (6.22)$$

Where P_s (kPa) is the saturated vapor pressure; T (℃) is the air temperature.

Therefore, the inlet air saturation vapor pressure,

P_{si} (kPa) = $0.61078\, e^{\left(\frac{17.24*40}{40+237.2}\right)}$ = 7.3501 kPa

Now, relative humidity at any specific temperature is calculated using equation (6.23)

$$RH = \frac{P_{ai}}{P_{si}}\, x\, 100 \quad (6.23)$$

Where, RH is the relative humidity; P_{ai} (kPa) is the partial vapor pressure of the inlet air; P_{si} (kPa) is the saturation vapor pressure of the inlet air at the same temperature.

As, inlet humidity, RH_i = 25% or 0.25

$$0.25 = \frac{P_a}{P_{si}}$$

$$0.25 = \frac{P_a}{7.3501}$$

Partial vapor pressure at an inlet temperature of 40 ℃, P_a = 1.8375 kPa

Now, the absolute humidity is given by equation (6.24)

$$H\ (kg\ water\ \ kg\ dry\ air^{-1}) = \frac{18.02\ P_a}{28.97(P_{atm} - P_a)} \quad (6.24)$$

Where P_a (kPa) is the partial vapor pressure of the air; P_{atm} (kPa) is the atmospheric pressure.

$$H_i\ (kg\ water\ \ kg\ dry\ air^{-1}) = \frac{18.02\ x\ 1.8375}{28.97(101.325 -\ 1.8375)}\ = 0.0114$$

Therefore, the inlet air absolute humidity, $H_i\ = 0.0114\ kg\ water\ \ kg\ dry\ air^{-1}$

6.3.2 Inlet Air Wet Bulb Temperature

Based on the equation describing wet bulb temperature T_w as a function of relative humidity RH and the inlet air temperature T (Stull, 2011).

$$T_w\ = T\ tan^{-1}(0.151977(\text{RH}\ +\ 8.313659)^{0.5}) +\ tan^{-1}(RH + T) -\ tan^{-1}(\text{RH}\ -\ 1.676331) +$$

$$0.0391838\ RH^{1.5} tan^{-1}(0.023101 * \text{RH}) - 4.686035$$

Substituting, T = 40 ℃ and RH = 25%

We obtain, wet bulb temperature of the inlet air, T_w = 26.70 ℃

6.3.3 Inlet Air Humid Volume

Now, the humid volume of the moist air is given by equation (6.25)

$$V_H\ \left(\frac{m^3}{kg\ dry\ air}\right) = (2.83\ x\ 10^{-3}\ \ + 4.56\ x\ 10^{-3}\ H)(273.15 + T) \qquad (6.25)$$

Where V_H is the humid volume, H is the absolute humidity and T is the temperature of air in ℃

Therefore, the humid volume of the inlet air

$$V_H\ \left(\frac{m^3}{kg\ dry\ air}\right) = (2.83\ x\ 10^{-3}\ \ + 4.56\ x\ 10^{-3} x\ 0.0032)(273.15 + 40) = 0.90\ m^3\ (\text{kg dry air})^{-1}$$

6.3.4 Inlet Air Density

Therefore, the density of inlet air, ρ = $\left(\frac{1+H}{V_H}\right)$ = (1+0.0124)/0.89 = 1.1206 (kg dry air + kg H_2O) m^{-3}

6.3.5 Average Humid Heat Over the Drying Bed

The inlet air saturation vapor pressure at the wet-bulb temperature T_w, kPa

$= P_w(kPa) = 0.61078 * e^{\left(\frac{17.24*26.70}{26.70+237.2}\right)} = 3.4965$ kPa

The inlet air wet bulb humidity is H_{iw}

$= H_{iw}\ (kg\ water\ \ kg\ dry\ air^{-1}) = \frac{18.02*3.4965}{28.97(101.325-\ 3.4965)}\ = 0.0222$

The average of the absolute humidity over the bed = $(H_i + H_{iw})/2$ = (0.0114 + 0.0222)/2 = 0.0168 kg water (kg dry air)$^{-1}$

Therefore, the average humid heat over the bed C_s = (1.005 + 1.88 H) kJ (kg dry air. K)$^{-1}$ = 1.005 + 1.88 x 0.0168 = 1036.69 J kg^{-1} K^{-1}

6.3.6 Void Fraction in The Drying Cabinet

Blade length = 25 inch = 635 mm

Blade width = 6 inch = 152 mm

Blade thickness = 2mm = 0.002 m

Box dimensions = 30 x 30 x 50 inch^3 = 0.7373 m^3

Therefore, single blade surface area = 2 x 25 inch x 6 inch = 300 inch^2 = 0.1935 m^2

Volume of single blade = 25 inch x 6 inch x 0.002 m = 0.0001935 m^3

Void fraction, ε = 1 – (Net volume of the blades/volume of the cabinet) = 1 – (no. of blades x volume of the single blade/volume of the cabinet) = 1-(28 x 0.0001935/0.7374) = 0.9853

Therefore, ε or void fraction = 0.9853

6.3.7 Superficial Velocity

As the void fraction is almost equal to 1, we can consider the superficial velocity will be equal to the inlet air velocity = 1m s^{-1}

6.3.8 Inlet Air Mass Velocity

Mass velocity of dry air (kg dry air s^{-1} m^{-2}) = Superficial velocity x density of inlet air x mass fraction of dry air in the inlet stream = 1m s^{-1} x 1.1206 (kg dry air + kg H_2O) m^{-3} x $\left(\frac{1}{1+0.0114}\right)$ = 1.107 kg dry air s^{-1} m^{-2}

6.3.9 Equivalent Diameter, D_p

D_p is the diameter in m of a sphere having the same surface area as the particle in the bed

Blade length = 25 inch = 635 mm

Blade width = 6 inch = 152 mm

Blade thickness = 2mm = 0.002 m

Therefore, single blade surface area = 2 x 25 inch x 6 inch = 300 $inch^2$ = 0.193548 m^2

Therefore, surface area of sphere, πD_p^2 = 2 x Blade length x Blade width,

πD_p^2 = 2 x 25 inch x 6 inch

So, D_p = 0.2482 m

6.3.10 Geometry Factor, a

a, net surface area of drying per unit volume of the drying cabinet, m^{-1}

Single blade surface area = 2 x 25 inch x 6 inch = 300 $inch^2$ = 0.193548 m^2

Surface area of 28 blades = 28 x 0.193548 m^2 = 5.419 m^2

Volume of the drying cabinet = 30 x 30 x 50 $inch^3$ = 0.7373 m^3

Therefore, a = 5.419/0.7373 = 7.35 m^{-1}

6.3.11 Reynolds Number for The Air Flow, N_{re}

Average air temperature, $(T_i + T_w)/2 = (40 + 26.70) = 33.35$ ℃

Therefore, average coefficient of viscosity $= 1.458\ x\ 10^{-6} x\ \frac{(273.15+33.35)^{1.5}}{(273.15+33.35+110.4)}$ = 1.8766 x 10^{-5} Pa.s

$G_{average}$ over the bed = $G_{inlet} + G_{inlet}$ x $H_{average}$ = 1.107 + 1.107 x 0.0168 = 1.1265 kg dry air s^{-1} m^{-2}

$N_{re} = G_{average}\ D_p/\mu$ = 1.1265 x 0.2482 x $(1.8766 \times 10^{-5})^{-1}$ = 14904.23

6.3.12 Convective Heat Transfer Coefficient, h

As, the N_{Re} is greater than 350

$G_{average}$ over the bed = $G_{inlet} + G_{inlet}$ x $H_{average}$ = 1.107 + 1.107 x 0.0168 = 1.1265 kg dry air s^{-1} m^{-2}

Therefore, $h = 0.151\ x\ \frac{(G_{average})^{0.59}}{(D_p)^{0.41}}$ = 35.95 W m^{-1} K^{-1}

6.3.13 Latent Heat at The Wet Bulb Temperature λ_w

$$\lambda_w = e^{\sqrt{\left(64.87678+11.76476\left[0.35\ln\left(\frac{1}{T_r}\right)-11.94431\left(\frac{1}{T_r}\right)^2+6.29015\left(\frac{1}{T_r}\right)^3-0.99893\left(\frac{1}{T_r}\right)^4\right]\right)}}$$

T_r is the reduced temperature and given by $T_w = \frac{T+273.15}{647.096}$

Therefore, at T_w (26.70 ℃), Tr = (273.15+26.70 ℃)/ 647.096 = 0.4633

Substituting Tr = 0.4633 in above equation we obtain, λ_w = 2551479.32 J kg^{-1}

6.3.14 Drying Time, t

On substituting all the variables in eq. 6.18, the calculated and experimental drying time was 3.13 hrs. and 3 hrs., respectively. This shows the developed model based on the assumption of drying kelp in a highly turbulent porous bed gives significantly closer values to the experimental values. The calculated values of the drying air and product parameters for different sets of inlet air temperature and relative humidity using the model are given in **Table 6.1**.

Table 6.1. The calculated drying vs the experimental drying for different inlet air temperature and humidity

Inlet air temperature, T_i	Inlet air relative humidity, H_i	No. of kelp blades	Calculated drying time (hrs.)	Experimental drying time (hrs.)
40 ℃	25%	28	3.13	3
	50%	28	4.98	N.A
70 ℃	25%	28	1.19	N.A
	50%	28	2.44	N.A

N.A = Not Available

Sugar kelp was dried at an air velocity of 1m s^{-1} from an initial moisture content of 92 kg water (100 kg sample)$^{-1}$ to final moisture content of 10 kg water (100 kg sample)$^{-1}$

6.4 Conclusions

Working and maintaining very low humidity conditions in big drying chambers is challenging due to the regular opening and closing of drying cabinet doors while taking sample measurements. For an initial run, the experiment conducted at an inlet air condition of 40 ℃ temperature and relative humidity of 25%, the developed model predicted similar drying time as compared to the experimental value. The rate of moisture removal from the kelp was assumed to be directly proportional to the moisture content of the drying kelp based on the premise that drying of the thin layer of kelp is characterized by a falling rate period. More experiments are required to validate the model for its possible application in high turbulence porous bed drying with well mixing of solids irrespective of the particle size. The successfully validated model can also be used in optimizing the power consumption in the air blower and heating unit of the dryer based on the calculated drying time.

CHAPTER 7

OVERALL CONCLUSIONS AND RECOMMENDATIONS

With the increasing population of the world (approximately 9 billion in 2050) and limited land holdings for agriculture, food security is a concern to feed all the people (Melorose et al. 2015). Moreover, in the past few decades, the overall food production across the globe has been stagnant in comparison to the exponential surge in the population (FAO 2013). The availability of high quality and nutritious foods with all the essential nutrients needed for people of all ages is a major challenge for the scientists and engineers, who endlessly investigate to develop better post-harvest processing methods and systems to improve shelf-life of processed food products; one option for providing nutritious products is to focus on marine aquaculture sources such as seaweeds. It has been observed through different studies seaweeds are a good source of dietary fibers, vitamins, minerals, antioxidants and bioactive compounds with medicinal effects.

Sugar kelp grown in Maine, USA is available seasonally and due to its limited shelf life, fresh sugar kelp is processed using basic principles of food preservation including the addition of heat, removal of moisture, fermentation, cold and refrigerated storage. Sun-drying is the most common process for drying seaweeds around the world due to less investment cost in energy. However, the product's textural, chemical and nutrient properties degrade significantly as compared to the other drying methods including freeze-drying and hot air convective drying. In the state of Maine, the average number of sunny days as compared to the US average is less as a result of higher precipitation in the form of snow, rain, sleet or hail, especially during the harvest season of kelp from April till June. In order to increase the dried seaweed producing capacity in Maine, farmers must rely on convective hot air dryers. These dryers require high capital and energy investment and might not be an affordable option for small scale farmers or wild harvesters. With the help of new technologies such as solar, heat pumps, ultrasound, microwave and infrared, now convective dryers are capable of processing large volumes of seaweed in less time to

produce premium quality products. Freeze-drying or lyophilization is used mostly in the extraction of beneficial compounds from the dried seaweeds in small scales. Application of several novel processing and extraction methods along with the knowledge of moisture sorption isotherm, glass transition temperature and freezing point of seaweeds might help in better processing, extending storage and retaining nutrient profile beneficial for overall human health and sustainability. Understanding seasonal variation in Maine, especially the available sunshine and water temperature over the period of growth can help in predicting the proximate composition (fats, carbohydrates, ash content, and proteins) of the kelp and thus, an appropriate harvesting, processing and storage strategy can be employed depending on the available capital, infrastructure, energy cost and intented use of the seaweeds.

The drying rates are usually estimated by experimental data fitted to empirical models including the Newton, Page and Henderson & Pabis kinetic models. The empirical approach is easy to handle compared to the analytical approach due to lower computational requirements and only it represents pure kinetics of the physical process. Also, experimentally determining the empirical relationships requires a lot of labor, time and the experimental data doesn't provide necessary information regarding the process variables such as pressure drop, temperature, and humidity and it is applicable only for certain processing conditions. To understand the microscopic movement of moisture inside kelp, the flow of air inside the sugar kelp packed bed, determining heat and mass transfer rates involves solving complex partial differential equations of heat and mass transfer phenomena. In the seaweed drying process, the thermophysical properties change continuously with the sample temperature and moisture content. Limited knowledge of the change in thermal properties during drying and the requirement of high computational power makes solving partial differential equationapproach less feasible. A simpler approach for modeling drying of sugar kelp packed bed in hot air convective dryer wass developed in this study as a highly turbulent porous bed for predicting the drying time using inlet air parameters, loading conditions of kelp inside the dryer, and initial and final moisture content of the product. The rate of water removal from the kelp was observed to be directly proportional to the moisture content of the drying kelp.

The successfully validated model can be used for optimizing the energy consumption in the heating and ventilation unit based on the required drying time.

As per the UN Intergovernmental Panel on Climate Change (IPCC), the mean Earth temperature is predicted to rise by 3°C by the end of the present century due to a continuous rise in the concentration of greenhouse gases (IPCC 2007). Consequently, over the past decade, the sea surface in the Gulf of Maine warmed faster than 99% of the global ocean resulting in prolonged summer conditions lasting two months longer than in 1982 (Pershing et al. 2015). With an increase in the ambient temperature, the moisture diffusion coefficient or the measure of the drying kinetics will likely increase resulting in more moisture migration from seaweeds. In closed greenhouse drying, an increase in ambient temperature will have a net positive effect on the performance of the solar collector and net heat loss reduction to the surrounding (Piacentini and Mujumdar 2009). However, in closed heat pump-based dryers the Carnot efficiency will decrease with an increase in the ambient temperature. Also, for land, the global surface specific humidity has significantly increased at the rate of 0.11 kg kg^{-1} per decade between 1977 and 2003 (Willet et al. 2008). The rise in evaporative water transpiration in the Gulf of Maine will produce more cloud coverage augmenting the overall solar irradiation. Together, these effects are likely to change the dynamics of open-air drying of seaweeds and could make the drying conditions less predictable due to an increase in the frequency of storms and strong winds, warmer average air and water temperatures, higher humidity and more cloud cover. Increased challenges will also arise from more rain events that will reduce the times available for drying, while greater cloud cover and higher humidity will slow down the rate of drying. Together with the increase in harvest volume associated with seaweed farming, these climate effects may increase the use of closed drying methods. This will require higher capital investments in drying equipment and the added expense of drying energy, which in turn will likely result in farmers choosing to increase the scale of their operations to justify and make use of this expanded infrastructure. Some of the climate changes that affect open-air drying will also have an impact on controlled environment drying, since the ambient air will on average become warmer and more humid,

which will help and impede drying, respectively. Investigations carried out through the Sustainable Ecological Aquaculture Network (SEANET) project at the University of Maine have shown that controlled environment drying can improve the predictability of drying dynamics and preservation of bioactive components in sea vegetables (Sappati et al. 2017, 2019). To reduce the carbon footprint of the conventional fossil fuel-based dryers, new solar dryers with non-concentrating or concentrating collectors need to be backed up for additional heating using latent heat phase change materials, photovoltaics, wind energy, or other renewables sources.

A search for alternative renewable energy and the development of its application for energy-efficient uses are on the rise. One such constant source of renewable energy is the ground source heat pump (GSHP). It relies on indirect heating of earth crust by the constant source of solar energy. Heat transfers from the surface of the earth to the lower levels through conduction and is stored in the available groundwater. Water having high specific heat capacity acts as good heat storage and maintains at a near-constant temperature even though the air temperature varies significantly throughout the year. This available energy can be used for heating, cooling and supplying hot water without relying on the burning of fossil fuels. The ground source heat pump (GSHP) is a system that uses the groundwater as a heat sink or heat source for operating refrigeration cycles used for either heating or cooling the surrounding space. Its indirect dependence on solar energy makes it a more reliable and feasible option for heating in very cold places (Maine, US) where the availability of solar energy is uncertain. The variation in groundwater temperature in Maine is very low (~7-10 ^{o}C) as compared to the variation in the ambient air temperature (~-20 to 30 ^{o}C). These conditions are suitable for the application of GSHP for providing heating during cold winters and cooling during summers. The US Environmental Protection Agency (EPA) and the Department of Energy (DOE) have done economic and energy analysis and concluded that the geothermal heat pumps are the most environmentally friendly and highly cost-efficient for heating and cooling the surrounding space.

In general, ground source heat pumps (GSHP) comprise two loops; the first is a refrigerant loop and the second is the groundwater loop. The refrigerant is a fluid which boils at very low temperature and has a high latent heat of evaporation for high absorption of heat at low temperatures. The refrigerant loop comprises four pieces of equipment (evaporator, compressor, condenser and expansion valve). In the evaporator, the refrigerant enters as liquid and starts absorbing latent heat from the surrounding air and changes its phase to gas. The surrounding air is cooled below its dew point for condensing the dew in the surrounding air, resulting in separating the moisture from the surrounding air. This method will be useful in generating de-humidified air, which can be used for low-temperature drying of heat-sensitive food materials. The hot refrigerant after the compression stage is cooled using the groundwater pumped in the second loop.

GSHP can be used to generate cold dehumidified air, which can be further heated by the superheated refrigerant after the compression stage through the heat exchanger. This hot dehumidified air can be used for the low-temperature drying of the seaweeds for producing high quality dried seaweed and will be helpful in boosting the Maine economy in an eco-friendly way. Also, to increase the productivity of the seaweed farmers in Maine, the whole process of harvesting and processing needs to be mechanized to reduce the physical labor and time involved. Currently, all the harvested sugar kelp is hung manually on the vertical lines in a drying chamber. Mechanizing this one aspect of the whole process of growing, harvesting and drying can certainly increase the overall productivity by decreasing the run time.

On the other hand, overconsumption of sugar kelp can also cause serious health concerns due to elevated levels of iodine, inducing either hyper or hypothyroidism and a substantial risk of thyroid cancer (Miyai et al. 2008; Teas et al. 2004). The presence of the inorganic form of arsenic in food can also have a carcinogenic effect leading to a higher incidence of skin, lung and urinary tract cancer (Wells et al. 2016; IARC 2012). However, aquatic life such as fish, crustaceans, mollusks and algae, detoxifies the inorganic arsenic by converting it to nontoxic organic forms such as arsenobetaine, arsenosugars and arsenophospholipids (Garcia-Salgado et al. 2012; Molin et al. 2015). Several researchers have conducted

studies on the bioaccumulation of heavy metals in the commercially available and processed dried seaweed products (Almeda et al., 2006; Besada et al., 2009) and found their concentration is less than the toxic limits. However, some brown seaweeds such as *Laminaria digitata* (Hansen et al. 2003) and *Laminaria hyperborean* (Taylor and Jackson 2016) tend to accumulate higher amount of the inorganic form of arsenic. Especially *Sargassum fusiforme*, commonly known as hijikia, contains levels of total arsenic and inorganic arsenic, 149 mg/kg dry solids and 117 mg/kg dry solids, respectively (Almela et al., 2006) far exceeding thelimit of 3 mg/kg dry solids or less by the French, Canadian, UK and US regulatory limits for food products (CFIA 2012; UK FSA 2016). It has been shown that the concentration of iodine and arsenic in the seaweed can be reduced considerably by cooking or rehydrating in boiling water (Ichikawa et al. 2006; Nitschke and Stengel, 2016) and found no significant change in concentration by applying drying methods. However, more studies are required to understand and quantify the toxicity, bioavailability, and metabolism of these minerals derived from seaweeds in the human digestive system, to potentially act as a supplemental source of essential macro and trace minerals.

Sixty-five percent of the total estuaries present in the contiguous US arebe moderately to severely degraded in terms of water quality and coastal ecosystems due to excess nutrient input from fertilizer runoff. Studies using model projects have shown promising results in reclaiming these estuaries by removing excess nutrients using bivalve aquaculture. These projects have also demonstrated that bivalve aquaculture requires less investment as compared to traditional nutrient-reduction methods including wastewater treatment improvements and best agricultural management practices. However, with the rise in ocean temperature and solubility of carbon dioxide, lowering of the seawater pH (ocean acidification) may prevent shell formation in bivalves resulting in lower yield and making it a less commercially viable option. The excess nutrient load in the form of nitrogen and phosphorus might be reduced by seaweeds, especially green seaweeds, due to their high nutrient tolerance. However, seaweeds harvested from eutrophic zones can possess food safety issues and might not be appealing to the consumers. Microalgae have been identified as a future source of producing biofuels due to theirits high lipid content as

compared to macroalgae. Converting green seaweeds grown in eutrophic zones into biofuels as compared to the other groups may provide a possible solution for producing alternative fuel options and restoring the native ecosystem in these dead zones. The process of producing biofuels is not yet profitable and commercially viable due to high energy/cost as compared to the conventional nonrenewable fuels. Alternatively, the seaweeds grown can also be utilized as animal feeds. A large number of studies have shown algal supplementation in the diets of aquaculture and land-based animals improved the animal health and quality of the finished products.

With reference to drying seaweeds, especially sugar kelp in Maine, seaweed farmers need to establish or identify a potential market and understand their customer behavior related to seaweed usage. Currently, several seaweed products are being consumed including extracts for cosmetics, animal feed, fertilizers, and human food (seaweed chips, food ingredients, dried sheets, flavor enhancers). This provides a huge opportunity for seaweed farmers in Maine to benefit economically and establish a sustainable seaweed industry. At present, sugar kelp is grown in aquaculture systems in Maine for the past seven years and the involved method of producing fully grown kelp from reproductive propagules is well understood. However, this study was done to provide the required information to seaweed farmers on the post-harvesting practices, especially drying and storage inputs to extend the shelf life of sugar kelp. Apart from drying, seaweed farmers can also look for other methods to process fresh seaweed including blanching, blanch freezing, and fermentation to produce different varieties of products. However, these processing methods further require additional infrastructure, energy inputs, and an in-depth understanding of the processing effects for producing high-quality finished products for consumers.

Conducting various scientific experiments and making a final conclusion based on the observation throughout this study has certain limitations. Sampling location was limited to one seaweed farm in Damariscotta bay, Maine to avoid the interference of geographical factors such as water temperature, available sunshine, and nutrient flux. In order to increase the accuracy of the study and make robust conclusions in future more sampling location and frequency over the harvesting period are needed.

This study can be further improved by quantifying specific minerals, amino acids, and fatty acids to better understand the impact of processing on the qualitative aspect of the final product. Scanning electron microscopy can also be used as an additional tool to assess the microscopic structural changes during drying processes under different conditions. Overall, seaweed farmers in Maine may rely on the results from this study to make decisions involving suitable harvesting period, post-harvest processing methods, and storage conditions to prolong the shelf life of sugar kelp for various applications and also extrapolate the same knowledge for other applicable seaweeds as well.

REFERENCES

Adams JM, Toop TA, Donnison IS, Gallagher JM (2011) Seasonal variation in *Laminaria digitata* and its impact on biochemical conversion routes to biofuels. Bioresour Technol 102:9976-9984.

Ahmedna M, Prinyawiwatkul W, Rao RM (1999) Solubilized wheat protein isolate: functional properties and potential food applications. J Agric Food Chem 47(4):1340-1345.

Airanthi M, Hosokawa M, Miyashita K (2011) Comparative antioxidant activity of edible Japanese brown seaweeds. J Food Sci 76:104-111.

Akonor PT, Ofori H, Dziedzoave NT, Kortei NK (2016) Drying Characteristics and Physical and Nutritional Properties of Shrimp Meat as Affected by Different Traditional Drying Techniques. Int J Food Sci 2016:1-5.

AOAC Method 993.13 (1990) Official Methods of Analysis (fifteenth ed.), Association of Official Analytical Chemists, Washington, DC.

AOAC (1999) Official Methods of Analysis (sixteenth ed.), Association of Official Analytical Chemists, Washington, DC.

AOAC Method 948.15 (2005) Fat (Crude) in Seafood Acid Hydrolysis Method. Official Methods of Analysis (eighteenth ed.), Association of Analytical Communities International, Gaithersburg, MD.

AOAC Official Method 967.21 (1968) Ascorbic Acid in Vitamin Preparations and Juices 2,6-Dichloroindophenol Titrimetric Method. First Action 1967, Final Action 1968.

AOAC Official Method 985.33 (1988) Vitamin C (Reduced Ascorbic Acid) in Ready-to- Feed Milk-Based Infant Formula. 2,6-Dichloroindophenol Titrimetric Method. First Action 1985, Final Action 1988.

Aquino-Bolaños EN, Mercado-Silva E (2004) Effects of polyphenol oxidase and peroxidase activity, phenolics and lignin content on the browning of cut jicama. Postharvest Biol Technol 33:275–283.

Argyropoulos D, Heindl A, Müller J (2011) Assessment of convection, hot-air combined with microwave-vacuum and freeze-drying methods for mushrooms with regard to product quality. Int JFood Sci Tech 46: 333–342.

Astorga-España MS, Galdón BR, Rodríguez ER, Romero CD (2015) Mineral and trace element concentrations in seaweeds from the sub-Antarctic ecoregion of Magallanes (Chile). J Food Compos Anal 39:69-76.

Badii F, Farahnaky A, Behmadi H (2014) Effect of Storage Relative Humidity on Physical Stability of Dried Fig. J Food Process Pres 38: 477–483.

Bai Y, Rahman MS, Perera CO et al (2001) State diagram of apple slices: Glass transition and freezing curves. Food Res 34: 89–95.

Balingasa C R, Elepaño AR (2009) Studies on engineering properties of red seaweed (Kappaphycus spp.). Philippines J Agr Bios Eng 7: 59-69.

Baur FJ Jr, Brown JB (1945) The fatty acids of corn oil. J Am Chem Soc 67(11):1899-1900.

Bennett AH, Chace Jr WG, Cubbedge RH (1969) Heat transfer properties and characteristics of Appalachian area 'Red Delicious' apple. ASHRAE Trans 75(2): 133.

Benzie IF, Strain JJ (1999) Ferric reducing/antioxidant power assay: direct measure of total antioxidant activity of biological fluids and modified version for simultaneous measurement of total antioxidant power and ascorbic acid concentration. Methods Enzymol 299:15-27.

Beppu F, Hosokawa M, Yim M, Shinoda T, Miyashita K (2013) Down-regulation of hepatic stearoyl-CoA desaturase-1 expression by fucoxanthin via leptin signaling in diabetic/obese KK-A(y) mice. Lipids 48(5):449-455.

Bhandari BR, Howes T (1999) Implication of glass transition for the drying and stability of dried foods. J Food Eng 40: 71–79.

Black WAP, Dewar ET (1949) Correlation of some of the physical and chemical properties of the sea with the chemical constitution of the algae. J Mar Biol Assoc U K 28(03):673-699. https://doi.org/10.1017/S002531540002350X

Black WAP (1950) The seasonal variation in weight and chemical composition of the common British Laminariaceae. J Mar Biol Assoc U K 29(1): 45-72.

Blois MS (1958) Antioxidant determinations by the use of a Stable Free Radical. Nature 181:1199-1200.

Boukouvalas Ch J, Krokida MK, Maroulis ZB, Marinos-Kouris D (2006) Effect of material moisture content and temperature on the true density of foods. Int J Food Prop 9(1):109-125.

Boukouvalas Ch J, Krokida MK, Maroulis ZB, Marinos-Kouris D (2006) Density and porosity: literature data compilation for foodstuffs. Int J Food Prop 9(4):715-746.

Braune W, Guiry MD (2011) Seaweeds: A Colour Guide to Common Benthic Green, Brown and Red Algae of the World's Oceans. Koeltz Scientific Books, Königstein, Germany.

Brewer DR, Franco JM, Garcia-Zapateiro LA (2016) Rheological properties of oil-in-water emulsions prepared with oil and protein isolates from sesame (Sesamum Indicum). Food Sci Technol 36(1):64-69.

Brunauer S, Deming LS, Teller E (1940) On a theory of Van der Waals adsorption of gases. J Am Chem Soc 62 (7): 1723-1732

Buera MP, Roos Y, Levine H, Slade L et al (2011) State diagrams for improving processing and storage of foods, biological materials, and pharmaceuticals (IUPAC Technical Report). Pure Appl Chem 83: 1567–1617.

Burtin P (2003) Nutritional value of seaweeds. Elect J Environ Agri Food Chem 2:498–510.

Camire ME, Flint SI (1991) Thermal processing effects on dietary fibre composition and hydration capacity in corn meal, oat meal and potato peels. Cereal Chem 68(6):645–647.

Campbell SJ, Bite JS, Burridge TR (1999) Seasonal patterns in the photosynthetic capacity, tissue pigment and nutrient content of different developmental stages of Undaria pinnatifida (Phaeophyta: Laminariales) in Port Phillip Bay, south-eastern Australia. Bot Mar 42:231-241.

Campo VL, Kawano DF, da Silva Jr, DB, Carvalho I (2009) Carrageenans: biological properties, chemical modifications and structural analysis – a review. Carbohydr Polym 77:167–180.

Caprez A, Arrigoni E, Amado R, Neukom H (1986) Influence of different types of thermal treatment on the chemical composition and physical properties of wheat bran. J Cereal Sci 4:233–239.

Carslaw HS, Jaeger JC (1959) Conduction of Heat in Solids. Clarendon Press, Oxford.

Chan JC-C, Cheung PC-K, Ang PO (1997) Comparative studies on the effect of three drying methods on the nutritional composition of seaweed Sargassum hemiphyllum (Turn.) C. Ag. J Agric Food Chem 45(8):3056-3059.

Chakraborty K, Maneesh A, Makkar F (2017) Antioxidant activity of brown seaweeds. J Aquat Food Prod T 26:406-419.

Chandini SK, Ganesan P, Bhaskar N (2008) In vitro antioxidant activities of three selected brown seaweeds of India. Food Chem 107:707-713.

Chapman ARO (1987) Population and community ecology of seaweeds. Adv mar Biol 23:1-161.

Chapman ARO, Craigie JS (1978) Seasonal growth in Laminaria longicuris: relations with reserve carbohydrate storage and production. Mar Biol 46(3):209-213.

Chapman ARO, Craigie JS (1997) Seasonal growth in Laminaria longicruris: relations with dissolved inorganic nutrients and internal reserves of nitrogen. Mar Biol 40(3):197-205.

Chen CS (1986) Effective molecular weight of aqueous solutions and liquid foods calculated from the freezing point depression. J Food Sci 51: 1537–1553.

Choi Y, MR Okos (1986) Effects of temperature and composition on the thermal properties of foods. Food Engineering and Process Applications 1:93-101. London: Elsevier Applied Science Publishers.

Chopin T, Yarish C, Wilkes R, Belyea E, Lu S, Mathieson A (1999) Developing Porphyra/salmon integrated aquaculture for bioremediation and diversification of the aquaculture industry. J Appl Phycol 11:463–472.

Clendenning K (2009) Determination of Fresh Weight, Solids, Ash and Equilibrium Moisture in Macrocystis pyrifera. Bot Mar 4:204-218.

Coimbra JSR, Gabas AL, Minim LA, Garcia Rojas EE, Telis VRN, Telis-Romero J (2006) Density, heat capacity and thermal conductivity of liquid egg products. J Food Eng 74(2):186-190.

Costa BR, Rocha SF, Rodrigues MCK, Pohndorf RS, Larrosa APQ, Pinto LAA (2015) Physicochemical characteristics of the Spirulina sp. dried in heat pump and conventional tray dryers. Int J Food Sci Technol 50:2614-2620.

Cumashi A, Ushakova NA, Preobrazhenskaya ME, D'Incecco A, Piccoli A, Totani L et al (2007) A comparative study of the anti-inflammatory, anticoagulant, antiangiogenic, and antiadhesive activities of nine different fucoidans from brown seaweeds. Glycobiology 17(5):541-552.

Craigie JS (2011) Seaweed extract stimuli in plant science and agriculture. J Appl Phycol 23: 321-335.

Crank J (1975) The Mathematics of Diffusion. (2nd ed., pp. 44-68). Oxford University Press, Oxford, UK.

Damonte E, Neyts J, Pujol CA, Snoeck R, Andrei G, Ikeda S et al (1994) Antiviral activity of a sulphated polysaccharide from the red seaweed nothogenia fastigiata. Biochem Pharmacol 47(12):2187-2192.

Dana D, Saguy IS (2006) Review: mechanism of oil uptake during deep-fat frying and the surfactant effect-theory and myth. Adv Colloid Interface Sci 128–130:267–272.

Dang TT, Vuong QV, Schreider MJ, Bowyer MC, Altena IAV, Scarlett CJ (2016) The Effects of drying on Physico-Chemical Properties and Antioxidant Capacity of the Brown Alga (Hormosira banksii(Turner) Decaisne). J Food Process Preserv 41: e13025.

Darcy-Vrillon, B., 1993. Nutritional aspects of the developing use of marine macroalgae for the human food industry. Int J Food Sci Nutr, 44, 23–35.

Das Purkayastha M, Nath A, Deka BC, Mahanta CL (2013) Thin layer drying of tomato slices. J Food Sci Technol 50(4):642-653.

Datta AK (2007a) Porous media approaches to studying simultaneous heat and mass transfer in food processes. I: problem formulations. J Food Eng 80(1): 80–95.

Datta AK (2007b) Porous media approaches to studying simultaneous heat and mass transfer in food processes. II: property data and representative results. J Food Eng, 80(1), 96–110.

Davis TA, Volesky B, Mucci A. 2003. A review of the biochemistry of heavy metal biosorption by brown algae. Water Res 37:4311-4330.

Dawczynski C, Schubert R, Jahreis G (2007) Amino acids, fatty acids, and dietary fiber in edible seaweed products. Food Chem 103:891-89

Delgado AE, Gallo A, De Piante D, Rubiolo A (1997) Thermal conductivity of unfrozen and frozen strawberry and spinach. J Food Eng 31(2): 137-146.

Demir V, Gunhan T, Yagcioglu AK, Degirmencioglu A (2004) Mathematical modelling and the determination of some quality parameters of air-dried bay leaves. Biosystems Engineering 88: 325–335.

Deng Y, Luo Y L, Wang YG, Zhao YY (2015). Effect of different drying methods on the myosin structure, amino acid composition, protein digestibility and volatile profile of squid fillets. Food Chem 171:168-176.

Deng Y, Wu J, Su SQ, Liu ZD, Ren L, Zhang YL (2011) Effect of far-infrared assisted heat pump drying on water status and moisture sorption isotherm of squid (Illex illecebrosus) fillets. Drying Technol 29(13):1580-1586.

Dickerson RW, Read RB (1975). Thermal diffusivity of meats. ASHRAE Trans 81(1):356.

Dillehay TD, Ramirez C, Pino M, Collins MB, Rossen J, Pinot-Navarro JD (2008) Monte Verde: seaweed, food, medicine and the peopling of South America. Science 320:784-789.

Djaeni M, Sari DA (2015) Low Temperature Seaweed Drying Using Dehumidified Air. Procedia Environmental Sciences 23: 2–10.

Doymaz I, Tugrul N, Pala M (2006) Drying characteristics of dill and parsley leaves. Journal of Food Engineering 77: 559–565.

Doymaz I (2006) Air-drying characteristics of tomatoes. Journal of Food Engineering 78: 1291– 1297.

Drążkiewicz M, Krupa Z (1991) The participation of chlorophyllase in chlorophyll metabolism. Acta Soc Bot Pol 60:139-154.

Eko Susanto et al (2017) Effects of Different Heat Processing on Fucoxanthin, Antioxidant Activity and Colour of Indonesian Brown Seaweeds. IOP Conf Ser: Earth Environ Sci 55 012063. http://iopscience.iop.org/article/10.1088/1755-1315/55/1/012063/pd.

Elansari AM, Hobani AI (2009) Effect of temperature and moisture content on thermal conductivity of four types of meat. Int J Food Prop 12(2): 308-315.

El Maghraby DM, Fakhry EM (2015) Lipid content and fatty acid composition of Mediterranean macro-algae as dynamic factors for biodiesel production. Oceanologia 57: 86-92.

Eonseon J, Polle JEW, Lee HK, Hyund SM, Chang M (2003) Xanthophylls in microalgae: from biosynthesis to biotechnological mass production and application. Microb Biotechnol 13:165-174

Erenturk S, Gulaboglu MS, Gultekin S (2005) The effects of cutting and drying medium on the vitamin C content of rosehip during drying. J Food Eng 68:513-

Erge HS, Karaden Z, Koca N, Soyer Y (2008) Effect of heat treatment on chlorophyll degradation and color loss in green peas. Gida 33:225-233.

Fadhel MI, Sopian K, Daud WRW (2010) Performance analysis of Solar-Assisted Chemical Heat-Pump Dryer. Sol. Energy 84:1920–1928

FAO (2013) FAO Statistical Yearbook 2013: World Food and Agriculture (pp. 123-201), Food and Agriculture Organisation of the United Nations (FAO), Rome, Italy

Fariman GA, Shastan SJ, Zahedi MM (2016) Seasonal variation of total lipid, fatty acids, fucoxanthin content, and antioxidant properties of two tropical brown algae (Nizamuddinia zanardinii and Cystoseira indica) from Iran. J Appl Phycol 28(2): 1323-1331.

Fasina O (2003) Infrared Heating of Food and Agricultural Materials. In ASAE Annual Meeting American Society of Agricultural and Biological Engineer, Las Vegas, USA.

Fleurence J (1999) Seaweed proteins biochemical, nutritional aspects and potential uses. Trends Food Sci Technol 10(1):25-8.

Fleurence J, Levine I (2016) Seaweed in Health and Disease Prevention. Academic Press, San Diego

Foti MC, Daquino C, Geraci C (2004) Electron-transfer reaction of cinnamic acids and their methyl esters with the DPPH radical in alcoholic solutions. J Org Chem 69: 2309-2314.

Gallali YM, Abujnah YS, Bannani FK (2000) Preservation of fruits and vegetables using solar drier: a comparative study of natural and solar drying, III; chemical analysis and sensory evaluation data of the dried samples (grapes, figs, tomatoes and onions). Renewable Energy 19: 203–212.

Geankoplis CJ (1993) Transport Processes and Unit Operations. Drying of Process Materials, 3rd edn. Prentice Hall Int, Englewood cliffs, New Jersey, USA, pp 520-583.

George M, Abraham TE (2006) Polyionic hydrocolloids for the intestinal delivery of protein drugs: Alginate and chitosan - a review. J Control Release 114(1):1-14.

Gonda S, Tóth L, Gyémánt G, Braun M, Emri T, Vasas G (2012) Effect of high relative humidity on dried plantago lanceolata L. leaves during long-term storage: Effects on chemical composition, colour and microbiological quality. Phytochem Analysis 23: 88–93.

Goula AM, Adamopoulos KG (2006) Retention of ascorbic acid during drying of tomato halves and tomato pulp. Drying Technol 24:57-64

Gordon M, Taylor JS (1952) Ideal copolymers and the second order transitions of synthetic rubbers. I. Non-crystalline copolymers. J Appl Chem 2: 493–500.

IFST (1993) Shelf life of foods: guidelines for its determination and prediction. Institute of Food Science and Technology (UK). London, UK.

Ikeguchi M, Yamamoto M, Arai Y et al (2011) Fucoidan reduces the toxicities of chemotherapy for patients with unresectable advanced or recurrent colorectal cancer. Oncol Lett 2(2):319-322.

Indegaard M, Ostgaard K (1991) Polysaccharides for food and pharmaceutical. In: Guiry MD, Blunden G (ed) Seaweed resources in Europe: uses and potential, John Wiley & Sons Ltd, Chichester, pp. 169-183

Ito K, Hori K (1989) Seaweed: Chemical composition and potential foods uses. Food Rev Int 5:101-144Johary, G.P., Hallbrucker, A., Mayer, E., 1987. The glass–liquid transition of hyperquenched water. Nature 330 (10): 552–553.

Jeffrey SW, Mantoura RFC, Bjørnland T (1997) Data for the identification of 47 key phytoplankton pigments. In: Jeffrey SW, Mantoura RFC, Wright SW (ed) Phytoplankton Pigments in Oceanography: Guidelines to Modern Methods, SCOR-UNESCO, Paris, France.

Jiménez-Escrig A, Goñi Cambrodón I (1999) Nutritional evaluation and physiological effects of edible seaweeds. Arch Latinoam Nutr 49(2):114.

Jones DB (1931) Factor for Converting Percentages of Nitrogen in Foods and Feeds into Percentages of Proteins. USDA Circ 1-22.

Kalogeras IM, Brostow W (2009) Glass transition temperatures in binary polymer blends. Journal of polymer science. Part B, Polymer physics 47: 80-95.

Kang S, Heo S, Kim K, Lee S, Yang H, Kim A, Jeon Y (2012) Molecular docking studies of a phlorotannin, dieckol isolated from Ecklonia cava with tyrosinase inhibitory activity. Bioorganic Med Chem Lett 20(1):311-316.

Karathanos VT, Kanellopoulos NK, Belessiotis VG (1996) Development of porous structure during air drying of agricultural plant products. J Food Eng 29: 167–183.

Katsube T, Tsurunaga Y, Sugiyama M, Furuno T, Yamasaki Y (2009) Effect of air-drying temperature on antioxidant capacity and stability of polyphenolic compounds in mulberry (Morus alba L.) leaves. Food Chem 113(4):964-969.

Kaya A, Aydın O, Kolaylı S (2010) Effect of different drying conditions on the vitamin C (ascorbic acid) content of Hayward kiwifruits (Actinidia deliciosa Planch). Food Bioprod Process 88(2):165-73

Kinsella E, Melachouris N (2009) Functional properties of proteins in foods: A survey. CRC Crit Rev Food Sci Nutr 7(3):219-280.

Khotimchenko SV, Gusarova IS (2004) Red algae of Peter the Great Bay as a source of arachidonic and eicosapentaenoic acids. Russ J Mar Biol 30:183-187.

Khotimchenko SV, Kulikova IV (2000) Lipids of different parts of the lamina of Laminaria japonica Aresch. Bot Mar 43:87-91.

Khotimchenko SV, Vaskovsky VE, Titlyanova TV (2002) Fatty acids of marine algae from the Pacific coast of North California. Bot Mar 45: 17-22.

Klein BP, Kurilich AC (2000) Processing effects of dietary antioxidants from plant food. Hortscience 35:580-584

Kotake-Nara E, Sugawara T, Nagao A (2005) Antiproliferative effect of neoxanthin and fucoxanthin on cultured cells. Fish. Sci. 71, 459-461. https://doi-org.prxy4.ursus.maine.edu/10.1111/j.1444-2906.2005.00986.x

Kraan S (2012) Algal polysaccharides, novel applications and outlook. In: Chang, CF (ed) Carbohydrates-Comprehensive Studies on Glycobiology and Glycotechnology, InTech, pp. 489–532.

Kumar CS, Ganesan P, Suresh P, Bhaskar N (2008) Seaweeds as a source of nutritionally beneficial compounds - A review. J Food Sci Technol 45:1-13.

Kumar PS, Sagar VR (2014) Drying kinetics and physico-chemical characteristics of osmo-dehydrated mango, guava and aonla under different drying conditions. J Food Sci Technol 51(8):1540-1546

Kumar Naidu BV, Sairam M, Raju KVSN, Aminabhavi TM (2005) Thermal, viscoelastic, solution and membrane properties of sodium alginate/hydroxyethylcellulose blends. Carbohydrate Polymers 61: 52–60.

Kurozawa, L.E., Hubinger, M.D., Park, K.J., 2012. Glass transition phenomenon on shrinkage of papaya during convective drying. J Food Eng 108, 43–50.

Kumar S, Sahoo D, Levine I (2015) Assessment of nutritional value in a brown seaweed Sargassum wightii and their seasonal variations. Algal Res 9: 117-125.

Kurozawa LE, Hubinger MD, Park KJ (2012) Glass transition phenomenon on shrinkage of papaya during convective drying. J Food Eng 108(1):43-50.

Lahsasni S, Kouhila M, Mahrouz M, Fliyou M (2003) Moisture adsorption-desorption isotherms of prickly pear cladode (Opuntia ficus indica) at different temperatures. Energy Convers Manag 44: 923–936.

Lann KL, Ferret C, VanMee E, Spagnol C, Lhuillery M, Payri C, Stiger-Pouvreau V (2012) Total phenolic, size-fractionated phenolics and fucoxanthin content of tropical Sargassaceae (Fucales, Phaeophyceae) from the South Pacific Ocean: Spatial and specific variability. Phycol Res 60(1):37-50.

Lann KL, Jegou C, Stiger-Pouvreau V (2008) Effect of different conditioning treatments on total phenolic content and antioxidant activities in two Sargassacean species: Comparison of the frondose Sargassum muticum (Yendo) Fensholt and the cylindrical Bifurcaria bifurcata R. Ross. Phycol Res 56(4):238-245.

Ling ALM, Yasir S, Matanjun P, Abu Bakar MF (2015) Effect of different drying techniques on the phytochemical content and antioxidant activity of Kappaphycus alvarezii. J Appl Phycol 27(4):1717-1723

Lebert A, Tharrault P, Rocha T, Marty-Audouin, C (1992) The drying kinetics of mint (Mentha spicata Huds.). J Food Eng 17: 15–28.

Lee HJ, Kim HC, Vitek L, Nam CM (2010) Algae consumption and risk of type 2 diabetes: Korean National Health and Nutrition Examination Survey in 2005. J Nutr Sci Vitaminol 56(1):13.

Lee KY, Mooney DJ (2012) Alginate: Properties and biomedical applications. Prog Polym Sci 37(1):106.

Lemus RA, Pérez M, Andrés A, Roco T, Tello CM, Vega A (2008) Kinetic study of dehydration and desorption isotherms of red alga Gracilaria. LWT - Food Sci Technol, 41:1592-1599.

Leopoldini M, Marino T, Russo N, Toscano M (2004) Antioxidant properties of phenolic compounds: H-atom versus electron transfer mechanism. J Phys Chem A 108(22):4916-4922.

Levi G, Karel M (1995) Volumetric shrinkage (collapse) in freeze-dried carbohydrates above their glass transition temperature. Food Res 28 (2): 145–151.

Lewicki PP, Jakubczyk E (2004) Effect of hot air temperature on mechanical properties of dried apples. J Food Eng 64: 307–314.

Lim YY, Murtijaya J (2007) Antioxidant properties of Phyllanthus amarus extracts as affected by different drying methods. LWT-Food Sci Technol 40:1664-1669.

Ling ALM, Yasir S, Matanjun P, Abu Bakar MF (2015) Effect of different drying techniques on the phytochemical content and antioxidant activity of Kappaphycus alvarezii. J Appl Phycol 27(4):1717-1723.

Lourenço SO, Barbarino E, De-Paula JC, Pereira L Oda S, Marquez UML (2002) Amino acid composition, protein content and calculation of nitrogen-to-protein conversion factors for 19 tropical seaweeds. Phycol Res 50:233-241.

Lüning K (1990) Seaweeds: Their Environment, Biogeography, and Ecophysiology. Wiley-Interscience Publication, New York.

Mabeau S, Fleurence J (1993) Seaweed in food products: biochemical and nutritional aspects. Trends Food Sci Technol 4(4):103-107.

Manns D, Nielsen MM, Bruhn A, Saake B, Meyer AS (2017) Compositional variations of brown seaweeds Laminaria digitata and Saccharina latissima in Danish waters. J Appl Phycol 29:1493-1506.

Martino MN, Otero L, Sanz PD, Zaritzky NE (1998) Size and location of ice crystals in pork frozen by high-pressure-assisted freezing as compared to classical methods. Meat Sci 50(3):303-13.

Maskan M (2001) Drying, shrinkage and rehydration characteristics of kiwifruits during hot air and microwave drying. J Food Eng 48(2):177-82.

Matanjun P, Mohamed S, Mustapha NM, Muhammad K (2009) Nutrient content of tropical edible seaweeds, Eucheuma cottonii, Caulerpa lentillifera and Sargassum polycystum. J Appl Phycol 21(1):75-80.

Mayor L, Sereno AM (2004) Modelling shrinkage during convective drying of food materials: A review. J Food Eng 61: 373–386.

McDermid KJ, Stuercke B (2003) Nutritional composition of edible Hawaiian seaweeds. J Appl Phycol 15(6):513-524.

Melo T, Alves E, Azevedo V, Martins AS, Neves B, Domingues P, Calado R, Abreu MH, Domingues MR (2015) Lipidomics as a new approach for the bioprospecting of marine macroalgae-unraveling the polar lipid and fatty acid composition of Chondrus crispus. Algal Res 8:181–191.

Merill AL and Watt BK (1973) Energy Values of Food: Basis and Derivation. United States Department of Agriculture, Washington, DC, Agriculture Handbook 74:2-3.

Miyashita K, Mikami N Hosokawa M (2013) Chemical and nutritional characteristics of brown seaweed lipids: A review. J Funct Foods 5(4):1507-1517.

Mohsenin NN (1986) Physical properties of plant and animal materials. Gordon and Breach Science Publishers, New York, NY.

Mori K, Ooi T, Hiraoka M, Oka N, Hamada H, Tamura M et al (2004) Fucoxanthin and Its Metabolites in Edible Brown Algae Cultivated in Deep Seawater. Mar Drugs 2(2):63-72.

Morrissey J, Kraan S, Guiry MD (2001) A guide to commercially important seaweeds on the Irish coast. Bord Iascaigh Mhara, Dublin 9:37.

Moser U, Bendich A. (1991) Vitamin C. In: Machlin LJ (ed) Handbook of Vitamins, Marcel Dekker, New York, pp 195-232

Mujumdar AS, Passos ML (2000) Drying: innovative technologies and trends in research and development. In: Mujumdar AS, Suvachittanont S (ed) Developments in Drying, Kasetsart University Press, Bangkok, Thailand, pp 235-268

Melorose J, Perroy R, Careas S (2015) World population prospects. United Nations.

Merill AL, Watt BK (1973) Energy values of food: basis and derivation (pp. 2-3). Agriculture Handbook No. 74, United States Department of Agriculture, Washington, DC.

Minh TV, Perry JS, Bennett AH (1969) Forced-air precooling of white potatoes in bulk. ASHRAE Trans 75(2): 87-94

Mirhosseini H, Amid BT (2013) Effect of different drying techniques on flowability characteristics and chemical properties of natural carbohydrate-protein Gum from durian fruit seed. Chem Cent J 7:1

Mišurcová L, Machů L, Orsavová J (2011) Seaweed minerals as nutraceuticals. Adv Food Nutr Res 64:371-390

Miura K, Kimura N, Suzuki H, Miyashita Y, Nishio Y (1999) Thermal and viscoelastic properties of alginate/poly(vinyl alcohol) crosslinked with calcium tetraborate. Carbohydrate Polymer 39: 139–144.

Mohamed LA, Kouhila M, Lahsasni S, Jamali A, Idlimam A et al (2005) Equilibrium moisture content and heat of sorption of Gelidium sesquipedale. J Stored Prod Res 41:199-209

Moraga, G., Martínez-Navarrete, N., Chiralt, A., 2006. Water sorption isotherms and phase transitions in kiwifruit. Journal of Food Engineering, 72, 147–156.

Moreira R, Chenlo F, Sineiro J, Sánchez M, Arufe S (2016) Water sorption isotherms and air drying kinetics modelling of the brown seaweed Bifurcaria bifurcata. J Appl Phycol 28: 609-618.

Moreira R, Chenlo F, Sineiro J, Arufe S, Sexto S (2017) Water Sorption Isotherms and Air Drying Kinetics of Fucus vesiculosus Brown Seaweed. J Food Process Preserv 41: e12997.

Morrissey J, Kraan S, Guiry MD (2001) Nutritional Analysis of Seaweeds - Sea Vegetables Sea Plants - Algae from Ireland - Taken from " A guide to Commercially Important Seaweeds on the Irish Coast ." Irish Govt 1–65.

Mune MAM, Sogi DS (2016) Emulsifying and Foaming Properties of Protein Concentrates Prepared from Cowpea and Bambara Bean Using Different Drying Methods. Int J Food Prop 19(2):371-384.

Murakami K, Yamaguchi Y, Noda K, Fujii T, Shinohara N, Ushirokawa T et al (2011) Seasonal variation in the chemical composition of a marine brown alga, Sargassum horneri (Turner) C. Agardh. J Food Compos Anal 24(2): 231-236

Muramatsu Y, Tagawa A, Kasai T (2005) Effective thermal conductivity of rice flour and whole and skim milk powder. J Food Sci 70: 279-28

Murphy RY, Marks BP, Marcy JA (1998) Apparent specific heat of chicken breast patties and their constituent proteins by differential scanning calorimetry. J Food Sci 63(1): 88-91

Murthy MVR (2009) A review of new technologies, models and experimental investigations of solar driers. Renew Sustain Energy Rev 13: 835-844.

Nash C (2010) The History of Aquaculture. John Wiley & Sons, Iowa, USA

Neoh YY, Matanjun P, Lee JS (2016) Comparative study of drying methods on chemical constituents of Malaysian red seaweed. Drying Technol 34(14):1745-1751.

Nisizawa K, Noda H, Kikuchi R, Watanabe T (1987) The main seaweed foods in Japan. In: Ragan MA, Bird CJ (eds) Twelfth International Seaweed Symposium. Developments in Hydrobiology 41. Springer, Dordrecht.

Nomura M, Kamogawa H, Susanto E, Kawagoe C, Yasui H, Saga N, Hosokawa M, Miyashita K (2013) Seasonal variations of total lipids, fatty acid composition, and fucoxanthin contents of Sargassum horneri (Turner) and Cystoseira hakodatensis (Yendo) from the northern seashore of Japan. J Appl Phycol 25:1159-1169.

Olofsson M, Lamela T, Nilsson E, Bergé JP, del Pino V, Uronen P, Legrand C (2012) Seasonal Variation of Lipids and Fatty Acids of the Microalgae Nannochloropsis oculata Grown in Outdoor Large-Scale Photobioreactors. Energies 5: 1577-1592.

Omotoso OT (2006) Nutritional quality, functional properties and anti-nutrient compositions of the larva of Cirina forda (Westwood) (Lepidoptera: Saturniidae). J Zhejiang Univ Sci B 7(1):51-55.

Othman MY, Mat S, Ruslan H, Sopian K, Goh LJ (2011) Review of heat pump systems for drying application. Renew Sust Energ Rev 15(9):4788-4796.

Panchariya PC, Popovic D, Sharma AL (2002) Thin-layer modelling of black tea drying process. Journal of Food Engineering 52(4): 349–357.

Park KJ (1998) Diffusional Model With and Without Shrinkage During Salted Fish Muscle Drying. Drying Technology 16: 889–905.

Pavia H, Cervin G, Lindgren A, Åberg P (1997) Effects of UV-B radiation and simulated herbivory on phlorotannins in the brown alga Ascophyllum nodosum. Mar Ecol Prog Ser 157:139–146.

Phinney DM, Frelka JC, Heldman DR (2017) Composition-based prediction of temperature-dependent thermophysical food properties: reevaluating component groups and prediction models: predicting thermophysical properties of foods. J Food Sci 82(1): 6-15.

Potisate Y, Phoungchandang S (2010) Chlorophyll Retention and Drying Characteristics of Ivy Gourd Leaf (Coccinia grandis Voigt) Using Tray and Heat Pump-Assisted Dehumidified Air Drying. Drying Technol 28(6):786-797.

Puttongsiri T, Choosakul N, Sakulwilaingam D (2012) Moisture Content and Physical Properties of Instant Mashed Potato. International Conference on Nutrition and Food Sciences IPCBEE 39.

Rahman MS (1995) Food Properties Handbook (2nd ed., pp. 68-143). CRC Press, Boca Raton FL.

Rahman MS (2001) Toward prediction of porosity in foods during drying: a brief review. Drying Technology 19 (1): 1–13

Rahman MS (2003) A Theoretical Model to Predict the Formation of Pores in Foods During Drying. Int J Food Prop 6(1): 61-72.

Rahman MS (2004) State Diagram of Date Flesh Using Differential Scanning Calorimetry (DSC). Int J Food Prop 7: 407–428.

Rahman MS (2006) State diagram of foods: Its potential use in food processing and product stability. Trends in Food Science and Technology 17: 129–141.

Rahman MS (2012) Applications of macro-micro region concept in the state diagram and critical temperature concepts in determining the food stability. Food Chemistry 132: 1679–1685.

Rahman MS, Sablani SS, Al-Habsi N, Al-Maskri S, Al-Belushi R (2005) State diagram of freeze-dried garlic powder by differential scanning calorimetry and cooling curve methods. Journal of Food Science 70 (2): 135–141.

Rajauria G, Foley B, Abu-Ghannam N (2016) Identification and characterization of phenolic antioxidant compounds from brown Irish seaweed Himanthalia elongata using LC-DAD–ESI-MS/MS. Innov Food Sci Emerg Technol 37:261-268.

Rajauria G, Jaiswal AK, Abu-Ghannam N, Gupta S (2010) Effect of hydrothermal processing on colour, antioxidant and free radical scavenging capacities of edible Irish brown seaweeds. Int J Food Sci Technol 45:2485-2493.

Randhir R, Kwon YI, Lin YT, Shetty K (2007) Effect of thermal processing on the phenolic associated health-relevant functionality of selected legume sprouts and seedlings. J Food Biochem 33:89-112

Rao MA (1975) Thermal conductivity and thermal diffusivity of process variety squash and white potatoes. Trans ASAE 18(6): 1188-1192.

Rao PVS, Mantri VA, Ganesan K (2007) Mineral composition of edible seaweed Porphyra vietnamensis. Food Chem 102:215-218.

Renaud SM, Luong-Van JT (2006) Seasonal variation in the chemical composition of tropical Australian marine macroalgae. J Appl Phycol 18:381-387

Riedel L (1969) Measurements of thermal diffusivity on foodstuffs rich in water. Kaltetechnik 21(11):315-316.

Ringeisen BM, Barrett D, Stroeve P (2014) Concentrated solar drying of tomatoes. Energy for Sustainable Development 19: 47–55.

Rioux LE, Turgeon SL, Beaulieu M (2010) Structural characterization of laminaran and galactofucan extracted from the brown seaweed Saccharina longicruris. Phytochemistry 71(13):1586-1595.

Rojas EEG, Coimbra JSR, Telis-Romero J (2013) Thermophysical properties of cotton, canola, sunflower and soybean oils as a function of temperature. Int J Food Prop 16(7): 1620-1629.

Roos YH (1987) Effect of moisture on the thermal behavior of strawberries studied using differential scanning calorimetry. Journal of Food Science 52 (1): 146–149.

Roos YH (2010) Glass Transition Temperature and Its Relevance in Food Processing. Annual Review of Food Science and Technology - (new in 2010): 469–496.

Rosell K, Srivastava LM (1984) Seasonal variation in the chemical constituents of the brown algae Macrocystis integrifolia and Nereocystis luetkeana. Can J Bot 62(11):2229-2236.

Rupeŕez P (2002) Mineral content of edible marine seaweeds. Food Chem 79:23-26.

Rupérez P, Saura-Calixto F (2001) Dietary fibre and physicochemical properties of edible Spanish seaweeds. Eur Food Res Technol 212(3):349-354.

Russo P, Adiletta G, Di Matteo M (2013) The influence of drying air temperature on the physical properties of dried and rehydrated eggplant. Food Bioprod Process 91(3):249-256.

Sablani SS, Andrews PK, Davies NM, Walters T, Saez H, Bastarrachea L (2011) Effects of Air and Freeze Drying on Phytochemical Content of Conventional and Organic Berries. Drying Technol 29(2):205-216

Sablani SS, Baik O, Marcotte M (2002) Neural networks for predicting thermal conductivity of bakery products. J Food Eng 52(3): 299-304.

Sablani SS, Bruno L, Kasapis S, Symaladevi RM (2009) Thermal transitions of rice: Development of a state diagram. Journal of Food Engineering 90: 110–118.

Sablani SS, Rahman MS (2002) Pore formation in selected foods as a function of shelf temperature during freeze drying. Drying Technol 20(7): 1379-1391.

Sablani SS, Syamaladevi RM, Swanson BG (2010) A review of methods, data and applications of state diagrams of food systems. Food Engineering Reviews: 168–203.

Sánchez-Machado DI, López-Cervantes J, López-Hernández J, Paseiro-Losada P (2004) Fatty acids, total lipid, protein and ash contents of processed edible seaweeds. Food Chem 85(3):439-444.

Sappati PK, Nayak B, van Walsum GP (2017) Effect of glass transition on the shrinkage of sugar kelp (Saccharina latissima) during hot air convective drying. J Food Eng 210:50-61.

Sappati PK, Nayak B, VanWalsum GP, Mulrey OT (2019) Combined effects of seasonal variation and drying methods on the physicochemical properties and antioxidant activity of sugar kelp (Saccharina latissima). J Appl Phycol 31(2):1311-1332.

Schiener P, Black KD, Stanley MS, Green, DH (2015) The seasonal variation in the chemical composition of the kelp species Laminaria digitata, Laminaria hyperborea, Saccharina latissima and Alaria esculenta. J Appl Phycol 27 (1):363-373.

Setiady D, Tang J, Younce F, Swanson BA, Rasco BA, Clary CD (2009) Porosity, Color, Texture, and Microscopic Structure of Russet Potatoes Dried Using Microwave Vacuum, Heated Air, and Freeze Drying. Appl Eng Agric 25(5):719-724.

Shi J, Maguer ML, Kakuda Y, Liptay A, Niekamp F (1999) Lycopene degradation and isomerization in tomato dehydration. Food Res Int 2(1):15-21.

Silva FM, Silva CLM (1999) Colour changes in thermally processed cupuaçu (Theobroma grandiflorum) puree: critical times and kinetics modelling. Int J Food Sci Technol 34:87-94.

Singh S, Shalini R (2016) Effect of Hurdle Technology in Food Preservation: A Review. Crit Rev Food Sci Nutr 56(4):641-649.

Smith DG, Young EG (1955) The combined amino acids in several species of marine algae. J Biol Chem 217:845–854.

Smith J, Summers G, Wong R (2010) Nutrient and heavy metal content of edible seaweeds in New Zealand. New Zeal J Crop Hort 38(1):19-28.

Sopade, PA, Halley PJ, D'arcy BR (2006) Specific heat capacity of Australian honeys from 35 to 165 C as a function of composition using differential scanning calorimetry: specific heat capacity of honeys. J Food Process Preserv 30(2): 99-109.

Stevenson A, Cray JA, Williams JP et al (2015) Is there a common water-activity limit for the three domains of life? ISME J 9:1333-1351.

Sugawara T, Matsubara K, Akagi R, Mori M, Hirata T (2006) Antiangiogenic activity of brown algae fucoxanthin and its deacetylated product, fucoxanthinol. J Agric Food Chem 54(26):9805-9810.

Sugimura R, Suda M, Sho Ayumi et al (2012) Stability of Fucoxanthin in Dried Undaria Pinnatifida (Wakame) and Baked Products (Scones) Containing Wakame Powder. Food Sci Technol Res 18 (5):687-693.

Suleria HAR, Osborne S, Masci P, Gobe G (2015) Marine-Based Nutraceuticals: An Innovative Trend in the Food and Supplement Industries. Mar Drugs 13(10): 6336-6351.

Suresh Kumar K, Ganesan K, Subba Rao PV (2015) Seasonal variation in nutritional composition of Kappaphycus alvarezii (Doty) Doty—an edible seaweed. J Food Sci Technol 52(5):2751-2760.

Susanto E, Fahmi AS, Abe M, Hosokawa M, Miyashita K (2016) Lipids, Fatty Acids, and Fucoxanthin Content from Temperate and Tropical Brown Seaweeds. Aquat Procedia 7:66-75.

Suzuki T, Ohsugi Y, Yoshie Y, Shirai T, Hirano T (1996) Dietary Fiber Content, Water-Holding Capacity and Binding Capacity of Seaweeds. Fisheries Science 62:454-461.

Suzuki K, Kubota K, Hasegawa T, Hosaka H (1976) Shrinkage in dehydration of root vegetables. Journal of Food Science 41 (5): 1189–1193

Sweat VE (1974) Experimental values of thermal conductivity of selected fruits and vegetables. J Food Sci 39: 1080-1083.

Syad AN, Shunmugiah KP, Kasi PD (2013) Seaweeds as nutritional supplements: analysis of nutritional profile, physicochemical properties and proximate composition of G. acerosa and S. wightii. Biomed Prev Nutr 3:139-144.

Syamaladevi RM, Sablani SS, Tang J, Powers J, Swanson BG (2009) State diagram and water adsorption isotherm of raspberry (Rubus idaeus). Journal of Food Engineering 91: 460–467.

Szcześniak L, Rachocki A, Tritt-Goc J (2008) Glass transition temperature and thermal decomposition of cellulose powder. Cellulose, 15, 445-451.

Tabarsa M, Rezaei M, Ramezanpour Z, Waaland J (2012) Chemical compositions of the marine algae Gracilaria salicornia (Rhodophyta) and Ulva lactuca (Chlorophyta) as a potential food source. J Sci Food Agric 92:2500-2505.

Taga MS, Miller EE, Pratt DE (1984) Chia seeds as a source of natural lipid antioxidants. J Am Oil Chem Soc 61: 928-931.

Takhar PS (2008) Role of glass-transition on fluid transport in porous food materials. International Journal of Food Engineering 4(7): 1-13.

Tang J, Sokhansanj S, Yannacopoulos S, Kasap SO (1991) Specific heat capacity of lentil seeds by differential scanning calorimetry. Transaction of the American Society of Agricultural Engineering 34: 517–522.

Taylor R, Krishna R (1993) Multicomponent Mass Transfer. The Maxwell-Stefen Relations (pp. 13-49). John Wiley & Sons Inc., NY , New York, USA.Telis, V.R.N., Sobral, P.J. A., 2001. Glass Transitions and State Diagram for Freeze-dried Pineapple. LWT - Food Science and Technology 34: 199–205.

Telis VRN, Sobral PJA (2002) Glass transitions for freeze-dried and air-dried tomato. Food Research International 35: 435–443.

Tello-Ireland C, Lemus-Mondaca R, Vega-Gálvez A, López J, Di Scala K (2011) Influence of hot-air temperature on drying kinetics, functional properties, colour, phycobiliproteins, antioxidant capacity, texture and agar yield of alga Gracilaria chilensis. Lebensm -Wiss Technol 44(10):2112-2118.

Tiwari B, Troy D (2015) Seaweed Sustainability: Food and Non-Food Applications. Academic Press Elsevier, San Diego, CA, USA

Tsami E, Marinos-Kouris D, Maroulis ZB (1990) Water Sorption Isotherms of Raisins, Currants, Figs, Prunes and Apricots. Journal of Food Science 55: 1594–1597.

Turkmen N, Poyrazoglu ES, Sari F, Sedat Velioglu Y (2006) Effects of cooking methods on chlorophylls, pheophytins and colour of selected green vegetables. Int J Food Sci Technol 41:281-288.

USDA (1996) Nutrient database for standard reference, release 11. U.S. Department of Agriculture, Washington, D.C.

Vairappan CS, Razalie R, Elias UM, Ramachandram T (2014) Effects of improved post-harvest handling on the chemical constituents and quality of carrageenan in red alga, Kappaphycus alvarezii Doty. J Appl Phycol 26(2):909-916.

Van Arsdel, W.B., 1973. Drying phenomena. In: W.B Van Arsdel, M.J Copley, A.I Morgan Jr. (Eds.), Food Dehydration Avi (pp. 22-57), Westport.

Vasquez G, Chenlo F, Moreira R, Carballo L (1999) Desorption isotherms of muscatel and aledo grapes, and the influence of pretreatments on muscatel isotherms. Journal of Food Engineering, 39(4), 409-414

Vega A, Fito P, Andrés A, Lemus R (2007) Mathematical modeling of hot-air drying kinetics of red bell pepper (var. Lamuyo). Journal of Food Engineering. 79, 1460–1466.

Vega-Gálvez A, Ayala-Aponte A, Notte E, Fuente L, Lemus-Mondaca R (2008) Mathematical modeling of mass transfer during convective dehydration of brown algae macrocystis pyrifera. Dry Technol 26(12):1610-1616.

Vilg JV, Nylund GM, Werner T, Qvirist L, Mayers JJ, Pavia H et al (2015) Seasonal and spatial variation in biochemical composition of Saccharina latissima during a potential harvesting season for Western Sweden. Bot Mar 58(6):435-47.

Wang BG, Zhang WW, Duan XJ, Li XM (2009) In vitro antioxidative activities of extract and semi-purified fractions of the marine red alga, Rhodomela confervoides (Rhodomelaceae). Food Chem 113:1101-1105.

Wang H, Ooi EV, Ang PO (2008a) Antiviral activities of extracts from Hong Kong seaweeds. Journal of Zhejiang University. Science. B, 9, 969–76.

Wang H, Zhang S, Chen G (2008b) Glass transition and state diagram for fresh and freeze-dried Chinese gooseberry. Journal of Food Engineering 84: 307–312

Wang N, Brennan JG (1995) Changes in structure, density and porosity of potato during dehydration. J Food Eng 24(1): 61-76

Wang J, Xiong YS, Yu Y (2004) Microwave Drying Characteristics of Potato and the Effect of Different Microwave Powers on the Dried Quality of Potato. Eur Food Res Technol 219: 500–506.

Wells ML, Potin P, Craigie JS et al (2016) Algae as nutritional and functional food sources: revisiting our understanding. J Appl Phycol 29(2):949-982.

Welty J, Wicks CE, Wilson RE, Rorrer GL (2008) Fundamentals of Momentum, Heat and Mass Transfer. Differential Equations of Mass Transfer (5th ed., pp. 433-451). John Wiley & Sons Inc., Hoboken, New Jersey, USA.Yang, J., Chen, J.F., Zhao, Y.Y., Mao, L.C., 2010. Effects of drying processes on the antioxidant properties in sweet potatoes. Agricultural Sciences in China 9: 1522–1529.

Wojdylo A, Figiel A, Legua P, Lech K, Carbonell-Barrachina AA, Hernández F (2016) Chemical composition, antioxidant capacity, and sensory quality of dried jujube fruits as affected by cultivar and drying method. Food Chem 207:170-179.

Wong K, Cheung PC (2001) Influence of drying treatment on three Sargassum species. J Appl Phycol 13(1):43-50.

Yang J, Chen JF, Zhao YY, Mao LC (2010) Effects of drying processes on the antioxidant properties in sweet potatoes. Agric Sci China 9:1522-1529

Yang L, Zhang L (2009) Chemical structural and chain conformational characterization of some bioactive polysaccharides isolated from natural sources. Carbohydr Polym 76(3):349-61.

Yan Z, Sousa-Gallagher MJ, Oliveira FAR (2008) Shrinkage and porosity of banana, pineapple and mango slices during air-drying. J Food Eng 84(3): 430-440.

Yeh C, Chang H, Pan W (2011) Time Trend of Obesity, the Metabolic Syndrome and Related Dietary Pattern in Taiwan: from NAHSIT 1993-1996 to NAHSIT 2005-2008. Asia Pac J of Clin Nutr 20(2):292-300.

Zabalaga RF, La Fuente CIA, Tadini CC (2016) Experimental determination of thermophysical properties of unripe banana slices (Musa cavendishii) during convective drying. J Food Eng 187: 62-69.

Zielinska M, Markowski M (2010) Air drying characteristics and moisture diffusivity of carrots. Chemical Engineering and Processing: Process Intensification 49: 212–218.

Zhang M, Tang J, Mujumdar AS, Wang S (2006) Trends in microwave-related drying of fruits and vegetables. Trends Food Sci and Technol 17: 524–534.

Zhao JH, Liu F,Wen X, Xiao HW, Ni YY (2015) State diagram for freeze-dried mango: freezing curve, glass transition line and maximal-freeze-concentration condition. J Food Eng 157: 49–56

Zhu M, Wang J, Perepezko JH, Yu L (2015) Possible existence of two amorphous phase of d-mannitol related by a forst order first-order transition. The J Chem Phys 142 (244504): 1–8.

Zubia M, Payri C, Deslandes E (2008) Alginate, mannitol, phenolic compounds and biological activities of two range-extending brown algae, Sargassum mangarevense and Turbinaria ornata (Phaeophyta: Fucales), from Tahiti (French Polynesia). J Appl Phycol 20:1033-1043

Zvyagintsevaa TN, Shevchenkoa NM, Popivnicha IB, Isakova VV, Scobunb AS, Sundukovaa EV, Elyakova LA (1999) A new procedure for the separation of water-soluble polysaccharides from brown seaweeds. Carbohydr Res 322(1–2):32-39.

BIOGRAPHY OF THE AUTHOR

Praveen Sappati was born in Srikakulam, Andhra Pradesh State in India on Jan 15, 1990. He was raised in Bhilai, Chhattisgarh, India. He graduated from Narayana Public School, Vishakhapatnam in 2007. He attended the Indian Institute of Technology Kharagpur in 2008 to receive a Bachelor of Technology in Agricultural and Food Engineering and Master of Technology in Food Process Engineering. He later worked in Godrej Agrovet Limited (GAVL), India and Indian Institute of Technology Kharagpur as a graduate engineer trainee and research assistant for 2 years. Praveen is a candidate for the Doctor of Philosophy degree in Food and Nutrition Sciences from the University of Maine in August 2020.